THE MORPHOLOGY OF THE INTRAPARIETAL SULCUS IN CHILDREN PRENATALLY EXPOSED TO ALCOHOL IN A SAMPLE OF CHILDREN FROM THE WESTERN CAPE, SOUTH AFRICA AND ITS POTENTIAL RELATIONSHIP WITH NUMBER PROCESSING.

MARLIE GREEFF

Supervisor: Christopher M. R. Warton

Co-Supervisors: Ernesta M. Meintjes and Fleur L. Warton

Presented for the Degree of

Doctor of Philosophy

Department of Human Biology

Faculty of Health Sciences

University of Cape Town

February 2020

Declaration

I, Marlie Greeff, declare that this thesis is my own unaided work, both in concept and execution, and that apart from the normal guidance from all my supervisors, I have received no other assistance.

Signature: Signed by candidate

Date: 10 February 2020

Abstract

The intraparietal sulcus (IPS) is a prominent feature in the parietal lobe and extends posteriorly from the postcentral sulcus through the parietal lobe to end in the occipital. It is involved in visuospatial functions and is known to play a critical role in number processing. Fetal alcohol spectrum disorders (FASD) result from prenatal exposure to alcohol and are particularly prevalent in the Western Cape region of South Africa. Arithmetic is a domain of cognitive function that is particularly sensitive to prenatal alcohol exposure, and effects on arithmetic remain significant after controlling for lower IQ. Magnetic resonance imaging (MRI) was used to investigate the morphology of the IPS and whether this morphology had a relation to the number processing abilities of children prenatally exposed to alcohol in a Western Cape community.

Participants were 9 to 14-year-old children from the same community in Cape Town, South Africa, who formed part of a study aimed at investigating the effects of prenatal alcohol exposure (PAE) on brain structure and function particularly during number processing. Mothers were interviewed regarding alcohol consumption during pregnancy using a timeline follow-back approach. The first analysis included designing a protocol for manually parcellating the IPS into two regions of interest (ROI): the medial wall (MIPS) and the lateral wall (LIPS) respectively. The neuroimaging program MultiTracer was used for the manual tracing and to calculate the volume of the cortex of both the MIPS and LIPS. The purpose of this first analysis was to examine the effects of PAE on IPS volume and asymmetry using manual tracing, the relation between IPS volume and number processing performance, and potential moderation by PAE of the relation between IPS volume and number processing performance. Results indicated that when comparing the FAS/PFAS (Fetal Alcohol Syndrome/Partial FAS) children to the controls, PAE had an effect on the left LIPS and higher arithmetic scores were associated with larger bilateral MIPS volumes suggesting that the effect of PAE on math may not be moderated by IPS volume. The left LIPS was significantly smaller in FAS/PFAS individuals when compared by FASD diagnosis, and this remained a trend after controlling for potential confounders. In the second analysis, the automated neuroimaging software program FreeSurfer was used to parcellate the IPS. These volumes were then compared with our previously manually traced volumes. Intra-rater reliability testing was statistically significant for consistency and absolute agreement indicating good retraceability of the designed protocol for manual tracing. Both left and right IPS volumes were significantly larger with the manually traced method compared to automated tracing. The manually traced left IPS yielded stronger results when comparing volumes

by diagnostic groups, conversely the automated volumes showed stronger associations with alcohol measures. A possible explanation is that FreeSurfer parcellated the IPS differently to our protocol and does not take into account the extensive variability of the morphology of the sulcus. BrainVoyager QX, another neuroimaging software program was used in the third analysis when looking at the BOLD fMRI data of the participants. For this analysis, the manually traced MIPS and LIPS were subdivided into five ROI's for the left and right hemispheres respectively: (1) the superior MIPS, (2) the medial branch of the MIPS, (3) the inferior MIPS, (4) the superior LIPS, and (5) the inferior LIPS. The percent signal change were calculated for each participant for the proximity judgement (PJ) tasks they performed inside the scanner. Associations of the percent signal change of the ROI's of the PAE children with absolute alcohol per occasion (oz) were all significant even after controlling for IQ except the left inferior LIPS, supporting what is found in the literature.

The current findings, in agreement with previous studies, demonstrate that PAE is associated with both structural and functional changes in the brain. While the morphology of the IPS may not moderate the effects of PAE on arithmetic function, some cortical volumes within the IPS were sensitive to PAE. Moreover, altered activation of the IPS in the performance of magnitude comparison tasks was strongly associated with PAE. The IPS is an extremely variable structure whose anatomy is often misunderstood, which emphasises the importance of anatomical knowledge for imaging studies. Future research will refine the protocol for manual tracing of the IPS, which may lead to greater understanding of the functions of the different areas. It is to be hoped that these findings will give more insight into understanding the functioning of children and adults with FASDs and contribute to more effective therapeutic interventions for these individuals.

Acknowledgments

Ek is tot alles in staat deur Hom wat my krag gee.

-Filipense 4:13-

I would like to thank the grants who supported this study from the National Institute on Alcohol Abuse and Alcoholism (R01 AA-016780, U01 AA014790); South African National Research Foundation; and the Lycaki/Young Fund, State of Michigan. We thank H.E. Hoyme, L.K. Robinson, and N. Khaole, who conducted the dysmorphology assessments; our University of Cape Town and Wayne State University research staff, M. Pienaar, M. September, R. Sun, and N. Dodge; and G. Adams, S. Heyne, P. Samuels, K. Salie, and N. Solomon, the MR technologists at the Cape Universities Brain Imaging Centre. Thank you to Profs. Sandra and Joe Jacobson for starting this study and or all their help on the project.

To my supervisors: Prof. Ernesta Meintjes for always pushing me to be a better researcher and for introducing me and allowing me to present our research at international conferences. Dr. Fleur Warton for being both my friend and supervisor. Thank you for always understanding and motivating me through the process. Dr. Christopher Warton, you are a mentor that every person needs. Thank you for your wisdom and extensive knowledge from my honours to PhD. You taught me a lot and always had an open door whenever I needed something. I give thanks to your wife Sarah and the rest of your wonderful family too.

For the people who helped me during the writing up process and to figure out confusing code on imaging software: Emmanuel Nwosu, thank you for your help with FreeSurfer, you were always kind and ready to help. Dr. Keri Woods, thank you for your extensive help with my functional data, you were so patient with me while I made stupid mistakes. Dr. Adhil Bhagwhandin, for being willing to help proof read chapters of my thesis and for giving advice on the write up process. Thank you Steven Randall for the all-nighters of work and for empathising with the stress of the PhD process. Stevie Biffen for always putting a smile on my face with her laughter.

To all my close friends for understanding and being patient with me through the years. You all mean a lot to me and I couldn't have done it without your love and friendship. Rhonwen, you entered my PhD journey in the last few months and helped me work through the last bit of it. Thank you so much

for caring and praying with me and reminding me that God is always there. You will never know how much your kindness and support means to me.

Finally I would like to thank my family without whom none of this would have been possible! To my eldest sister Louisa, thank you for all the food and supply of 2-minute noodles! You were also my safe haven in Cape Town when I needed comfort and motivation. To my crazy sister Johanetta, thank you for being the good kind of crazy and motivating me to keep exercising (this thesis is my comrades marathon…I'm not doing the real one with you) Thank you for the visits, love and karaoke! A special thank you to my mom, Marlene. You started this journey with me 10 years ago. You accepted what I wanted to study and was and is always supporting me, emotionally and financially. You are a great mother and I love you very much. Thank you for everything.

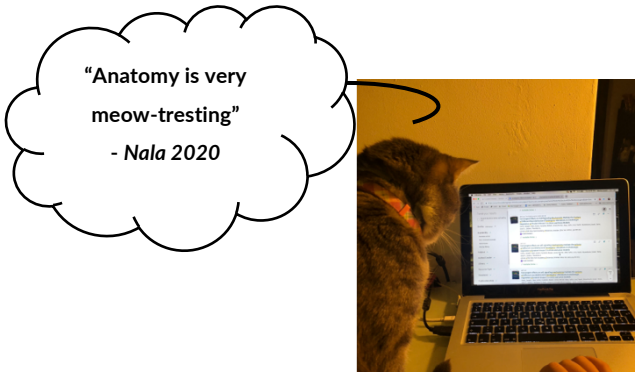

Preface

In these studies magnetic resonance imaging (MRI) and functional magnetic resonance imaging (fMRI) were used to investigate the effects of prenatal alcohol exposure on the intraparietal sulcus (IPS) of the brain and its function as an arithmetic hub. Prenatal alcohol exposure (PAE) is sadly a major social problem in the Western Cape Province of South Africa and extensive research has been done on cohorts of certain communities in the province. This thesis presents work that forms part of a longitudinal study of PAE in the Western Cape that has done a considerable amount of research on various areas of brain structure and function in children exposed to the teratogenic effects of alcohol *in utero*.

Chapters three to five are presented as individual original articles that will be prepared for publication after submission of the thesis. As the chapters are written as independent articles, there will be repetition in the introductions, methods, results and discussions. Following below is a synopsis of each chapter and the co-authors who contributed to each study.

Chapter one gives a short introduction to Fetal Alcohol Spectrum Disorder, the parietal lobe and imaging. It also explains the need for the study and the aims that we wanted to achieve with the research.

Chapter two provides background information on the important elements of the thesis. The anatomy of the parietal lobe and intraparietal sulcus is discussed and the imaging methods used in this study are briefly explained. Additional information on the methodology of the longitudinal study that this thesis forms part of is also explained at the end of chapter two.

Chapter three is the first of the three original articles which will be submitted for publication. In this chapter my primary supervisor, Dr. Christopher M R Warton and I, created a novel protocol for manually tracing the cortex of the intraparietal sulcus. These tracings allowed us to analyse the associations of maternal alcohol consumption with the volume of the IPS cortex and the children's performance on arithmetic tasks.

Chapter four used the protocol created in chapter three and compares the volumetric results to the same subjects measured by an automated software. Emmanuel Nwosu helped with the coding in the automated software and provided guidance for using the software. This chapter aimed to show the advantages and disadvantages of manual- and automated -parcellation of a sulcus.

Chapter five, the final of the three articles is an fMRI study that used region of interest analysis to determine activation of manually traced subdivisions of the intraparietal sulcus. The protocol in chapter three for manual parcellation was used in this chapter to subdivide each wall of the intraparietal sulcus into smaller regions. Dr. Keri Woods assisted in the fMRI analysis an provided guidance with the software used.

Chapter six is the final chapter of the thesis and discusses all the studies done from chapter three to five. This chapter evaluates all the conclusions of the three studies and gives a conclusion of the significance of the research done for this thesis.

My co-supervisors Prof. Ernesta M Meintjes and Dr. Fleur L Warton provided assistance with the statistical analysis in chapters three to five. In addition, Prof. Meintjes was involved in the initial design of the project and provided valuable guidance throughout. Dr. Christopher M R Warton provided the main supervision for the project and all three supervisors aided in editing the drafts of all chapters in this thesis.

Table of Contents

Abbreviations

A	Anterior
AA	Absolute alcohol
AG	Angular gyrus
ARBD	Alcohol-related birth defects
ARND	Alcohol-related neurodevelopmental disorder
BOLD	Blood oxygenation level dependent
CI	Confidence interval
CNS	Central nervous system
CS	Central sulcus
CSF	Cerebrospinal fluid
FAS	Fetal alcohol syndrome
FASD	Fetal Alcohol Spectrum Disorder
fMRI	Functional magnetic resonance imaging
GLM	General linear model
HE	Non-syndromal heavily exposed
HRF	Hemodynamic response function
I	Inferior
ICC	Intraclass correlation coefficient
IPL	Inferior parietal lobule
IPS	Intraparietal sulcus
L	Left
LIPS	Lateral wall of the intraparietal sulcus
MIPS	Medial wall of the intraparietal sulcus
MRI	Magnetic resonance imaging
P	Posterior
PCS	Post-central sulcus
PEA	Prenatal alcohol exposure
PFAS	Partial fetal alcohol syndrome
PJ	Proximity judgement
POS	Parietal-occipital sulcus
PSPL	Posterior superior parietal lobe

R	Right
RF	Radio frequency
ROI	Region of interest
S	Superior
SI	Primary somatosensory cortex
SII	Secondary somatosensory cortex
SPL	Superior parietal lobule
TC	Tailarach coordinates
TE	Echo time
TR	Repetition time

Chapter 1

INTRODUCTION

Prenatal alcohol exposure (PAE) can be detrimental to a developing fetus. The development of the human embryo and fetus is a very sophisticated and complex process and it is very sensitive to outside influences. Those factors which result in abnormal development are called teratogens.

Teratogens include drugs such as cocaine, methamphetamines and tobacco. Alcohol is another major substance with teratogenic effects *in vivo* (Riley, Infante and Warren, 2011). The origin of the word 'teratogen' comes from Greek '*teras*' and '*geneim*' meaning 'to produce'. Thus a teratogen is any agent chemical or otherwise that can cause an abnormality in the embryo or fetus (*Mosby's Dictionary of Medicine, Nursing & Health Professions*. 8th edn, 2009).

PAE affects each fetus differently depending on the timing and amount of consumption and therefore PAE itself is not a diagnosis. The term fetal alcohol spectrum disorder (FASD) was first used in April 2004 (Bertrand *et al.*, 2005; Hoyme *et al.*, 2016), and is an umbrella term for a range of diagnoses which include fetal alcohol syndrome (FAS), partial fetal alcohol syndrome (PFAS), alcohol-related neurodevelopmental disorder (ARND) and alcohol-related birth defects (ARBD) (Riley *et al.*, 2010; Hoyme *et al.*, 2016). Jones and Smith (1973) first described the most severe of FASDs, FAS, in their 1973 paper: "Recognition of the fetal alcohol syndrome in early infancy". The current criteria (figure 1.1) for a diagnosis of FAS/PFAS are detailed and specific and include growth retardation and craniofacial abnormalities including short palpebral fissures, thin vermillion border of the upper lip, absent or reduced philtrum and small head circumference (Hoyme *et al.*, 2016). A large proportion of exposed children, however, lack the characteristic FAS facial features but may exhibit attention, cognitive and/or behavioural deficits. These are diagnosed as having ARND. In our study, children with confirmed heavy PAE who lack the facial dysmorphology have been termed nonsyndromal heavily exposed (HE). Certain communities in the Western Cape Province of South Africa have amongst the highest reported incidence rates of FAS in the world (Croxford and Viljoen, 1999; May *et al.*, 2000; Jacobson *et al.*, 2006, 2008).

Alcohol consumption by pregnant mothers may occur continuously throughout pregnancy or by episodes of binge drinking. Variations in the timing of consumption may affect the developing embryo in different ways. The brain is one of the organs most profoundly sensitive to the teratogenic effects of alcohol (Riley, Infante and Warren, 2011; Guerri and Pascual, 2017). Deficits in learning, memory, language, motor abilities and visuospatial functioning (Mattson and Riley, 1998; Nunez, Roussotte and Sowell, 2011) have been reported, as well as global and regional volume reductions (Archibald et al., 2001; Blair & O'Connor, 2007; Clarren & Smith, 1978; Jones & Smith, 1973; Mattson et al., 1996; Sowell et al., 2002; Swayze et al., 1997; Wisniewski, Dambska, Sher, & Qazi, 1983). Some

anatomically affected domains include the caudate nucleus and hippocampus (Biffen *et al.*, 2018), and parietal, temporal and frontal cortical regions (Sowell et al., 2008).

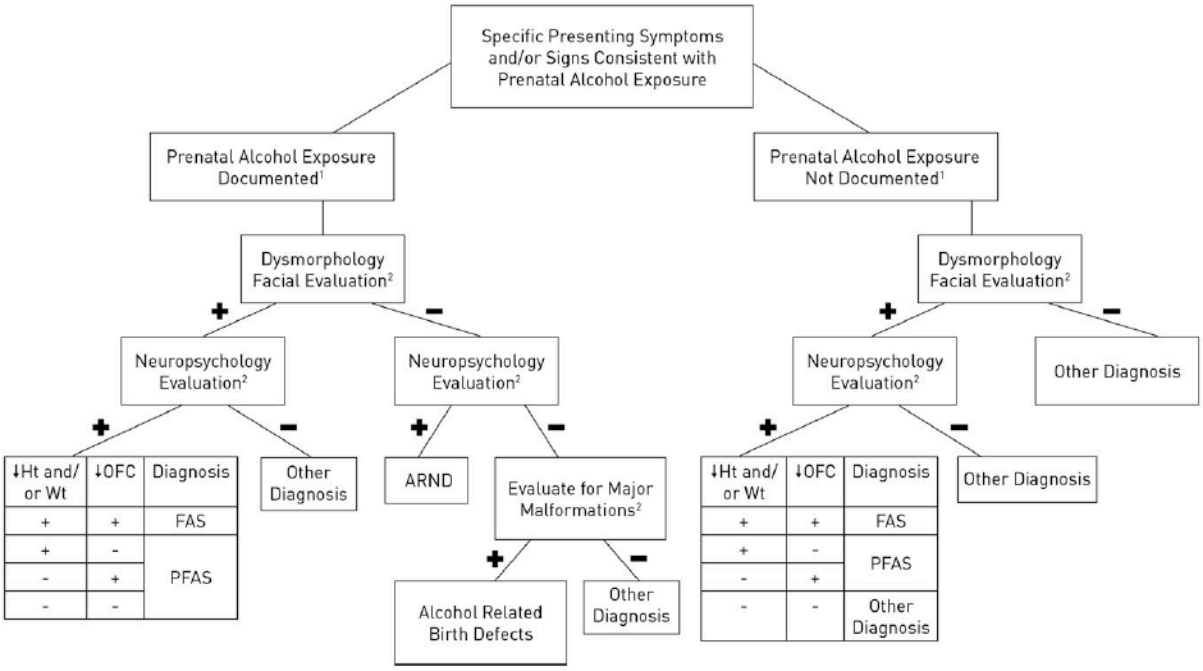

Figure 1.1: The FASD diagnostic algorithm as presented by Hoyme *et al.* (2016). Two of the three cardinal facial characteristics are needed for a positive 'dysmorphological facial evaluation'. (From Hoyme *et al.* (2016))

The parietal lobe cortex hosts a variety of visuospatial functions which are implicated in FASDs (Mattson and Riley, 1998). Areas in the lobe linked to number processing have also been consistently linked to PAE (Meintjes *et al.*, 2010; Woods *et al.*, 2015). A particular structure in the parietal lobe linked to number processing is the intraparietal sulcus (IPS) (Coull and Frith, 1998; Delazer *et al.*, 2003; Molko *et al.*, 2003; Piazza *et al.*, 2004; Venkatraman, Ansari and Chee, 2005; Ashkenazi *et al.*, 2008; Bugden *et al.*, 2012). The IPS comprises 5 functional subdivisions known as the posterior- (PIP), anterior- (AIP), medial- (MIP), lateral- (LIP), and ventral (VIP) IPS. The anterior IPS plays a greater role in somatosensory processing while the posterior IPS is more involved in processing of visual signals. Neurons in the medial bank or wall of the sulcus are more involved in arm movements, while those in the lateral bank play a greater role in eye movements (Clark, Boutros and Mendez, 2010). Functional MRI (fMRI) studies have demonstrated that similar brain regions are involved in visuospatial and number processing tasks, (Simon *et al.*, 2002; Dehaene *et al.*, 2003) suggesting that visuospatial ability may be indicative of number processing skills. Data from lesion and fMRI studies have linked bilateral activation of the anterior IPS with representation of semantic information about magnitude (Cohen and Dehaene, 1995; Naccache and Dehaene, 2001) and activations in this region have been shown to increase as the complexity of the calculation increases (Menon *et al.*, 2000). Reduced grey matter density has also been reported in the left IPS in children with dyscalculia (Isaacs

et al., 2001). Dehaene and associates (2004) suggest that basic number sense is acquired from an early age in the IPS. In view of the recognised role of the IPS in number sense, the studies examined whether alterations in the structure or volume of the IPS would be related to arithmetic performance in PAE children. Dehaene *et al.*, (2004) suggest that disorganisation in functional domains involved in number processing could cause impairment in arithmetic when alterations occur at an early age.

Although certain automated segmentation tools are able to parcellate the IPS, there is concern that automated segmentation of pediatric brains may not be optimal (Bigler *et al.*, 2010; Ghosh *et al.*, 2010) as atlases used in the construction of the automated labeling software are based on images and/or manual tracings of adult brains (Destrieux *et al.*, 2010). Children's brains are rapidly developing and as such relative sizes of different structures may differ from those in adults. There also exists a need for manual tracing of the IPS in children to examine relationships between morphology from manual tracing and direct observations with those from automated segmentation. Further, it is known that prenatal alcohol exposure results in reduced brain size and affects different brain regions disproportionately (Jones and Smith, 1973; Clarren and Smith, 1978; Wisniewski *et al.*, 1983; Mattson *et al.*, 1996; Swayze *et al.*, 1997; Archibald *et al.*, 2001; Blair and O'Connor, 2007), which may exacerbate the problems associated with automated segmentation. In view of the variability of the IPS, inconsistent branching, and the fact that most automated segmentation tools are based on adult data, 'gold standard' manual tracing was used in this study.

This project used neuroimaging data acquired as part of ongoing studies of brain development in children with prenatal alcohol exposure in Cape Town, South Africa (Jacobson *et al.*, 2008, 2011). Its focus is to examine the incidence of structural alterations and volume reductions in the IPS in children with FASD, and the potential role of these alterations in number processing performance. This study also aimed to clarify the extent to which manual tracing and automated segmentation correspond in a pre-adolescent cohort which includes normative controls and children with PAE-related deficits.

Chapter 2

BACKGROUND

2.1 The Parietal Lobe – '*Lobus Parietalis*'

(Cunningham, 1892; Sacks, 1985; Rizzolatti, 1997; Culham and Kanwisher, 2001; Culham and Valyear, 2006; Husain and Nachev, 2007; *Mosby's Dictionary of Medicine, Nursing & Health Professions*. 8th edn, 2009; Clark, Boutros and Mendez, 2010; Mancall and Brock, 2011; Martinez *et al.*, 2013; Crossman and Neary, 2014; Hendelman, 2015; Hall, 2016; Caspers and Zilles, 2018; Harding-Forrester and Feldman, 2018)

The parietal lobe is one of the four main lobes of the cerebral hemisphere (the insula is sometimes considered a lobe of its own). Each lobe has its own functions but they all work together in an extremely complex multi-modal way which is slowly being elucidated. The name 'parietal' comes from the Latin 'Paries' meaning 'wall'. The lobe itself was named after the 'parietal bone' of the skull which overlies it. The parietal lobe has had its name for centuries, and while its basic form has long been well established its functions still require much research. Both somato-sensory and visuospatial information are integrated in the lobe. All of the body's sensory nerve networks and the comprehension of visual stimuli with their spatial relationships are controlled by the multimodal network that centres in the parietal lobe. Sensory information from the body enters the spinal cord through the dorsal roots of the spinal nerves from where the information is carried to the thalamus, primarily via one of two sensory pathways – the dorsal column-medial lemniscal system and the anterolateral system. Considered as his greatest masterpiece, Professor Macdonald Critchley, a British Neurologist of the 20th century, wrote a book entitled 'The Parietal Lobes'. He went into great detail explaining everything about the lobe, from anatomy to spatial disorders etc. This foundational work showed that the parietal lobe holds many mysteries and needs much exploration. Most of the functional research came from experiments on Macaque monkeys. Although the research on primates has provided a great deal of knowledge, the cortical maps of humans and primates are by no means identical and therefore the imaging research on humans is, among many other modalities, essential. Primates have many more functional areas in the parietal lobe compared to humans. This may be because of their need to survive in the wild and for this, their need for spatial awareness is much greater.

2.1.1 The anatomy and functions of the parietal lobe

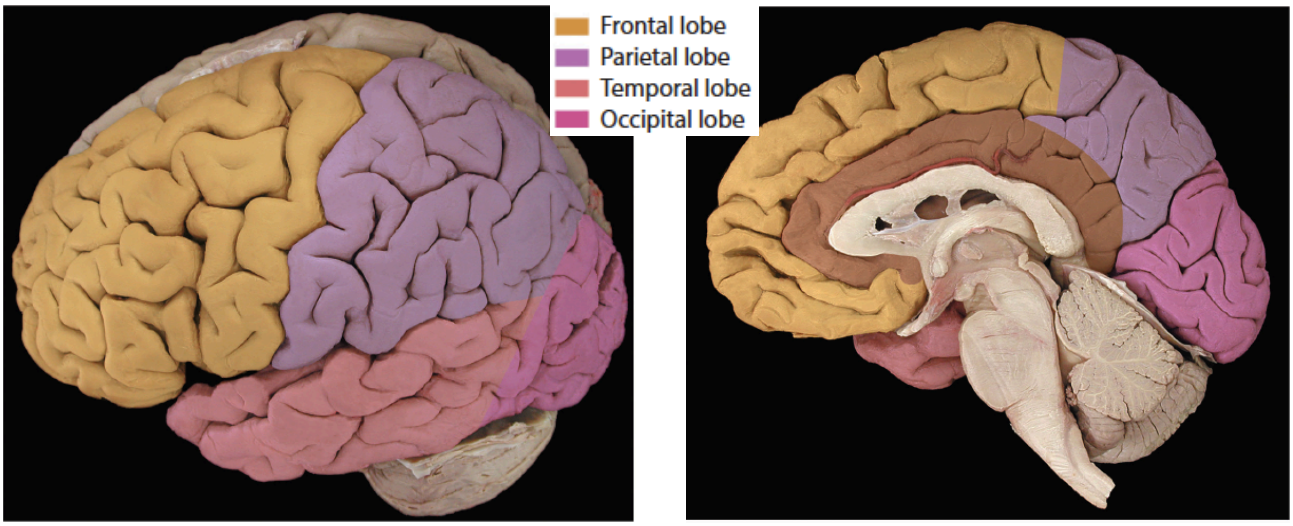

Figure 2.1: (Left) A lateral view of the brain showing the different lobes of the brain and the position of the parietal lobe. (Right) A medial view of the brain showing the medial borders of the parietal lobe. (From Hendelman (2015)).

The parietal lobe (figure 2.1) lies posterior to the frontal lobe, anterosuperior to the occipital and superior to the temporal. The borders of the lobe are the central sulcus anteriorly, the lateral sulcus (temporal lobe) inferiorly and the parieto-occiptal sulcus posteroinferiorly. If the cingulate gyrus is to be regarded as part of the "limbic lobe" it then forms the inferior boundary on the medial surface of the hemisphere.

The parietal lobe is divided into the postcentral gyrus, superior and inferior parietal lobules and the intraparietal sulcus on the superolateral surface and the paracentral lobule and precuneus on the medial surface.

The post-central gyrus and paracentral lobule

As the name suggests, this gyrus is immediately posterior to the central sulcus with the postcentral sulcus lying posteriorly. It passes over the superior surface of the hemisphere and ends on the medial surface by forming the posterior part of the paracentral lobule. It usually ends inferolaterally by joining the lateral sulcus. Functionally it forms the primary somatosensory cortex (SI). The SI contains a sensory homunculus with the areas of the body represented functionally in the form of a map on the cortex. The area for the head lies inferolaterally and the body parts arranged as a figure with the lower limb areas uppermost and extending onto the medial surface in the paracentral lobule. Some areas such as the lips and hands are represented as larger areas due to the larger number of sensory neurons in those particular areas. The post-central gyrus (PCG) allows us to experience touch, pain, temperature, pressure and proprioceptive information. This information passes to the brainstem via the dorsal column, anterolateral (spinothalamic) and trigeminothalamic pathways. The pathways

relay in the thalamus before passing to the gyrus. The sensory pathways cross the midline so the left side of the body is represented in the right postcentral gyrus and vice versa. Just below SI, in the upper wall of the lateral sulcus, is the parietal operculum that houses the second somatosensory cortex (SII). The localization of body areas in SII are poor compared to the precise localisation in SI. Signals from the brainstem to SII are bilateral and usually projections from SI are required for its functioning.

Superior parietal lobule

When you want to take your car keys out of your pocket or bag, you will immediately be able to identify them by touch. This involves the activity of the superior parietal lobule. If it is damaged you may be unable to recognise objects by touch with the contralateral hand. The superior parietal lobule (SPL) is the somesthetic association cortex. The SPL is concerned with identifying an object by touch and locating it in space. It also monitors our own body position moment by moment. It activates saccadic eye movements and also contributes to the control of movement of a body part to act out the movement needed for a certain action. The right anterior SPL is suggested to be involved in the exploration of objects while the same area on the left is said to remember information about objects in the working memory such as their shape. There exist various 'maps' in the brain representing our body in space and our immediate environment. They include somatotopic, retinotopic, allocentric and egocentric maps. The egocentric map is located in the superior parietal lobule and acts as our "internal GPS" monitoring moment by moment the space in front, behind and left and right of us and also our own body position in that space. The left SPL monitors the right side of the body but the right serves both sides. For this reason a right sided lesion has more profound effects on awareness of the body than the left. The somatotopic map lies on the postcentral gyrus, The retinotopic map in the primary visual cortex, and the allocentric map, which functions like an internal "atlas" is housed in the hippocampus.

Inferior parietal lobule

While the SPL busies itself with figuring out the position of the body and the objects around oneself, the inferior parietal lobule (IPL) is more involved in higher intellectual functions. Anatomical components located in the IPL are the supramarginal and angular gyrus. The IPL works closely with the superior part of the temporal lobe in processing speech. Seen words, coming from the occipital lobe are interpreted as their auditory equivalents. This is mostly the work of the angular gyrus. The supramarginal gyrus also acts as a kind of memory centre in the IPL storing information about movements of limbs and positions of the hands from previous experiences. The language functions occur predominantly in the dominant hemisphere of the individual.

Intraparietal sulcus

This large sulcus runs anteroposteriorly separating superior and inferior parietal lobules. It is discussed in more detail below.

Precuneus

This area makes up most of the medial surface of the parietal lobe. It is involved, among other things, with consciousness, visuospatial imagery and self-awareness.

The effect of alcohol on the development of the parietal lobe

(Archibald *et al.*, 2001; Sowell *et al.*, 2001, 2002, 2008; Lebel, Roussotte and Sowell, 2011)

Prenatal alcohol exposure (PAE) is known to effect the whole brain. The teratogenic effects of alcohol on the fetus lead to whole brain volume reduction and deficits in functionality of all four lobes. The parietal lobe has been well established as a domain sensitive to PAE with both visuospatial- and arithmetic -functioning being effected. Both white- and grey -matter volume have been suggested to be decreased compared to controls whereas cortical thickness and grey matter density have been increased.

2.2 The Intraparietal Sulcus

2.2.1 The history of the anatomy of the intraparietal sulcus

(Turner, 1866; Cunningham, 1890; 'DANIEL JOHN CUNNINGHAM, M.D., F.R.S', 1909; Wessels, Correia and Taylor, 2016)

This significant landmark in the parietal lobe runs horizontally and divides the superior parietal lobule from the inferior parietal lobule. The intraparietal cortex is a galaxy of neurons involved in many functions of visuo-spatiality and numerosity. Its history in anatomy runs back all the way to the 1800's when it was identified in both human and animal brains.

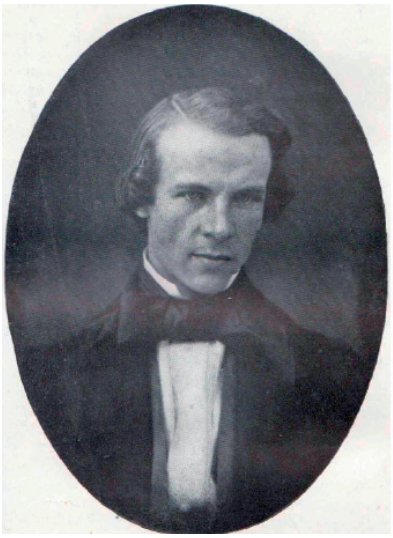

Figure 2.2: Sir William Turner in 1854. From Wessels *et al.* (2015).

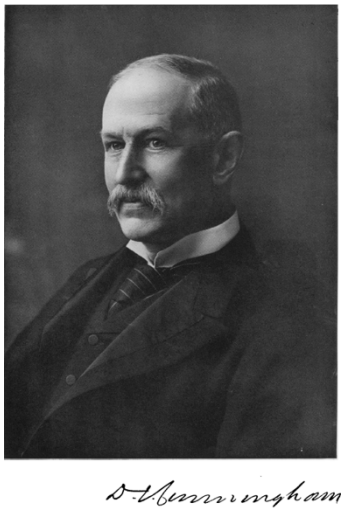

Figure 2.3: Professor Daniel John Cunningham (1850 – 1909). From his obituary in 1909.

The intraparietal sulcus was first described by Sir William Turner, and for some time the sulcus was referred to as 'the intraparietal sulcus of Turner'. Turner was born in Lancashire, England in 1832 and passed away in February of 1916. He was regarded as a "physiological anatomist" at the University of Edinburgh where he published many papers on anatomy. In 1866 he published his work on the IPS and it's morphology on the chimpanzee and human brain, and named the sulcus the 'Intra-parietal fissure':

> *"Not only in the brain of the Chimpanzee, but in those of all the apes in which the various parietal convolutions are differentiated, the fissure which separates the angular convolution from the second ascending parietal and its posterior lobule is so clearly marked that it deserves to be recognised by a distinctive term ; but as none has as*

yet been applied to it, I would suggest that it should be called the intra-parietal fissure (IP). This fissure commences anteriorly behind the fissure of Rolando, at first ascends almost parallel to it, and then runs backwards and joins posteriorly the parieto-occipital fissure."

Turner became a mentor and friend to Daniel John Cunningham who furthered the research on the IPS and described its anatomy in more detail. Daniel John Cunningham, who like his mentor Turner, was also a Professor of Anatomy at the University of Edinburgh and was born in Crieff, Scotland in 1850. Unfortunately and unlike his mentor Turner, Cunningham passed away at a young age of 59 in 1909.

Cunningham's work on the IPS identified five anatomical variations of the sulcus. His description of the morphology of the IPS based on 62 human brains described the IPS as comprising three major parts: *the ramus horizontalis*, *the ramus verticalis superior* and the *ramus verticalis inferior*. The *ramus verticalis superior* and *inferior* are now collectively known as the post central sulcus (PCS), and the *ramus horizontalis* as the IPS. Cunningham's five proposed variations were: (I) All three parts of the sulcus are separate; (II) the inferior portion of the PCS is confluent with the intraparietal sulcus, but the superior portion of the PCS is separate; (III) the PCS is confluent, but separate from the intraparietal sulcus; (IV) all three parts of the sulcus are confluent; and (V) the superior part of the PCS is confluent with the IPS, but the inferior part of the PCS is separate.

Presently, the PCS is usually regarded as a separate structure from the IPS. Many research papers refer to the IPS as the 'HIPS' regarding the 'horizontal' portion running down the parietal lobe as the entire sulcus.

2.2.2 Visuospatial functions

(Bremmer *et al.*, 2001; Cooke *et al.*, 2003; Grefkes and Fink, 2005; Shikata *et al.*, 2008; Clark, Boutros and Mendez, 2010; Binkofski, Klann and Caspers, 2016; Harvey, Ferri and Orban, 2017)

Extensive research into the functional organization of the IPS has been done on Macaque monkeys. Seventeen functional areas have been discovered thus far in Macaques. Currently, five functional regions have been identified in the human IPS. These areas help us to know where we find ourselves in the space around us and what objects are in our direct vicinity. Even though some research has been done on the functional areas in humans, it is still not clear where exactly the boundaries of

these areas are. Some areas that are medial in primates may lie more laterally in humans. It is already clear, however, that the components of the IPS communicates heavily with each other and surrounding cortical areas.

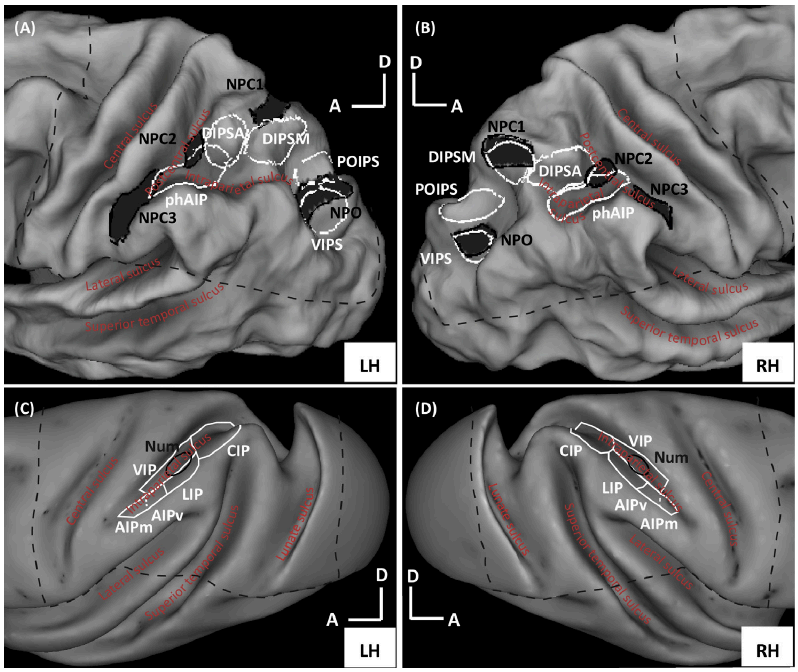

Figure 2.4: The difference in the Macaque and Human IPS in the left and right hemishperes. The image show where the different functional areas are located. (A) and (B) are human IPS; and (C) and (D) are Macaque IPS. Abbreviations of the functional areas mentioned in text: AIP, anterior intraparietal area; CIP (PIP), posterior intraparietal; LIP, lateral intraparietal area; phAIP, putative human AIP; VIP, ventral intraparietal area; VIPS, ventral IPS. (From Harvey *et al.* (2017))

The five functional areas of the IPS are:-

Anterior intraparietal area (AIP)

This 'parietal grasp region' is located in the anterior portion of the IPS on the lateral wall. When, for example, a person is reaching to pick up their car-keys or a pen, the neurons in this area are activated and know the size, shape and location of the object. This area also allows us to feel differences in the 3-D shapes of objects in order to identify them by touch. Therefore we know when we touch an object in our pockets that it is our car-keys. The AIP is regarded as the "parietal grasp region".

Posterior intraparietal area (PIP)

In primates this area is suggested to be located on the lateral bank of the IPS close to the occipital lobe. In humans, however, it is the opposite, the PIP is located on the medial bank. Similarly to the AIP, the PIP analyses the 3-D shape of objects but focusses more on the texture.

Ventral intraparietal area (VIP)

Deep inside the IPS cortex overlapping both the medial- and lateral -walls is the VIP. The VIP is a polymodal network incorporating visual, auditory, vestibular and somatosensory information. This area is important for self-awareness of the space around us. In primates it has been found that the VIP is most active with awareness around the head. In humans activation of the VIP was seen when a person looked at their own hand.

Medial intraparietal area (MIP)

The MIP is suggested to be close to the occipital lobe on the medial wall of the IPS. As the AIP is the 'parietal grasp region', the MIP is the 'parietal reach region'. The MIP aids in controlling and planning of motor movements by the upper limb.

Lateral intraparietal area (LIP)

This area has been extensively researched in primates and in which it lies close to the occipital lobe on the lateral wall of the IPS. However, some studies have shown this area to be on the medial wall in humans rather than the lateral, but certain related tasks still activate the lateral wall in humans. It also appears to be active during saccadic eye movements. When the head is turned a certain way, the LIP monitors the position of the eyes.

2.2.3 Arithmetic

(Dehaene *et al.*, 2003; Fehr, Code and Herrmann, 2007; Dehaene, 2009; Zamarian, Ischebeck and Delazer, 2009; Woods *et al.*, 2015; Peters and De Smedt, 2018)

Basic arithmetic is taught to us from a young age and is the foundation of the mathematics that we use in everyday life, even if we aren't mathematicians by trade. It has also been shown that we have an intuition for basic number sense from infancy. Arithmetic is important in development of children as it has been shown to play a role in their future academic achievement. Both non-symbolic and symbolic arithmetic processes activate the same brain region. Symbolic numerosity as the name suggests refers to how we interpret numbers (such as 5 and 7) and their respective number words (i.e. 'five' and 'seven'). Non- symbolic numerosity involves how we interpret the number objects such as dots or pictures. The parietal lobe and the IPS is known to play a crucial role in number processing. Numerous imaging studies have provided evidence for this. Dehaene and associates (2003) proposed a parietal network consisting of three circuits of how the parietal lobe processes arithmetic tasks. The three circuits were termed: quantity, verbal and attention circuits. Five key parietal regions were identified with each region being important in one of the three circuits. The five regions included

were bilateral posterior superior parietal lobules, the left angular gyrus and bilateral IPS. The left angular gyrus (AG) is part of the verbal system and lies posteroinferior to the IPS. It is more active when one recalls exact calculation tasks such as multiplication tables. The bilateral posterior superior parietal lobules (PSPL) are part of the attention circuit and as the name suggests, this region lies posteriorly on the superior parietal lobule and medial to the IPS. Similar to the IPS's visuospatial functions, the PSPL activates in processes involving grasping and eye-movements, any function that requires attention. Arithmetic tasks involved in number comparison, approximation and subtraction activate the PSPL and the suggested hypothesis is that because this region is active during attentional processes in space, it will be active during attentional number processes too. The bilateral IPS make up the quantity circuit. The quantity system allows us to process basic subtraction, addition, multiplication and number comparison problems with a semantic representation. The IPS has been shown to be particularly active when quantity manipulation of numbers is needed. It also shows more activity when computing subtraction because addition and multiplication can be stored in verbal memory whereas subtraction still requires some quantity processing. Even though studies have shown the right IPS to show greater activation in certain tasks, there is always bilateral activation. Throughout the meta-analysis, Dehaene *et al*., (2003) supplies evidence that the IPS is able to process the quantity that the numbers represent in the language that our brain understands, i.e. "is it a large number, is the distance between two numbers large or small". For this reason, they proposed that there exists a 'number line' in this area, a scale for the semantic representation. Furthermore, this helps us to understand why a highly visuospatial area such as the IPS is active when computing certain arithmetic tasks. Because the IPS can understand and process how far or close certain objects are in the space around us, it is able to process number scales.

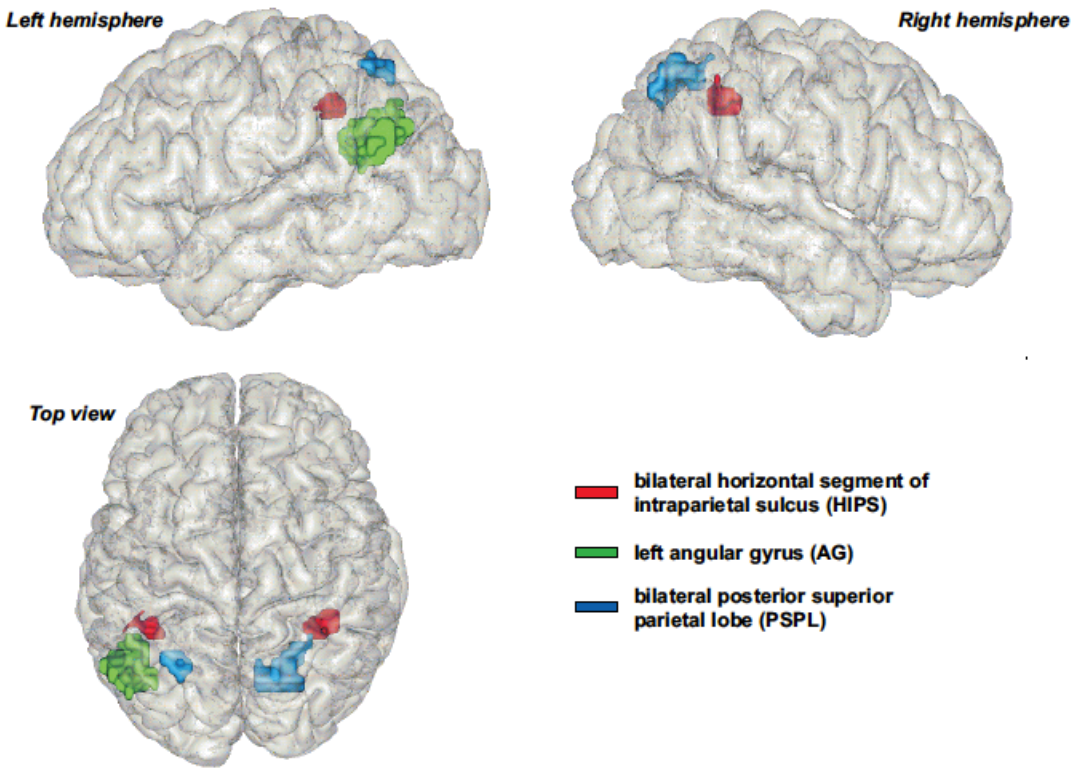

Figure 2.5: The five key parietal regions that make up the quantity, verbal and attention circuits for number processing. (From Dehaene *et al*., (2003))

Deficits in arithmetic may be caused by numerous external or internal factors. The teratogenic effect of alcohol is one factor that can influence an individual's number sense. Research has shown that in children, the IPS had less activation when performing magnitude comparison task with more PAE (Woods *et al*., 2015).

2.3 Neuroimaging

There are many modalities of brain imaging: EEG, SPECT, PET, CAT, to name a few. They allow us to have an insider view of the brain and make discoveries and diagnoses. MRI and fMRI give us a 3D view of the brain and uses sophisticated physics allowing us to identify functional areas important for everyday living. Here we will be looking at MRI and fMRI specifically due to their importance and use in our study. Both MRI and fMRI involve sophisticated physics which is beyond the scope of this thesis. This is brief overview.

2.3.1 Magnetic Resonance Imaging (MRI)

(Schild, 1990; McRobbie *et al.*, 2006; Weishaupt, Köchli and Marincek, 2008; Hashemi and Bradley, 2010)

An easy way to look at MRI may be to define and understand the science of each of the words that make up the term 'Magnetic Resonance Imaging':

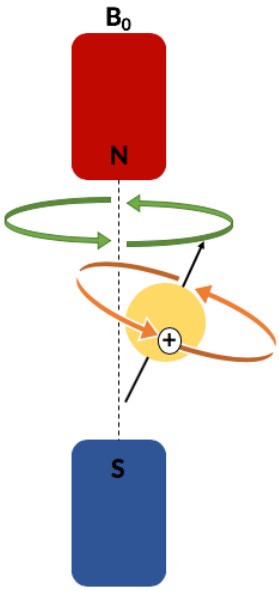

Figure 2.6: Adapted from Schild (1990)

Magnetic

The tissues in our bodies contain a large percentage of hydrogen atoms. These hydrogen (^1H) atoms possess a many qualities, one of which is that they act like little magnets. Each ^1H atom consists of a positively charged proton and a negatively charged electron that orbits around it making the atom electrically neutral. The protons in the nucleus possess 'spin' because they are constantly turning around an axis. It is for this reason that the protons in the nuclei of ^1H acts like magnets, the spin induces electrical current which in turn induces a magnetic field. When an external magnetic field (B_0) is applied to the protons, they will align either parallel or anti-parallel to B_0. While the protons are spinning about their own axis, they will also spin around the axis of B_0, this is called precession.

Resonance

Within an MRI scanner, there are different types of coils. One of the types of coils is called 'radio frequency coils'. As mentioned above, the protons are precessing in the direction of B_0 but we ultimately want to have an image of the tissues and for this the protons are made to align with a secondary energy source that is transverse to B_0. For the protons to absorb the energy from this source, they need to have the same frequency as the radio frequency source. Therefore, a radio frequency pulse (RF) pulse is transmitted to the protons in our body from the coils. This causes them

to align transverse to B_0 and they now move in sync or "in phase". This phenomenon is termed 'resonance'. We therefore have a longitudinal magnetization vector (M_z) which refers to the patient's body becoming a magnetic field and is parallel to B_0. This magnetic force cannot be measured due to the fact that it is parallel to the external magnetic field. The RF pulse thus causes a transversal

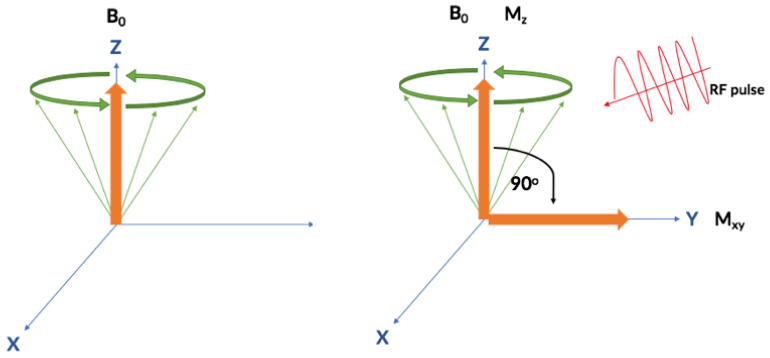

Figure 2.7: Resonance. Adapted from Schild (1990) and Weishaupt et al (2008)

magnetization (M_{xy}) by decreasing M_z.

Imaging

Retrieving the image from the scanner involves 'relaxation'. The precessing protons that were in phase transversely, will now return to their original longitudinal plane where they are precessing with B_0. Relaxation happens when the RF pulse is switched off. M_{xy} is reduced by two independent relaxation processes and they cause the protons to return to a lower energy state from their higher energy state that they were in with the RF pulse. There exist two types of independent relaxation processes because each is helpful in different diagnostic ways. The two processes are: (1) spin-lattice interaction which causes T1 relaxation; and (2) spin-spin interaction which causes T2 relaxation. To understand relaxation, it is helpful to know that different tissues have different densities, i.e. the fat in the myelin in our brain tissue has a different density to bone or CSF and therefore will have a different contrast on the MR image. These densities will appear differently on the image when different relaxation types are measured. It all depends on how the protons 'loose' their energy.

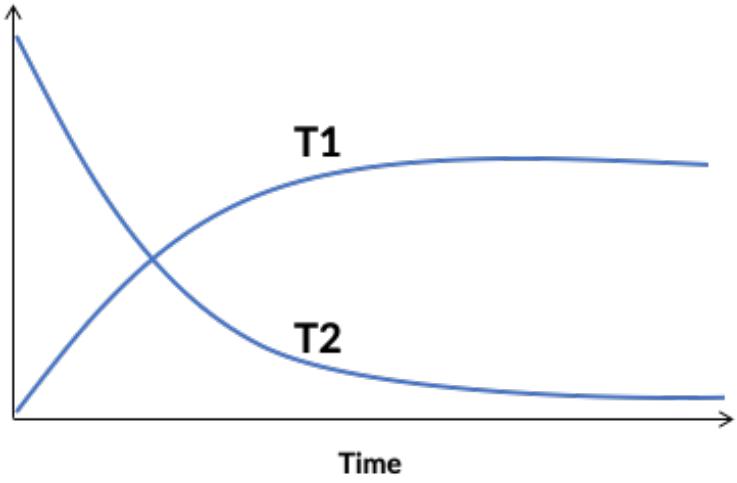

Figure 2.8: T1 and T2 time constants representing longitudinal and transverse relaxation respectively. Adapted from Schild (1990) and Weishaupt et al (2008)

In T1 relaxation, the protons are releasing energy into their surroundings which is why this is termed 'spin-lattice-relaxation'. It should also be noted that not all the protons 'relax' at the same time, it is more of a continuous process. While this gradual decaying of M_{xy} is occurring, M_z is slowly being restored and this is termed 'longitudinal relaxation'. Every relaxation process happens with a time constant for the recovery that is taking place, and in longitudinal relaxation this is T1. T1 is dependent of two factors: (a) the strength of B_0; and (b) the internal motion of the molecules, also known as Brownian motion.

In T1, the protons released energy into the lattice, its surroundings, in T2 (transverse relaxation) the time constants rely on inhomogeneities of the local magnetic field and of B_0. As mentioned above, when the RF pulse is applied, the protons move 'in phase' and therefore have phase coherence. Because the nuclei of the protons possess their own individual magnetic vectors independent from B_0, phase coherence is lost due to the individual magnetic vectors cancelling each other out after excitation. This causes M_{xy} and the MR-signal to eventually disappear which is why this is termed transverse relaxation. T1 and T2 happen at the same time but it should be noted that they are independent of each other.

In short, different tissues have different rates for their protons to return back to B_0 after the RF pulse and this is described by T1 and T2 as explained above. Two types of images are produced according to the relaxation times of the tissues: T1-weighted and T2-weighted images. In order to retrieve the desired MR image with the best contrast needed to view certain tissues, timing values are required and can be set accordingly. These timing values are termed: repetition time (TR); and echo time (TE). After two RF pulses are applied to the desired tissue, TR is the time interval between the excitations.

TE is the time interval between excitation with a pulse and the retrieval of the MR signal. Changing TE and TR will render different image qualities and therefore different weighted images. For instance, a longer TR will lower the effect of T1, and a longer TE will make the effect of T1 stronger. Therefore, a T1-weighted image is produced by both a short TR and TE, and a T2-weighted image is produced by both a long TR and TE. T1- weighted images are helpful when looking at structures of the brain and are more anatomically desired, whereas T2-weighted images are helpful to look at pathologies.

2.3.2 Functional magnetic resonance imaging (fMRI)

(Ogawa *et al.*, 1990, 1990(a); Ogawa *et al.*, 1990(b); Ogawa *et al.*, 1992; Huttenlocher, 2002; Gore, 2003; Jezzard, Matthews and Smith, 2003; Matthews and Jezzard, 2004; Amaro and Barker, 2006; Lindquist, 2008; Logothetis, 2008; Coles and Li, 2011; Poldrack, Nichols and Mumford, 2011; Goebel, 2012; Ogawa, 2012; Soares *et al.*, 2016)

It is impossible to open a person's skull and look at each part of their brain to see the activity. fMRI solves this problem and gives researchers a look at the functions of the structures of the brain. fMRI works on the principle that increased blood flow (therefore oxygen) to a specific area in the brain suggests that the area is being used.

How does fMRI work

Blood oxygenation level dependent (BOLD) fMRI measures the ratio of oxygenated blood to deoxygenated haemoglobin in the blood. BOLD fMRI was discovered in the early nineties by Seiji Ogawa. Erythrocytes are the oxygen carriers of the blood. When a certain activity is performed by the body, the blood vessels in the area of the brain that controls it vasodilates, inviting more blood and oxygen to flow to this area. The body contains ^{1}H which have a magnetic field and will be attracted to the magnet of the MRI machine. Deoxygenated blood causes the ^{1}H to 'spin' out of time, whereas oxygenated blood causes the ^{1}H to spin in sync with each other causing a rise in signal that can be picked up by the scanner. Therefore, if neurons are firing in a particular area, more blood arrives to supply these neurons with oxygen, resulting in a higher MR signal. The change in MR signal due to neuronal activity is described by the hemodynamic response function (HRF) of neuronal activity (figure 2.14). Simply described, after neuronal metabolic activity takes place, there is a brief period of increased blood flow to the area. Then follows an undershoot of blood flow which takes a few seconds to return to the baseline. fMRI has many advantages in that it is non-invasive and provides high spatial resolution. However, fMRI only measures neuronal activity indirectly and has low temporal resolution.

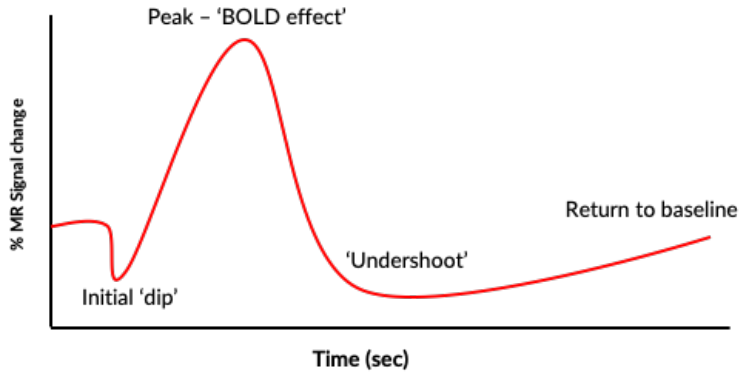

Figure 2.9: The hemodynamic response function (Adapted from Amaro & Barker (2006))

Task-based fMRI?

There are two types of task-based designs in fMRI: block design and event-related design. Only block design will be discussed here because it was the only design used in this study.

As the name suggests, in a block design trials are grouped together into blocks (figure 2.15). Task blocks contain multiple trials of a task which stimulate the processes of interest. However, the task will include aspects not related to the process of interest, such as visual stimuli and motor response. For this reason, task blocks are often alternated with control blocks. The control trials should visually will look the same as the task trials, but lack the process of interest. Additionally, rest blocks are usually included. In this study the task and control blocks were each 40s long and the rest blocks were 20s. The advantage of using a block design is that it has high statistical power. However, if the task block is too long, the subject may get bored, which make is prone to confounders, such as habituation.

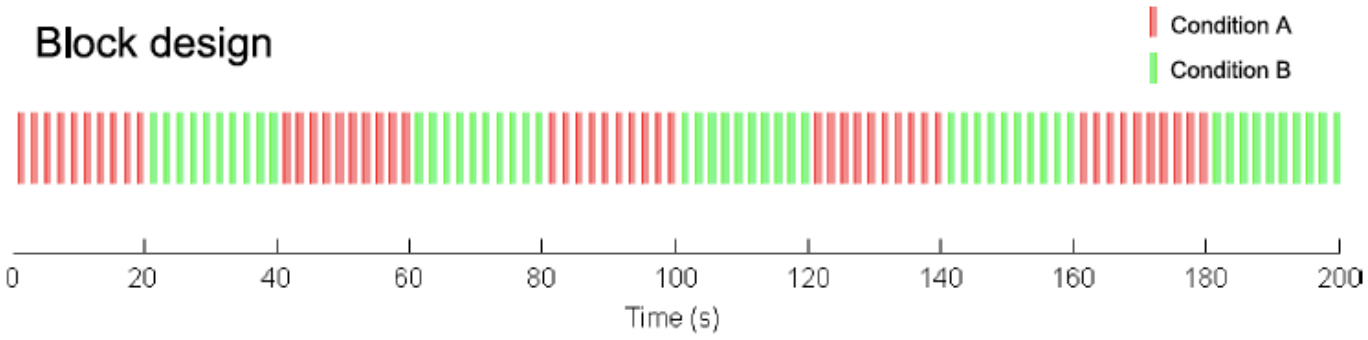

Figure 2.10: An example of a block design for task- based fMRI studies. Condition A is the task and Condition B is rest. (From Lindquist (2008))

Preprocessing

There are many software programs that make the preprocessing of fMRI easy for the user. In this study, the software BrainVoyager QX (Brain Innovation, Maastricht, the Netherlands) was used for all functional analysis. Preprocessing of fMRI data is necessary to prepare the data for the statistical analyses that need to be performed in order to get results.

fMRI measures the same brain volume multiple times across time. Each of the volumes consists out of a number of voxels (roughly 100 000). Each voxel has its own spatial location and has a number associated with it that represents its intensity. Because the same brain volume is measured multiple times and each slice in the volumes are scanned at different times, slice timing correction needs to be done. This is done to make it seem as if all the slices were obtained at the same time. Motion correction takes into account subject motion by aligning each volume to a reference volume. Spatial and temporal smoothing are performed to increase the signal to noise ratio. Once these initial steps have been done, coregistration and normalization are next. Coregistration aligns the structural MR image with the functional one so that the functional data can be visualized over the high resolution structural image. Normalization is done by using aligning the structural data to a template in order to 'normalize' each subject to a standardized template brain, enabling group analyses to be performed. In this case, Talairach alignment was used.

fMRI statistical analysis

The most commonly used approach to statistical analysis in fMRI is the general linear model (GLM). The GLM will ultimately show whether the stimulus created any significant signal changes in the subject's brain. A model of the expected response to the stimulus over time is created, taking into account the HRF. The model of the stimulus is convolved with the HRF to mimic the brain's response to the stimulus. For each voxel, a GLM is used to fit the actual signal to the model. If the expected model fits the fMRI data, it means that the particular part of the brain may be responding to the stimulus.

For this study, a multi-subject region of interest (ROI) analysis was done. In an ROI analysis, only a specified number of voxels in a specific area are analysed which provides for increased statistical power. Therefore, for this study for each subject a GLM was run on each voxel in the ROI, and the results were averaged to give the average activation within the region for that subject.

2.4 Additional details on the methodology of this project

2.4.1 Recruitment of the participants

(Jacobson *et al.*, 2008, 2011)

Participants were 52 right-handed, 9- to 14-year-old children from the same community in Cape Town, South Africa, who formed part of a study aimed at investigating the effects of PAE on brain structure and function during number processing. Within this sample, 15 had been diagnosed with FAS/PFAS, 13 were heavily exposed non-syndromal (HE) and 24 were controls. 20 of the 52 participants form part of a prospective longitudinal study investigating the effects of PAE. The mothers of these children were recruited from an antenatal clinic of a midwife obstetric unit that serves an economically disadvantaged community between July 1999 and January 2002. Mothers were included in the study if they drank on average at least 1.0 oz absolute alcohol (AA) per day (2 standard drinks), or reported at least 2 incidents of binge drinking (5 standard drinks/occasion) during the first trimester of pregnancy. Additionally, women initiating antenatal care were invited to participate if they drank <0.5 oz AA/day and if they did not binge drink during the first trimester. Mothers were excluded from the study if they were younger than 18 years of age and suffered from diabetes, epilepsy, or cardiac problems requiring treatment. Additionally excluded were women who were religiously observant Muslims because their religious beliefs prohibit them from consuming alcoholic beverages. The reason for this exclusion is that the Muslim women would have been disproportionately represented among the controls. Infants were excluded if they presented with major chromosomal anomalies, neural tube defects, seizures, and if they were part of multiple births. The other 32 participants are from a cross-sectional study who were identified by screening children from an elementary school in a rural section of Cape Town where alcohol abuse among local farm workers is high.

2.4.2 Procedure

(Bowman, Stein and Newton, 1975; Sokol *et al.*, 1985; Lanphear, 2000; Jacobson *et al.*, 2002, 2008; Chiodo, Jacobson and Jacobson, 2004)

Both mother and child were transported from their home to our child developmental research laboratory at the Faculty of Health Sciences campus of the University of Cape Town (UCT) by our driver. Each mother completed a written informed consent and each child a written assent. Breakfast,

lunch and snacks were provided for the mothers and children at each of their laboratory visits. Each mother received monetary compensation for every visit and each child was rewarded a small gift. A neuropsychological and a neuroimaging (at Groote Schuur Hospital) assessment was administered on each child for which the examiners where blind regarding the FASD diagnoses. FASD were obvious for some cases and were exceptions. The Wayne State University Human Investigation committee and the UCT Faculty of Health Sciences Human Research Ethics Committee approved the study for human research. (Ethical clearance number from UCT for the study presented in this thesis and for the cohort used: 516/2015)

Mothers were interviewed regarding alcohol consumption during pregnancy using a timeline follow-back approach. Interviews were conducted in the mother's primary language (English or Afrikaans). The volume for each type of beverage consumed each day was recorded and using multipliers proposed by Bowman *et al.*, (1975), the volume was converted to absolute alcohol (AA) (liquor – 0.4, beer – 0.04, wine – 0.2). This could then be averaged providing summary measures of alcohol consumption during pregnancy. Data from the alcohol consumption interviews provide three continuous measures of drinking during pregnancy: average oz AA consumed per day, AA/drinking day (dose/occasion) and frequency of drinking (days/week). Two groups of children were recruited: (1) children whose mothers were heavy drinkers, who consumed at least 14 standard drinks per week (1.0 oz AA/day) on average or engaged in binge drinking (5 or more drinks/occasion) and (2) controls whose mothers abstained or drank only minimally during pregnancy. Number of cigarettes smoked per day was also recorded, as was the use of illicit drugs (days/week). Mothers were also interviewed regarding their education. A venous blood sample was taken from each child to examine the lead concentration in the blood as certain levels could have an effect on cognitive function. H.E. Hoyme, MD, and L.K. Robinson, MD, two U.S.-based FAS dysmorphologists examined each child at a clinic organized in September 2005 for growth and FAS dysmorphology using the Hoyme *et al.*, (2005) protocol. N. Khaole, MD, a Cape Town based dysmophologist, examined the two children who were not able to attend the clinic. Considerable agreement between the examiners was reached on all the dysmorphic features assessed and a consensus on FAS/PFAS diagnosis was reached during a case conference which included the dysmorphologists and SWJ, JLJ and CDM.

2.4.3 Neuropsychological assessment

(Annett, 1970; Sattler, 1992; Kopera-Frye, Dehaene and Streissguth, 1996; Jacobson *et al.*, 2011)

Each child had been previously administered computer-based number processing tests designed by Dehaene, adapted by Jacobson *et al.*, (2011). The assessments contained seven 32-problem subtests: Exact Addition (EA), Exact Subtraction (ES), Exact Multiplication (EM), Proximity Judgment (PJ), Approximate Addition and Approximate Subtraction. The two latter tests were not used in this current study. Before each task the examiner would provide an explanation to the participant on how to complete the task. This was preceded by a practice round consisting of 10 items. An equation was present on the screen for EA, ES and EM (e.g., 2 + 5 = ?) and the participant had to enter their answer on the computer keypad. For the PJ task, a number would appear at the top of the screen with two numbers bellow it. The participant used the mouse to indicate which number was larger. IQ was estimated from 7 of the 10 subtests from the Wechsler Intelligence Scale for Children, Third Edition (WISC-III)—Similarities, Arithmetic, Digit Span, Symbol Search, Coding, Block Design, and Picture Completion—and Matrix Reasoning from the WISC-IV. Sattler's (1992) formula for computing Short Form IQ was used to estimate the IQ of the children using the afore mentioned subtests. Handedness assessment used the Annett (1970) Behavioral Handedness Inventory.

Chapter 3

THE MORPHOLOGY OF THE INTRAPARIETAL SULCUS AND ITS EFFECT ON NUMBER PROCESSING

3.1 Introduction

Prenatal exposure to alcohol has a teratogenic effect on the fetus and may lead to a range of structural and functional consequences including growth retardation and typical facies, as well as mental retardation (Jones and Smith, 1973; Hoyme, 2005). Fetal Alcohol Spectrum Disorder (FASD) is an umbrella term encompassing the range of disorders that may arise as a result of prenatal alcohol exposure (PAE), including fetal alcohol syndrome (FAS), partial FAS (PFAS) and alcohol-related neurodevelopmental disorder (ARND) (Bertrand *et al*., 2005; Hoyme, 2005). FAS was first diagnosed by Jones and Smith (1973) and refers to the most severe diagnosis within FASD. FAS is characterized by a distinctive craniofacial dysmorphology (small palpebral fissures, thin upper lip and flat philtrum), small head circumference, and pre- and/or postnatal growth retardation (Hoyme, 2005). A diagnosis of PFAS requires the presence of at least two of the facial features as well as either small head circumference, retarded growth, or neurobehavioral impairment and confirmation that the mother drank during pregnancy (Hoyme, 2005). A large proportion of exposed children, however, lack the characteristic FAS facial features but may exhibit attention, cognitive and/or behavioural deficits (Hoyme, 2005). Certain communities in the Western Cape Province of South Africa have amongst the highest reported incidence rates of FAS in the world (Croxford and Viljoen, 1999; May *et al*., 2000; Jacobson *et al*., 2006, 2008).

Imaging studies have provided evidence that cortical volume (of different structures and areas in the brain) is significantly affected in children prenatally exposed to alcohol (Rajaprakash *et al*., 2013; Migliorini *et al*., 2015). In particular, the volume (Archibald *et al*., 2001; Lebel *et al*., 2012; Rajaprakash *et al*., 2013; Meintjes *et al*., 2014) and function (Woods *et al*., 2015, 2018; Infante *et al*., 2017) of the parietal cortex appears to be frequently affected. Number processing is a recognized function of a number of areas of parietal cortex including the posterior part of the superior parietal lobule and the intraparietal sulcus (IPS) (Dehaene *et al*., 2003). The IPS is a region in the parietal lobe that plays a critical role in number processing (Cohen and Dehaene, 1995; Naccache and Dehaene, 2001; Dehaene et al., 2003; Menon *et al*., 2000; Isaacs *et al*., 2001) – one of the most sensitive neurocognitive impairments associated with PAE (Streissguth *et al*., 1989, 1994; Kopera-Frye, Dehaene and Streissguth, 1996; Burden *et al*., 2005; Howell *et al*., 2006).

The IPS, first described from chimpanzee brains by neuro-anatomist and -physiologist Sir William Turner, has been a topic of research since the 19th century (Cunningham, 1890). The IPS is a prominent feature in the parietal lobe that runs between the superior parietal lobule (SPL) and the inferior parietal lobule (IPL), providing a horizontal division (Clark, Boutros and Mendez, 2010). The

starting point is the post-central sulcus (PCS) from where it continues posteriorly all the way into the occipital lobe (Clark, Boutros and Mendez, 2010; Rubin and Safdieh, Joseph, 2016). Along its route this sulcus is frequently interrupted and has a variable pattern of branching both on medial and lateral walls. Although studies have attempted to establish a pattern of morphological variation (Cunningham, 1890; Zlatkina and Petrides, 2014), this has yet to be included in atlases used in automated analyses of imaging data.

Studies in macaque monkeys and humans have identified five functional subdivisions, namely, the anterior- (AIP), medial- (MIP), lateral- (LIP), ventral- (VIP), and posterior- (PIP) IPS. (Lewis and Van Essen, 2000b; Grefkes and Fink, 2005). The AIP plays an important role in somatosensory processing (Tunik, Frey and Grafton, 2005; Buxbaum *et al.*, 2007; Pa and Hickok, 2008), while the PIP is more involved in processing of visual signals (Tsutsui *et al.*, 2002; Grefkes and Fink, 2005). Neurons in the medial bank are more involved in arm movements (Connolly, Andersen and Goodale, 2003; Himmelbach *et al.*, 2006), while those in the lateral bank play a greater role in eye movements (Andersen, 1997; Koyama *et al.*, 2004; Ipata, 2006). The VIP contains a somatotopic map and enables the body to navigate in its surroundings (Lewis and Van Essen, 2000a; Schlack, Hoffmann and Bremmer, 2002, 2003; Bremmer, 2005; Graziano and Cooke, 2006). Combined these areas form a multi-modal visuospatial network (Clark, Boutros and Mendez, 2010) that has been linked to number processing (Coull and Frith, 1998; Delazer *et al.*, 2003; Molko *et al.*, 2003; Piazza *et al.*, 2004; Venkatraman, Ansari and Chee, 2005; Ashkenazi *et al.*, 2008; Bugden *et al.*, 2012; Simon *et al.*, 2002; Dehaene *et al.*, 2003; Cohen and Dehaene, 1995; Naccache and Dehaene, 2001; Menon *et al.*, 2000; Isaacs *et al.*, 2001).

In view of the recognised role of the IPS in number sense, we were interested in whether the poorer arithmetic performance observed in children prenatally exposed to alcohol could be related to alterations in the structure or volume of the IPS. Morphometric findings in the parietal lobe following PAE have, however, been inconsistent with some studies showing both grey and white matter volume reductions (Archibald *et al.*, 2001) and others grey matter increases in the left cortex (Sowell *et al.*, 2001). The present study examines the effects of PAE on IPS volume and asymmetry using manual tracing, the relation between IPS volume and number processing performance, and potential moderation by PAE of the relation between IPS volume and number processing performance.

3.2 Methods

3.2.1 Participants

Participants were 52 right-handed, 9- to 14-year-old children from the same community in Cape Town, South Africa, who formed part of a study aimed at investigating the effects of PAE on brain structure and function during number processing (Jacobson *et al.*, 2008; Jacobson *et al.*, 2011). Within this sample, 15 had been diagnosed with FAS/PFAS, 13 were heavily exposed non-syndromal (HE) and 24 were non- or minimally exposed controls. In our study, children with confirmed heavy PAE who lack the facial dysmorphology have been termed non-syndromal heavily exposed (HE). Due to small sample sizes, children with FAS or PFAS were grouped together.

Twenty of the 52 participants were from our prospective longitudinal cohort (Jacobson *et al.*, 2008). The mothers of these children were recruited from an antenatal clinic of a midwife obstetric unit that serves an economically disadvantaged community between July 1999 and January 2002. Mothers were included in the study if they averaged at least 1.0 oz absolute alcohol (AA) per day (2 standard drinks), or reported at least 2 incidents of binge drinking (5 standard drinks/occasion) during the first trimester of pregnancy. Additionally, women initiating antenatal care were invited to participate if they drank <0.5 oz AA/day and if they did not binge drink during the first trimester. These women were the mothers of the control children. Mothers were excluded from the study if they were younger than 18 years of age and suffered from diabetes, epilepsy, or cardiac problems requiring treatment. Infants were excluded if they presented with major chromosomal anomalies, neural tube defects, seizures, or if they were part of a multiple-gestation pregnancy. For children from this cohort, prospective alcohol exposure data are available from timeline follow-back interviews (Jacobson *et al.*, 2002) conducted with the mothers during pregnancy.

The other 32 participants were from our cross-sectional cohort who were identified by screening children from an elementary school in a rural section of Cape Town where there is a high level of alcohol abuse among local farm workers (Jacobson et al., 2011). Two groups of children were recruited: (1) children whose mothers were heavy drinkers during pregnancy consuming at least 14 standard drinks per week (1.0 oz AA/day) on average or engaged in binge drinking (5 or more drinks/occasion), and (2) controls whose mothers abstained or drank only minimally during pregnancy (≤2 drinks per occasion).

3.2.2 Procedure

Mothers and children were transported to the Child Development Research Laboratory at the Faculty of Health Sciences campus of the University of Cape Town (UCT) by our driver, and on a separate day to the Cape Universities Brain Imaging Centre (CUBIC) at Tygerberg Hospital. Each mother completed a written informed consent and each child a written assent. Breakfast, lunch and snacks were provided for the mothers and children at each of their visits. Each mother received monetary compensation for every visit and each child a small gift. Neuropsychological and neuroimaging assessments were administered to each child by examiners who were blind regarding the FASD diagnoses, except in a small subset of the cases where the FAS diagnosis was obvious from facial features. Ethics approval for the study was obtained from the Wayne State University Human Investigation committee and the UCT Faculty of Health Sciences Human Research Ethics Committee.

3.2.3 Neuropsychological assessment

Each child had previously been administered computer-based number processing tests designed by Dehaene (Kopera-Frye, Dehaene and Streissguth, 1996), adapted by Jacobson et. al. 2011, including a 32-problem Proximity Judgement (PJ) subtest. During this test, a number appeared at the top of the screen with two numbers below it, and the participant used the mouse to indicate which of the bottom numbers was closer to the number at the top. IQ was estimated from 7 of the 10 subtests from the Wechsler Intelligence Scale for Children, Third Edition (WISC-III)—Similarities, Arithmetic, Digit Span, Symbol Search, Coding, Block Design, and Picture Completion—and Matrix Reasoning from the WISC-IV. Sattler's (1992) formula for computing Short Form IQ was used to estimate the IQ of the children using the aforementioned subtests. Handedness assessment used the Annett (1970) Behavioral Handedness Inventory.

3.2.4 Neuroimaging assessment

Magnetic resonance imaging protocol

All children completed neuroimaging on a 3T Allegra MRI scanner (Siemens Medical Systems, Erlangen, Germany) using the single channel head coil. High-resolution anatomical images for the 32 participants of the cross-sectional cohort were acquired in the sagittal plane using a magnetization prepared rapid gradient echo (MPRAGE) sequence (TR 2300 ms, TE 3.93 ms, TI 1100 ms, 160 slices, flip angle 12°, 1.3 × 1.0 × 1.0 mm^3, 6.03 min). The high-resolution T1 weighted images of the participants from the longitudinal cohort were acquired using a volumetric navigated (Tisdall *et al.*, 2012) multi-echo magnetization prepared rapid gradient echo (MEMPRAGE) (van der Kouwe *et al.*, 2008) sequence (FOV 256 mm × 256 mm, 128 sagittal slices, TR 2530 ms, TE 1.53/3.21/4.89/6.57 ms, TI 1100 ms, flip angle 7°, 1.3 × 1.0 × 1.3 mm^3, 8.07 min).

3.2.5 MRI analysis

The IPS was manually traced and volumes generated using MultiTracer java-based software (Woods, 2003). A protocol for manually tracing the cortex volume of the IPS was developed by CW and MG (Figure 3.1). The protocol comprised two parts for each hemisphere: (1) tracing all the medial walls of the IPS (MIPS) and (2) tracing the entire sulcus by adding the lateral wall (LIPS). The volume of the LIPS was calculated by subtracting the volume of the MIPS from the total sulcal volume.

On sagittal and axial planes the postcentral and parieto-occipital sulci were identified to delimit the anterior and posterior boundaries of the parietal portion of the IPS (Figure 3.1 a, b and e). The occipital portion was excluded. The IPS was first traced on the axial sections as the patterns and branches were more clearly visible (Figure 3.1 c). These tracings were then used to guide the tracing on the coronal sections. Tracings on coronal sections were used to compute volumes. A prominent medial branch was consistently present posteriorly for the MIPS and was included in the measurements (Figure 3.1 d). Other sulci from the superior parietal lobule (SPL) that joined the MIPS in a few cases were excluded. All sulci branching from the LIPS into the inferior parietal lobule (IPL) were excluded. We compare volumes of two regions of interest (ROI) in each hemisphere: left and right MIPS, and left and right LIPS.

3.2.6 Statistical analyses

Statistical analyses were performed using SPSS (version 25, IBM). All variables were normally distributed. The following variables had outliers greater than 3 SD beyond the mean, which were recoded to one unit greater than the next highest value (Winer, 1971): cigarettes per day (*n*=1), lead exposure (*n*=1), AA/occasion (*n*=1) and proportional drinking days (*n*=2). AA/day was positively skewed and was log transformed.

Seven control variables were considered and assessed as potential confounders: total intracranial volume (TIV; mm^3), age at scan (years), sex of child, MRI sequence used, socioeconomic status (Hollingshead, 2011), lead exposure (µg/dl) and maternal cigarette use during pregnancy (number of cigarettes smoked per day).

Analyses of the data included examining the differences in ROI volumes between exposure groups (FAS/PFAS, HE, controls), associations of alcohol exposure measures with ROI volumes, and whether alcohol moderates the relationship between regional IPS volume and math performance. One-way ANOVA was used to examine group differences and ANCOVA to control for potential confounders. To examine specifically whether observed group differences were attributable to smoking or

reductions in total brain volume, we first controlled separately for smoking and TIV only. Analyses were then repeated in regions showing group differences controlling for all potential confounders associated with the dependent variables at $p < 0.10$.

Associations between ROI volumes and measures of alcohol exposure were examined using linear regression. In regions showing association, multiple regression was used to control separately for TIV, and for potential confounding variables weakly associated with the outcome ($p < 0.10$).

Potential effects of alcohol exposure on brain asymmetry were examined by comparing volumes of each region between left and right hemispheres within each group separately. Finally, in each region we examined associations between ROI volumes and math performance on the PJ, WISC Arithmetic. Scaled Score and WISC Digit Span tasks. Multiple regression was used to control for effects of alcohol exposure and to examine interaction effects.

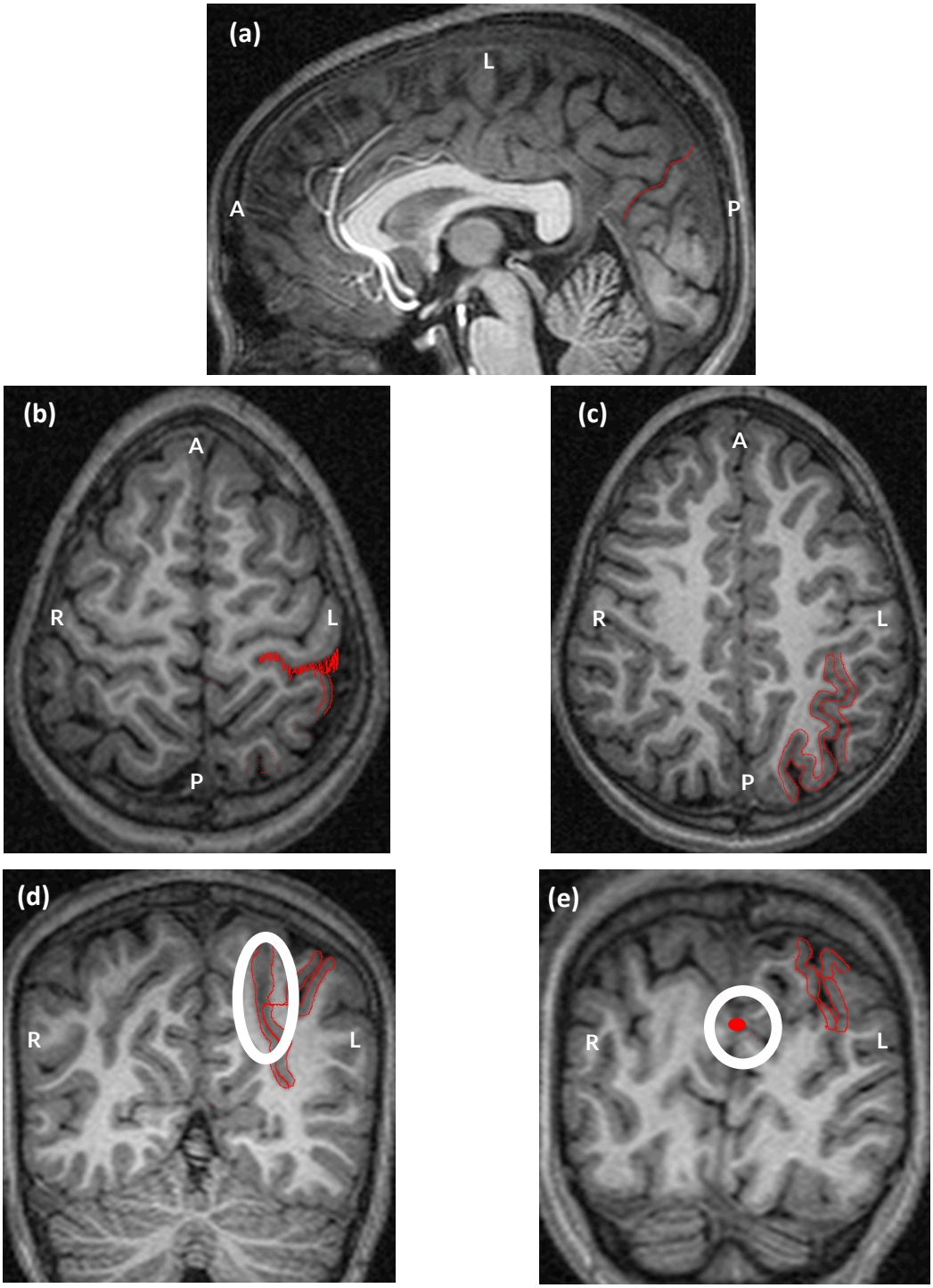

Figure 3.1: The protocol for manually parcellating the IPS shown on the left hemisphere of a FAS/PFAS subject. Both the MIPS and LIPS are traced. **(a)** On the sagittal plane the parieto-occipital sulcus was identified to indicate the end of the parietal portion of the IPS. **(b)** On the horizontal planes the postcentral sulcus was identified indicating the start of the IPS and **(c)** further tracings on this plane identified the pattern of the sulcus. **(d)** The IPS could finally be traced on the coronal sections and a medial branch was always present near the end of the parietal portion. **(e)** The tracings on the sagittal slice were visible on the coronal planes and clearly indicated the parietal border of the IPS.

3.3 Results

3.3.1 Sample characteristics

Table 3.1: Sample characteristics

	Alcohol exposed					
	FAS/PFAS	**HE**	**Control**	**Total**		
	(*n*=15)	**(*n*=13)**	**(*n*=24)**	**(*N*=52)**	***F* or χ2**	***p***
Child						
Sex: *n* = Male (%)	8 (15.4)	6 (11.5)	12 (23.1)	26 (50.0)	0.144	0.931
Child age (yr) at scan	10.9 (1.1)	11.4 (0.9)	11.2 (1.1)	11.2 (1.1)	0.619	0.543
Total Intracranial Volume (x 10^6mm^3)(TIV)[a]	1.29 (0.17)	1.43 (0.15)	1.53 (0.14)	1.43 (0.18)	10.952	**<0.001**
WISC IQ[b]	64.5 (8.4)	65.3 (10.9)	75.6 (1.0)	69.8 (11.0)	7.735	**0.001**
Blood lead concentration (µg/dl)[c]	10.4 (6.3)	7.9 (4.0)	6.4 (2.1)	7.9 (4.4)	4.374	**0.018**
Math scores						
Proximity judgment[#]	13.7 (3.1)	12.4 (3.5)	14.8 (1.3)	13.8 (2.8)	2.965	0.062
WISC Arithmetic Scaled Score	6.0 (2.4)	6.0 (2.6)	7.9 (3.1)	6.9 (2.9)	2.940	0.062
WISC Digit Span Scaled Score	7.1 (3.2)	7.2 (2.4)	7.9 (2.6)	7.9 (2.6)	0.473	0.626
Maternal						
Education (yr)[*]	7.9 (3.0)	8.1 (2.1)	8.9 (1.8)	8.4 (2.3)	1.253	0.295
Mother's age at delivery (yr)	28.1 (7.8)	25.5 (5.1)	27.4 (4.7)	27.2 (5.8)	0.738	0.483
Socio-economic status (SES)[♣]	17.1 (6.89)	19.7 (10.38)	20.8 (8.86)	19.5 (8.73)	0.802	0.454
Maternal substance use during pregnancy[∃]						
Absolute alcohol/day (oz)[d]	2.1 (2.7)	1.6 (1.3)	0.002 (0.01)	0.1 (1.8)	8.854	**0.001**
Absolute alcohol/occasion (oz)[e]	4.5 (2.3)	5.4 (3.7)	0.1 (0.3)	2.7 (3.3)	31.467	**<0.001**
Frequency (days/week)[f]	2.5 (2.0)	1.9 (1.0)	0.01 (0.1)	1.2 (1.6)	26.149	**<0.001**
Cigarettes/day[g,h]	8.3 (5.7)	10.6 (2.2)	3.7 (8.5)	6.8 (8.1)	3.827	**0.029**

All variables are Mean(SD). Bold print denotes significance at $p \leq 0.05$. FAS = fetal alcohol syndrome. PFAS = partial fetal alcohol syndrome. HE = nonsyndromal heavy alcohol exposed. WISC = Wechsler Intelligence Scale for Children. 1 oz absolute alcohol ≈ 2 standard drinks. [*]Of *N*=52, 48 primary caregivers were the biological mothers of the children: 2 (HE) were the fathers, 1 (Control) was the grandmother, and 1 (FAS/PFAS) was another relative. [♣]Hollingshead (2011) Four Factor Index of Socio Economic Scale. [#]Missing for 7 control children (*N*=45). [∃]One mother of a FAS child used Marijuana 0.87 days/month during pregnancy. [a]FAS/PFAS<Controls (p<0.001), [b]FAS/PFAS<Controls (p=0.004); HE<Controls (p=0.01), [c]FAS/PFAS>Controls (p=0.013), [d]FAS/PFAS>Controls (p=0.001), HE>Controls (p=0.016), [e]FAS/PFAS, HE>Controls (p<0.001), [f]FAS/PFAS, HE>Controls (p<0.001), [g]HE>Controls (p=0.032). [h]Average computed using all mothers, including those who did not smoke.

Sample characteristics are shown in Table 3.1. There was no difference between groups in sex, age, maternal age, maternal education or socioeconomic status. Children with FAS/PFAS had smaller TIV and higher blood lead concentrations than controls, and children in both alcohol exposed groups had lower WISC IQ scores than controls. Mothers of children in the HE group smoked more heavily than controls. All but two mothers of the control children abstained from drinking: one drank 2 standard alcoholic beverages on one occasion, and the other drank 2 standard alcoholic beverages about once every month. Although the mothers of children with FAS/PFAS on average drank fewer drinks per occasion than mothers of children with HE (9 standard drinks compared to 10.8), mothers of the

FAS/PFAS children drank more frequently (2.5 days per week compared to 1.9). Although not significant, children in both alcohol exposed groups tended to have lower WISC Arithmetic Scaled Scores than controls (FAS/PFAS < controls, p = 0.111; HE < controls, p = 0.133). While FAS/PFAS children performed similarly to controls on PJ (Tukey p=0.5), HE children performed more poorly (Tukey p = 0.049).

3.3.2 Relation of PAE with IPS volumes

Table 3.2: Associations of volumes with potential confounders (N = 52)

	TIV		IMAGING SEQUENCE#		AGE AT SCAN		SEX OF CHILD#		SES		CIG/DAY*		LEAD EXPOSURE*	
	r	*p*	*r*	*P*	*r*	*p*	*r*	*p*	*r*	*p*	*r*	*p*	*r*	*p*
Left MIPS	0.383	**0.005**	0.105	0.460	-0.179	0.204	0.014	0.919	0.041	0.774	-0.242	**0.083**	-0.171	0.225
Right MIPS	0.271	**0.052**	0.082	0.561	-0.164	0.246	-0.004	0.976	-0.11	0.436	0.022	0.879	-0.050	0.725
Left LIPS	0.260	**0.062**	0.311	**0.025**	-0.051	0.719	-1.852	**0.070**	-0.072	0.610	-0.179	0.204	-0.223	0.112
Right LIPS	0.223	0.112	0.224	0.110	-0.147	0.299	0.079	0.580	-0.047	0.742	0.037	0.796	-0.049	0.728

Values are Pearson correlation coefficients. #For categorical variables, point biserial correlation was used.*One outlier (>3SD beyond the mean) recoded to 1 unit higher than next highest value.

Table 3.2 shows the associations of volumes in each region with potential confounders. TIV was related to 3 of the 4 ROI volumes, but imaging sequence, smoking and sex each showed association with 1 ROI volume only.

Table 3.3: Comparison of volumes by FASD diagnosis (N = 52)

	GROUP MEANS											
	FAS/PFAS (n=15) Mean (SD)	HE (n=13) Mean (SD)	CONTROL (n=24) Mean (SD)	*F*	*P*	F^1	P^1	F^2	P^2	F^3	P^3
Left MIPS[c]	5457.77 (1168.47)	6127.99 (995.3)	6527.71 (1529.56)	3.053	**0.056**#	2.205	0.121	0.603	0.552	0.555	0.578
Right MIPS	5799.63 (940.91)	5645.06 (2016.36)	6303.42 (1368.5)	1.045	0.359						
Left LIPS[a,b]	2871.29 (669.64)	3647.76 (1023.35)	3757.67 (941.39)	4.854	**0.012***	4.253	**0.020**	2.896	**0.065**	2.645	**0.082**
Right LIPS	2668.24 (726.1)	2915.44 (1038.1)	3210.74 (1071.53)	1.463	0.241						

Controlling for [1]Cig/day, [2]TIV, [3]TIV and: [a]Imaging sequence, [b]Sex of child, [c]Cig/day. *Post Hocs* (reflecting main effects): #FAS/PFAS<Controls (p=0.044), *FAS/PFAS<Controls (p=0.011).

Although left MIPS and left LIPS were smaller in children with FAS/PFAS than controls, differences in left MIPS did not survive after control for smoking or TIV, separately or combined (Table 3.3). By contrast, left LIPS volume was significantly smaller in the FAS/ PFAS group following control for smoking, and remained smaller, albeit below conventional levels of significance, after adjustment for

potential confounding by TIV, imaging sequence and sex. Figure 3.2 shows group means and 95% confidence intervals for the left LIPS and MIPS.

Table 3.4: Associations of volumes with level of prenatal alcohol exposure (*N* = 52)

	Absolute alcohol/day (oz)		Absolute alcohol/occasion (oz)#		Proportional drinking days+					
	r	*P*	*r*	*p*	*r*	*p*	β^1	p^1	β^2	p^2
Left MIPS	-0.130	0.360	-0.117	0.407	-0.155	0.273				
Right MIPS	-0.073	0.609	-0.102	0.470	-0.068	0.632				
Left LIPS[a,b]	-0.137	0.333	-0.044	0.757	-0.237	**0.090**	-0.156	0.303	-0.215	0.148
Right LIPS	-0.063	0.655	-0.104	0.463	-0.076	0.590				

#One and +two outliers (> mean + 3SD) were recoded to 1 unit higher that the next highest value. *r* : Pearson correlation. β: Standardized regression coefficient after adjustment for [1]TIV, [2]TIV and: [a]Imaging sequence, [b]Sex of child

While none of the regions showed association of volume with level of alcohol exposure per day or per occasion, higher frequency of drinking was weakly associated with smaller volumes of the left LIPS, an effect that did not survive after control for confounders (Table 3.4).

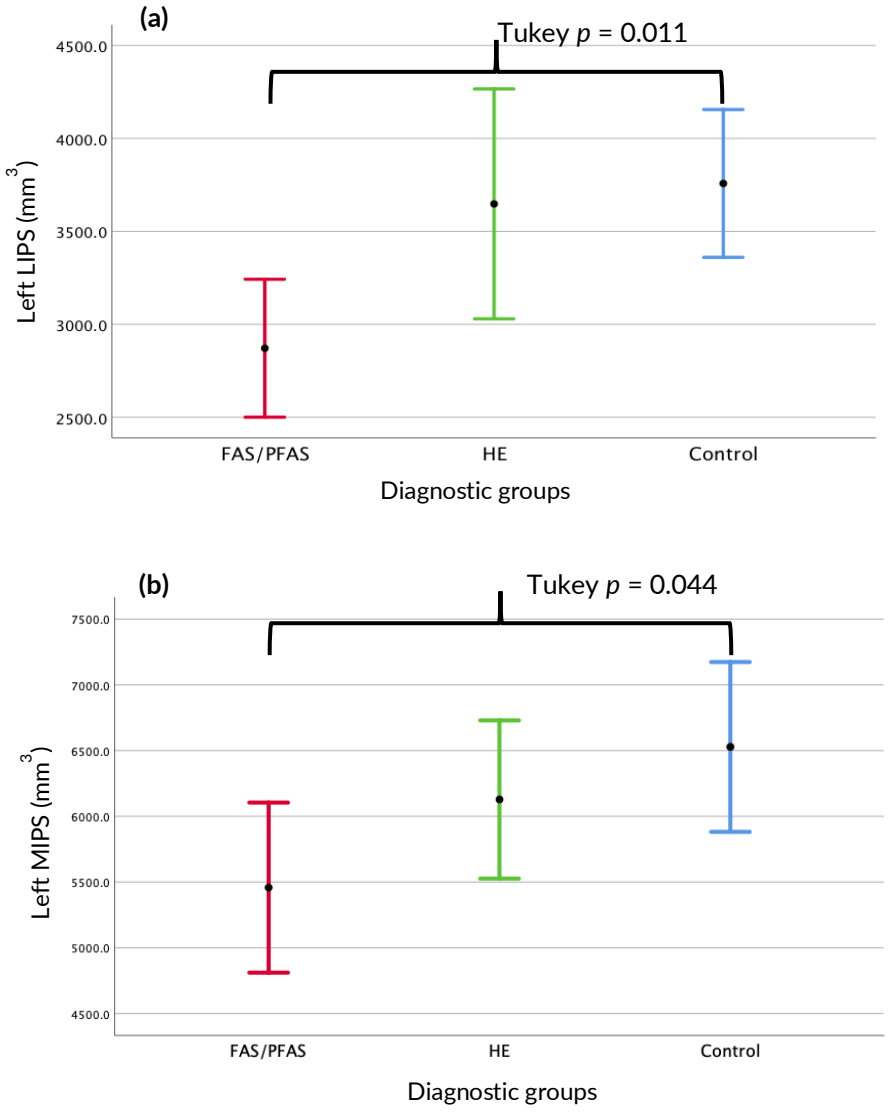

Figure 3.2: (a) Comparison of the left lateral (L) IPS volumes -and **(b)** comparison of the left medial (M) IPS volumes -by diagnostic group (mean ± 95%) CI).

Table 3.5: Comparison of hemispheric asymmetry by FASD diagnosis (*N* = 52)

	FAS/PFAS (*n*=15)			HE (*n*=13)			CONTROL (*n*=24)		
	Mean (SD)	***t***	***p***	**Mean (SD)**	***t***	***p***	**Mean (SD)**	***t***	***p***
Left MIPS	5457.77 (1168.47)	-1.452	0.168	6127.99 (995.3)	1.221	0.246	6527.71 (1529.56)	0.952	0.351
Right MIPS	5799.63 (940.91)			5645.06 (2016.36)			6303.42 (1368.5)		
Left LIPS	2871.29 (669.64)	1.123	0.280	3647.76 (1023.35)	2.102	**0.057**	3757.67 (941.39)	2.533	**0.019**
Right LIPS	2668.24 (726.1)			2915.44 (1038.1)			3210.74 (1071.53)		

Table 3.5 shows the comparison of volumes between the left and right hemispheres within each diagnostic group. While the MIPS demonstrated no volume asymmetry in any of the groups, the volume of the left LIPS was significantly greater than the right LIPS in the HE and control groups, but not in children with FAS/PFAS.

Table 3.6: Relations between math performance and regional IPS volumes

		Left MIPS			Right MIPS			Left LIPS			Right LIPS		
	N	***r* (*p*)**	**β^1 (*p*)**	**β^2 (*p*)**	***r* (*p*)**	**β^1 (*p*)**	**β^2 (*p*)**	***r* (*p*)**	**β^1 (*p*)**	**β^2 (*p*)**	***r* (*p*)**	**β^1 (*p*)**	**β^2 (*p*)**
Proximity judgement*	**45**	-0.16 (0.311)	-0.18 (0.200)	-0.20 (0.147)	0.05 (0.736)	-0.06 (0.647)	-0.06 (0.669)	**-0.25 (0.098)**	**-0.27 (0.051)**	-0.22 (0.106)	-0.03 (0.833)	0.04 (0.783)	-0.08 (0.569)
WISC Arithmetic scaled score	**52**	**0.35 (0.012)**	**0.30 (0.020)**	**0.28 (0.027)**	**0.30 (0.029)**	**0.27 (0.031)**	**0.27 (0.031)**	0.04 (0.806)	-0.03 (0.859)	-0.03 (0.851)	0.02 (0.868)	-0.03 (0.850)	<0.01 (0.975)
WISC Digit span scaled score	**52**	0.16 (0.272)	0.12 (0.378)	0.11 (0.446)	0.132 (0.350)	0.11 (0.412)	0.11 (0.418)	0.06 (0.690)	0.02 (0.884)	0.02 (0.906)	<0.01 (0.993)	-0.016 (0.909)	-0.13 (0.390)

*One outlier (>3SD beyond the mean) recoded to 1 unit higher than next highest value. *r* : Pearson correlation. β^1: Standardized regression coefficient after adjustment for the degree of alcohol exposure (AA/day (oz)), β^2: Standardized regression coefficient after adjustment for AA/day (oz) and potential interaction effects.

Increasing volumes of both the left and right MIPS were associated with higher WISC Arithmetic Scaled Scores (Table 3.6, Figure 3.3a, b). Both of these associations remained significant after adjustment for AA/day (oz) and potential interaction effects. By contrast, increasing left LIPS volumes showed weak association with poorer performance on PJ (Figure 3.3c). No regions showed association with WISC digit span scores.

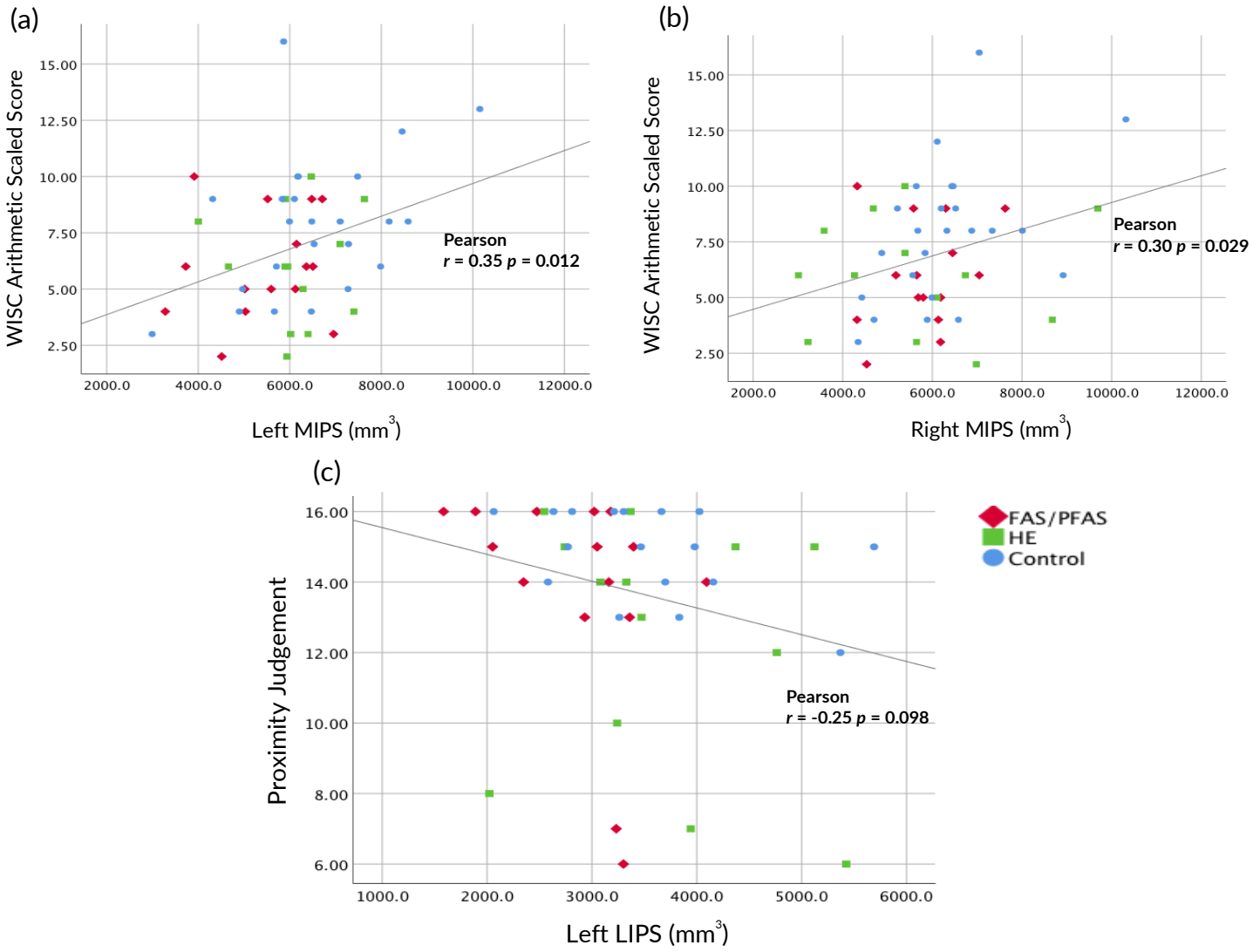

Figure 3.3: Associations of (a) WISC Arithmetic Scaled scores with left medial IPS (MIPS) volumes; **(b)** WISC Arithmetic Scaled scores with right MIPS volumes; and **(c)** Proximity judgement scores with left lateral (L) IPS volumes.

3.4 Discussion

In this study we developed a protocol for manual parcellation of the IPS to investigate potential effects of PAE on the volume of the IPS, and to determine whether alterations in IPS volume play a role in number processing deficits observed in PAE (Meintjes *et al.*, 2010; Woods *et al.*, 2015). Our results show that both the MIPS and LIPS of the left IPS are smaller in children with FAS/PFAS than in control children. While reductions in the left MIPS were, however, not disproportionate to the overall reductions in brain size seen in children with FAS/PFAS, the left LIPS remained smaller even after adjustment for smaller overall brain size. Our results show that left LIPS size is impacted more by how frequently the mother drank during pregnancy than the amount of alcohol she consumed. Notably, the larger volumes of the left LIPS compared to the right seen in HE and control children, were not evident in children with FAS/PFAS, which may account for volume reductions seen in these children in this region. Bilaterally, larger volumes of the MIPS were associated with better performance on the WISC Arithmetic scales, while larger LIPS were associated with poorer PJ.

Although numerous studies have examined effects of PAE on brain volumes (for a review see Lebel, Roussotte and Sowell, 2011), none have focused specifically on the IPS. Our results extend findings from Archibald *et al*. (2001) of parietal lobe reductions in 11- to 13-year-old children with FAS to a specific structure. Similar to Sowell *et al*. (2001) who found structural abnormalities in PAE individuals aged 8 - 22 years predominantly in the *left* posterior temporo-parietal cortices, we found *only* the left IPS to be smaller in children with FAS/PFAS. Although both the MIPS and LIPS were smaller, decreasing volumes of the MIPS were related to increased maternal smoking during pregnancy and alcohol effects in this region did not survive after adjustment for smoking. Prenatal exposure to nicotine has been associated with reduced brain volumes of the frontal lobe and cerebellum (Ekblad *et al.*, 2010), as well as increased activity in the left SPL during tasks involving working memory (Longo *et al.*, 2014).

Our observation of reduced volume in the left LIPS raises the question as to which of the functional domains of the IPS could be affected. The functional areas of the IPS that extend onto the LIPS include the AIP (anterior part of the LIPS), LIP (lies near the occipital lobe on the LIPS and MIPS), and VIP (lies deep in the sulcus and stretches over both the LIPS and MIPS) (Culham and Valyear, 2006). The LIP – a region that has been extensively studied in primates but is less understood in humans – is hypothesised to be involved in saccadic eye movements (Koyama *et al.*, 2004). Since our tracing protocol excluded the occipital region of the IPS, our finding of smaller LIPS volume may not point to deficits in saccadic eye movements. In contrast, the AIP, which overlaps significantly with the LIPS

where we see volume reductions, plays a role in goal-directed movements for grasping objects (Tunik, Frey and Grafton, 2005). In addition to well documented effects of PAE on motor abilities and development (Kalberg *et al.*, 2006), deficits in isometric force have been reported in children prenatally exposed to alcohol when conducting fine motor movements like grasping (Simmons *et al.*, 2012).The VIP, which like the LIP has mainly been studied in primates, has been suggested to be functionally similar in humans (Bremmer *et al.*, 2001; Cooke *et al.*, 2003; Beck *et al.*, 2015). The VIP is suggested to be a polymodal network of neurons that incorporates vestibular, visual, auditory and touch stimuli and creates a sense of self-awareness in the space around you to act on the mentioned stimuli (Bremmer *et al.*, 2001; Beck *et al.*, 2015). PAE individuals have been shown to perform similarly to control subjects in a task of spatial navigation, which may rely on activation of the VIP (Hamilton *et al.*, 2003). Those findings and the fact that the VIP lies deep in the IPS and only a small portion may overlap the LIPS, suggests that this area is probably not functionally affected by reduced volume of the LIPS. The five functional areas in the IPS have not, to our knowledge, been directly studied in subjects with PAE, and may be a promising avenue for future research.

The role of the IPS in arithmetic is well-established (Cohen and Dehaene, 1995; Menon *et al.*, 2000; Isaacs *et al.*, 2001; Naccache and Dehaene, 2001; Dehaene *et al.*, 2003). Localizing the exact areas within the IPS involved in arithmetic could aid in better understanding the impact of the PAE-related structural alterations on mathematical abilities. In our study, both the left- and right MIPS volumes were associated with WISC arithmetic scores, but not the LIPS. Associations remained essentially unchanged after adjustment for degree of alcohol exposure and potential interaction effects. Five key parietal areas for number processing have been suggested, including the left and right posterior superior parietal lobule (PSPL) and the IPS, with its anterior portion being most active during interpretation of magnitude (Dehaene *et al.*, 2003). The location of the PSPL delineated by Dehaene *et al.*, (2003) and used by Woods *et al.*, (2015) in fMRI studies of number processing, corresponds neuroanatomically with the medial branch of the MIPS in the current study. The PSPL is activated during certain arithmetic calculations such as counting (Piazza *et al.*, 2003) and number comparison (Pinel *et al.*, 2001). Since the PSPL and anterior portion of the IPS make up most of our MIPS volumes, it is not surprising that children with larger MIPS volumes performed better on the WISC arithmetic assessments. The observed association of larger left LIPS volumes with poorer PJ performance requires further investigation. This finding may be artefactual due to the extremely simplified nature of the PJ task and the concatenated range of scores.

During the process of manual tracing, extreme inter-subject variations were observed in the branching patterns and shapes of the sulcus between hemispheres. Interhemispheric asymmetry

observed in the LIPS volume in controls and HE children was not seen in children with FAS/PFAS, or in the MIPS in any of the diagnostic group. Structural asymmetry is known to be typical in healthy brains (Watkins, 2001). Although PAE-related changes in typical asymmetry have been reported previously (Sowell *et al.*, 2002), the asymmetry of the IPS has not been studied.

A limitation in this study was the small group sizes of the FAS/PFAS and HE children, which were both smaller than the control group. Two MRI sequences (MPRAGE for n = 32; and MEMPRAGE for n = 20) were used for the subjects which may have altered the MR images slightly and could have affected the volume results. This was, however, accounted for by including imaging sequence as a potential confounder. The simplified PJ task resulted in many participants across groups achieving 100% leading to a concatenated range of scores. Since the children in our cohort were also recruited from an educationally and socio-economically deprived community, our findings may not be representative of children raised in less deprived areas. Strengths of the current project included the use of the timeline follow-back approach that allowed the researchers to examine dose dependent effects, and manual tracing allowing an expert neuro-anatomist to make informed decisions related to branching and structural variations.

This study designed a protocol for manual parcellation of the IPS and applied it to examine effects of PAE. In contrast to other studies that examined volumes of the parietal lobe as a whole, our study examined the volume of the IPS specifically. The left IPS was found to be smaller in children with FAS/PFAS, with reductions in the lateral wall remaining significant after adjustment for overall reductions in brain size and potential confounding. This volume reduction results in loss of the LIPS asymmetry seen in controls and HE children. Bilaterally, increasing MIPS volumes were associated with better WISC arithmetic performance.

Chapter 4

COMPARING MANUAL AND AUTOMATED PARCELLATION MODALITIES ON THE INTRAPARIETAL SULCUS IN CHILDREN PRENATALLY EXPOSED TO ALCOHOL

4.1 Introduction

Measuring the volume of brain structures provides a strategy to identify areas compromised by pathological processes. Magnetic Resonance scanning creates a window through which we can examine and quantify the structures with minimal risk in living subjects. The volumes of the structures can be measured using a variety of methods.

In manual segmentation, an anatomical protocol is defined for a structure that is hand-traced slice by slice. The tracing is performed by trained personnel who has in-depth knowledge of the structures involved. The advantage of manual segmentation is that throughout the tracing procedure, an expert is defining the boundaries. For this reason, manual tracing is regarded as "the gold standard" (Mikhael et al., 2019). The primary disadvantage is the labour and time involved. Automated techniques are thus more commonly used, especially for large datasets (Morey *et al.*, 2009). Automated programmes make use of previous manually-traced brains where a template is created from the defined regions. The regional boundaries are usually defined according to an atlas (Fischl *et al.*, 2004; Desikan *et al.*, 2006; Destrieux *et al.*, 2010; Klein and Tourville, 2012). The programme then automatically separates the image into defined areas. The advantage of this method is that it is much quicker and less labour-intensive than manual tracing. It does not require the involvement of expert neuroanatomists, and the results are thoroughly reproduceable. The primary disadvantage is that the structures may be incorrectly delineated which may lead to some doubt as to the validity of the volumes generated (Mikhael, Hoogendoorn, Valdes-Hernandez, & Pernet, 2018; Mikhael et al., 2019).

Some subcortical structures, such as the caudate nucleus or corpus callosum, are easily identified and defined. Areas of cerebral cortex, however, provide particular challenges. Variations in position and shape or even the absence of the structure concerned may make it difficult to define an area (Cunningham, 1890; Kruggel, 2018). Absence of a structure does not necessarily indicate that a functional area is missing, but rather that a sulcus, which defines it, may not be present. In addition to variations in shape, sulci are frequently interrupted (Cunningham, 1890; Destrieux *et al.*, 2010). These interruptions may vary from subject to subject and provide a challenge to interpretation. In addition sulci are frequently branched, or merged with other sulci, and these features vary from brain to brain. Decisions, therefore, have to be made as to which branches to include or exclude. A factor which is of particular relevance to the functional significance of areas traced is the considerable depth of some sulci, such as the intraparietal sulcus (IPS). Areas on one or other wall at the surface of the sulcus appear on a whole brain or fMRI scan to be very close to one another. They may,

however, be several centimetres apart in terms of the distance along the cortical surface between the two of them. In addition to all this, boundaries frequently need to be defined quite arbitrarily.

The parietal lobe is divided into superior and inferior lobules by the longitudinally running IPS (Clark, Boutros and Mendez, 2010). Frequently, however, this is referred to as the "HIPS" – horizontal portion of the intraparietal sulcus, an example of the variations of nomenclature, which bedevil studies of cortical morphology and function. The history of the sulcus in anatomical literature is relevant here. Sir William Turner (1832-1916) a prominent 19th century anatomist was the first to name this sulcus in 1866 (Turner, 1866). He defined it as starting directly posterior to the inferior end of the central sulcus (CS), ascending parallel to it and then turning posteriorly into the parietal lobe. Its posterior termination was variable. The postcentral sulcus (PCS) had not been defined at that time. Cunningham studied it in more detail in cadaver specimens and spoke of 5 different variations (Cunningham, 1890). These relate to the manner of branching and interruptions in the sulcus. He described the IPS as comprising three major parts: *the ramus horizontalis*, *the ramus verticalis superior* and the *ramus verticalis inferior*. Currently, the *ramus verticalis superior* and *inferior* are collectively known as the PCS, and the *ramus horizontalis* as the IPS. Cunningham's five proposed variations were: (I) All three parts of the sulcus are separate; (II) the inferior portion of the PCS is confluent with the IPS, but the superior portion of the PCS is separate; (III) the PCS is confluent but separate from the IPS; (IV) all three parts of the sulcus are confluent; and (V) the superior part of the PCS is confluent with the IPS, but the inferior part of the PCS is separate. Subsequently the part parallel to the CS has been named the ascending portion (Duvernoy, 1999), or alternatively included as the inferior portion of the PCS (Clark, Boutros and Mendez, 2010; Zlatkina and Petrides, 2014). The part running posteriorly through the parietal lobe became the horizontal part of the IPS (HIPS) which is frequently mentioned in imaging literature (Dehaene *et al.*, 2003; Piazza *et al.*, 2004; Fias *et al.*, 2007; Meintjes *et al.*, 2010). The descending portion extends from this into the occipital lobe (Duvernoy, 1999). Unsurprisingly the sulcus has a variable number of branches and connections. Destrieux *et al.*, (2010) referred to additional inconstant sulci, the transverse parietal sulci, which originate at right angles to the IPS and may attain the superior edge of the hemisphere.

This study aimed to compare volumes traced on MultiTracer and FreeSurfer in order to establish if there are correlations between the two modalities when tracing a variable brain structure such as a sulcus. We hypothesised that the 'gold-standard' manual tracing would be a more trustworthy method as subject variation is taken into account with this method.

4.2 Methods

4.2.1 Participants

This study forms part of an extensive ongoing longitudinal study researching the effects of maternal alcohol consumption during pregnancy on the developing child (Jacobson *et al.*, 2008, 2011; Meintjes *et al.*, 2010; Biffen *et al.*, 2018). The study involves neurocognitive assessments, morphological measurements and MRI scans at various ages. A total of 52 right-handed children aged 9- to 14 from the Cape Coloured (mixed ancestry) community in Cape Town, South Africa were the participants for this study. Within the sample, 15 were diagnosed as having fetal alcohol syndrome or partial fetal alcohol syndrome (FAS/PFAS); 13 were heavily exposed non-syndromal (HE) and 24 were non-or minimally exposed controls. Children with confirmed heavy prenatal alcohol exposure who lack facial dysmorphology have been termed HE in our study. Due to small sample size, children with a diagnosis of FAS or PFAS were grouped together.

Twenty of the 52 participants form part of our prospective longitudinal cohort (Jacobson *et al.*, 2008). The mothers of these children were recruited from an antenatal clinic of a midwife obstetric unit that serves an economically disadvantaged community between July 1999 and January 2002. Mothers were included in the study if they averaged at least 1.0 oz absolute alcohol (AA) per day (2 standard drinks), or reported at least 2 incidents of binge drinking (5 standard drinks/occasion) during the first trimester of pregnancy. Additionally, women initiating antenatal care were invited to participate as control subjects if they drank <0.5 oz AA/day and if they did not binge drink during the first trimester. Mothers were excluded from the study if they were younger than 18 years of age and suffered from diabetes, epilepsy, or cardiac problems requiring treatment. Infants were excluded if they presented with major chromosomal anomalies, neural tube defects, seizures, and if they were part of multiple births. For children from this cohort, prospective alcohol exposure data are available from timeline follow-back interviews conducted with the mothers during pregnancy. The other 32 participants are from our cross-sectional cohort who were identified by screening children from an elementary school in a rural section of Cape Town where alcohol abuse among local farm workers is high (Jacobson *et al.*, 2011). Two groups of children were recruited: (1) children whose mothers were heavy drinkers, who consumed at least 14 standard drinks per week (1.0 oz AA/day) on average or engaged in binge drinking (5 or more drinks/occasion) during pregnancy and (2) controls whose mothers abstained or drank only minimally during pregnancy (≤2 drinks per occasion).

4.2.2 Procedure

Mothers and children were transported to the Child Development Research Laboratory at the Faculty of Health Sciences campus of the University of Cape Town (UCT) by our driver, and on a separate day to the Cape Universities Brain Imaging Centre (CUBIC) at Tygerberg Hospital. Each mother completed a written informed consent and each child a written assent. Breakfast, lunch and snacks were provided for the mothers and children at each of their visits. Each mother received monetary compensation for every visit and each child a small gift. Neuropsychological and neuroimaging assessments were administered to each child by examiners who were blind regarding the FASD diagnoses, except in a small subset of the cases where the FAS diagnosis was obvious from facial features. Ethics approval for the study was obtained from the Wayne State University Human Investigation committee and the UCT Faculty of Health Sciences Human Research Ethics Committee.

4.2.3 Neuroimaging assessment

Magnetic resonance imaging protocol

All children received neuroimaging on a 3T Allegra MRI scanner (Siemens Medical Systems, Erlangen, Germany) using the single channel head coil. High-resolution anatomical images for the 32 participants of the cross-sectional cohort were acquired in the sagittal plane using a magnetization prepared rapid gradient echo (MPRAGE) sequence (TR 2300 ms, TE 3.93 ms, TI 1100 ms, 160 slices, flip angle 12°, 1.3 × 1.0 × 1.0 mm^3, 6.03 min). The high-resolution T1 weighted images of the 17 participants from the longitudinal cohort were acquired using a volumetric navigated (Tisdall *et al.*, 2012) multi-echo magnetization prepared rapid gradient echo (MEMPRAGE) (van der Kouwe *et al.*, 2008) sequence (FOV 256 mm × 256 mm, 128 sagittal slices, TR 2530 ms, TE 1.53/3.21/4.89/6.57 ms, TI 1100 ms, flip angle 7°, 1.3 × 1.0 × 1.3 mm^3, 8.07 min).

4.2.4 MRI analysis

Manual parcellation

A number of programmes are available for manual tracing (Woods, 2003; Rosset, Spadola and Ratib, 2004; Yushkevich *et al.*, 2006; Keller and Roberts, 2009). We chose to use Multitracer (Woods, 2003). This is a user friendly, freely available Java based tool which permits separate tracings in the three orthogonal planes. The image is smoothed and then the tracings appear as lines on the computer interface. When the view is switched to a different plane the tracings appear as coloured dots on the screen. This permits the tracer to trace in one plane and then use that tracing to guide the tracing in another plane. The benefit of this is that structures are generally more easily defined in one or other plane depending on their orientation (Randall *et al.*, 2017; Biffen *et al.*, 2018).

A protocol for the tracing was designed as follows. Fifty- two brains (104 hemispheres) were each traced by two trained neuroanatomists (MG and CMRW). All sets of tracings were then discussed slice by slice to reach agreement on the details of the protocol. The need for this is the considerable variation between subjects in relation to the nature of the origin of the sulcus from the postcentral sulcus, variation in branches of the sulcus and their frequency, interruptions in the sulcus and the best manner to trace them, variations in the position and shape of the parieto-occipital sulcus and which aspect of it to take as the posterior boundary of the parietal lobe, and which approach to adopt to the large constant medial branch of the posterior part of the sulcus.

The origin of the sulcus from the postcentral sulcus varied in its position and the angle of the connection. When the confluence of the sulci was superiorly placed the angle of the junction was roughly a right angle. Lower intersections had more acute angles as viewed from the superior aspect of the IPS, with the IPS at times descending parallel to the PSC before joining it. The point of junction was adjudged by the point of maximal curvature as the wall of the IPS merged with the PCS. The medial wall of the IPS was traced first and then the lateral wall added to this. This is relevant to note as, in general, the angle of junction of the medial wall was more acute than the lateral.

With regards to branches of the IPS, all branches of the lateral wall were excluded as they were taken as part of the inferior parietal lobule. The posterior extension of the lateral sulcus and that of the superior temporal sulcus connected in some brains with the IPS. It was clearly not functionally appropriate to include these with the IPS, and was thus deemed wiser to exclude all branches of the lateral wall. Near the posterior end of the IPS a large medial branch was present in every brain on both sides. This branch frequently divided into further branches beneath the surface of the hemisphere. We included it as part of the IPS. Further anteriorly in the superior parietal lobule smaller sulci were present which frequently joined the postcentral sulcus anteriorly. In a minority of cases these sulci joined the IPS, but because of their variability we excluded them from the tracings, regarding them as features of the inferior parietal lobule as did Destrieux *et al*., (2010).

Interruptions in the sulcus were traced as follows. The initial tracings were performed in the horizontal plane. From this view the whole sulcus was generally well seen and interruptions identified along with the portions of the sulcus on either side. The final tracings used for volumetric assessment were then done, in each case in the coronal plane. Using the dots visible from the horizontal plane coronal tracings of the sulcus were relatively easy to perform. In particular the depths of the sulcus were better traced in coronal slices as they are difficult to see precisely in horizontal ones. Since we were attempting to trace the IPS within the parietal lobe the parieto-occipital sulcus must define the

posterior extremity of our tracings. The question was, however, how to define the appropriate part of the parieto-occipital sulcus. On the medial surface of the hemisphere the sulcus is visible as the prominent single groove familiar to neuroanatomists. As it passes laterally into the hemisphere, however, it branches extensively and becomes very complex, making decisions as to what was anterior to it very difficult. For consistency therefore we defined the posterior boundary of the parietal lobe as being the parieto-occipital sulcus on the medial surface of the hemisphere which we traced on the saggital sections of the brains. Lines were then drawn directly laterally from this boundary. The coronal tracings to be used for volumetric purposes used this as the posterior boundary.

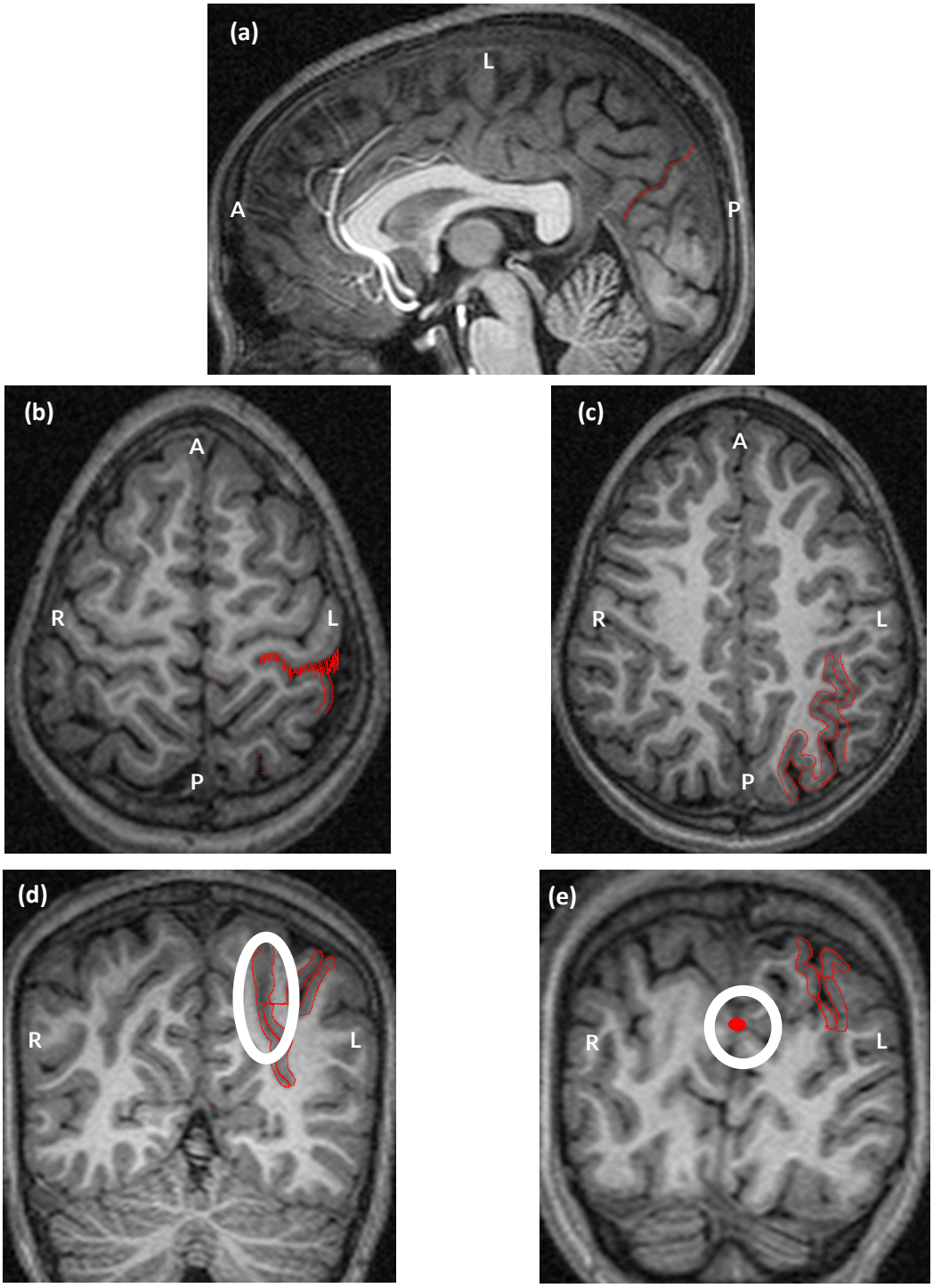

Figure 4.1: The protocol for manually parcellating the IPS shown on the left hemisphere of a PFAS subject. Both the MIPS and LIPS are traced. **(a)** On the sagittal plane the parieto-occipital sulcus was identified to indicate the end of the parietal portion of the IPS. **(b)** On the horizontal planes the postcentral sulcus was identified indicating the start of the IPS and **(c)** further tracings on this plane identified the pattern of the sulcus. **(d)** The IPS could finally be traced on the coronal sections and a medial branch was always present near the end of the parietal portion. **(e)** The tracings on the sagittal slice were visible on the coronal planes and clearly indicated the parietal border of the IPS.

In summary, the tracings were performed using the following steps:-

1. In the saggital plane near the midline, the parieto-occipital sulcus was identified and traced to define the posterior boundary.
2. The central and thus postcentral sulcus were identified in the horizontal plane. .
3. In the horizontal plane the medial wall of the IPS and the prominent posterior medial branch were traced. These tracings were terminated at the position of the parieto-occipital sulcus as described above.
4. The whole medial wall of the sulcus was traced in coronal sections. At this point we obtained the volume of the medial wall from MultiTracer.
5. The lateral wall was traced in horizontal sections. The anterior extremity of the IPS was easier to position on the medial wall where the junction is more acute. This facilitated the more difficult positioning of the anterior end of the lateral wall.
6. The lateral wall was traced in coronal sections as per the medial wall. These were traced as add-ons to the medial wall in each slice excluding the CSF-containing spaces between medial and lateral walls. When tracings were complete, the combined volume of the medial and lateral walls was obtained from Multitracer.

The protocol was designed by the two neuroanatomists MG and CMRW following which the entire set was traced by MG. Ten brains were then randomly selected from the sample and retraced using this protocol by the same researcher for intra-rater analysis.

Automated parcellation

FreeSurfer is open-source software used for the processing of MR images (https://surfer.nmr.mgh.harvard.edu/). The FreeSurfer software package performs detailed steps of cortical surface reconstruction to ultimately supply the researcher with the desired volumetric measurements. The steps for cortical surface reconstruction involves algorithms that perform steps to take high resolution T1-weighted images and transform them into a readable format for FreeSurfer to work with. After the MR images are normalized and 'skull-stripped', the software constructs a boundary between the white matter and cortical grey matter. Once this is manually checked for any inconsistencies, the cortical surfaces are aligned with a cortical surface-based atlas (Destrieux *et al.*, 2010) and the volumetric measurements may be retrieved. For this study, version 6.0.0 of the software suite was used to generate voxel-based volumes for the IPS. FreeSurfer automatically assigns a neuroanatomical label to each location on a cortical surface model based on probabilistic information estimated from a manually labeled training set. The labeling scheme used by Destrieux and colleagues (Destrieux *et al.*, 2010) to construct the automated labeling software included in the

FreeSurfer package since August 2009 (Freesurfer v4.5, aparc.a2009s/Destrieux.simple.2009-07-29.gcs atlas), includes a region denoted "intraparietal-and_parietal_transverse sulci". In addition with the inconstant 'transverse parietal sulci' mentioned above, the authors also noted that the IPS comprised varying numbers of segments on the inflated view, ranging from 1 to 3 with 2 segments being most common. Figure 4.2 shows pial (left) and inflated (right) views of the parcellations for one hemisphere. Since sulci are only visible on the inflated view, FreeSurfer outputs surface areas for these regions.

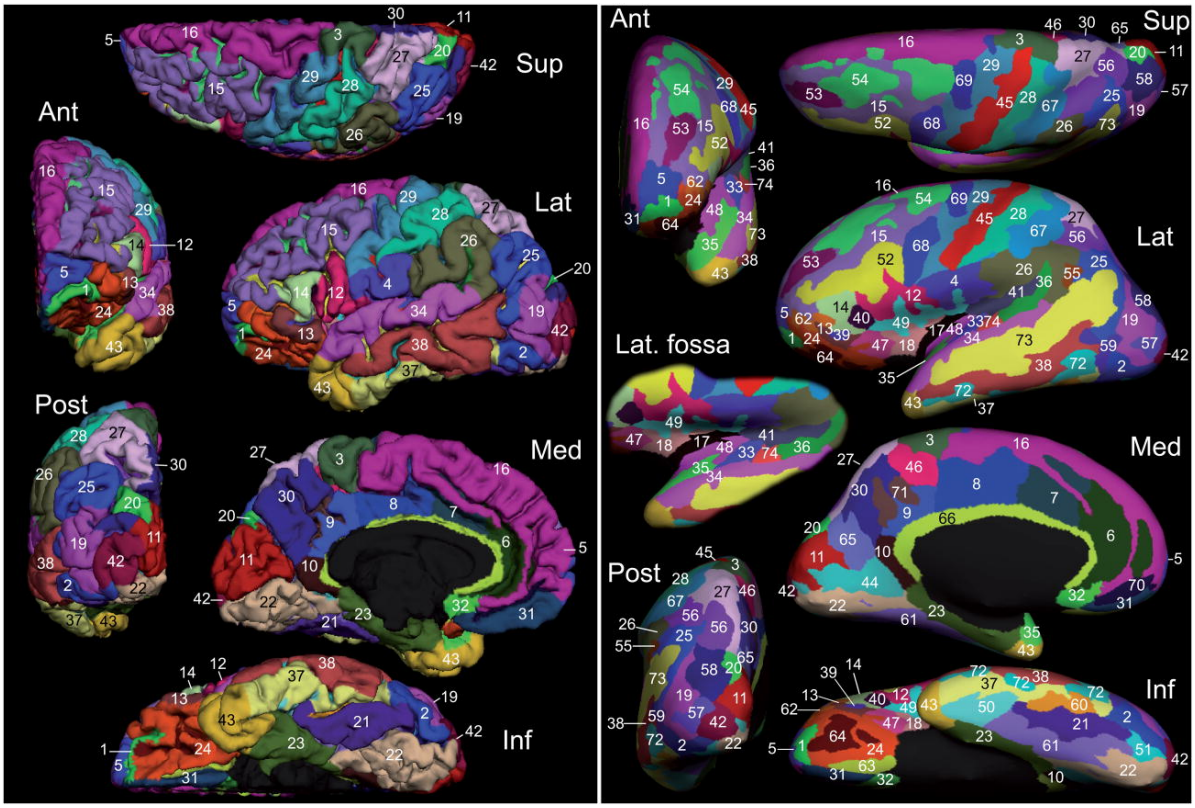

Figure 4.2: Pial (left) and inflated (right) views showing parcellations for one hemisphere. (From: Destrieux et al. Neuroimage. 2010 Oct 15; 53(1): 1–15.) The intraparietal sulcus (label 56) is visible on the superior, lateral and posterior views of the inflated brain. Label assignments: 28 postcentral gyrus; 27 superior parietal lobule; 26 supramarginal gyrus (anterior portion of inferior parietal lobe); 25 angular gyrus (posterior portion of the inferior parietal lobe); 67 postcentral sulcus; 56 intraparietal sulcus.

4.2.5 Statistical analyses

Statistical analyses were performed using SPSS (version 25, IBM). All variables were normally distributed except the following which had outliers greater than 3 SD beyond the mean, which were therefore recoded to one unit higher than the next data point (Winer, 1971): cigarettes per day (n=1), lead exposure (n=1) and proportional drinking days (n=2). AA/day was positively skewed and was log transformed.

Control variables that were considered as potential confounders included: total intracranial volume (mm^3) (TIV), child age at scan (yr), sex of the child, MRI sequence used, socioeconomic status (SES)

(Hollingshead, 2011), lead exposure (μg/dl) and maternal cigarette use during pregnancy (number of cigarettes smoked per day).

To determine intra-rater reliability for the manual parcellation, Pearson correlations were used to assess the correspondence between the first and second tracings for the two ROIs in the ten retraced brains. Intraclass correlation (ICC) was then used to test the reliability of the manual tracings, and to indicate if the parcellation protocol could be consistently repeated. Using a two-way mixed-effects model, the 'consistency' and 'absolute agreement' coefficients were determined. The same analyses were used to determine consistency and absolute agreement coefficients between the two parcellation methods (manual and automated).

The volumes for the two ROIs were compared between the parcellation methods using paired t-tests. ANOVA was used to examine diagnostic group differences and ANCOVA to control for potential confounders associated with the ROI volumes at $p<0.1$. TIV was added to the final step after controlling for confounders to determine if ROI volumes are disproportionately affected by PAE.

Associations of the volumes with alcohol measures were examined using linear regression. Multiple regression was used to control for potential confounders, and TIV was added in the last step.

4.3 Results

4.3.1 Sample characteristics

Table 4.1: Sample characteristics

	Alcohol exposed					
	FAS/PFAS	HE	Control	Total	*F or* χ2	*p*
	(*n*=14)	(*n*=11)	(*n*=24)	(*N*=49)		
Demographic background						
Child						
Sex: *n* = Male (%)	7 (14.3)	7 (14.3)	12 (24.5)	26 (53.1)	0.637	0.727
Child age (yr) at scan	11.0 (1.12)	11.5 (0.90)	11.2 (1.11)	11.2 (1.06)	0.801	0.455
Total Intracranial Volume (TIV)[a] (x 10^5 mm^3)[a]	12.9 (17.65)	14.1 (15.80)	15.3 (14.44)	14.4 (18.433)	10.052	**<0.001**
WISC IQ[b]	64.7 (8.66)	63.7 (11.06)	75.5 (10.00)	69.8 (11.24)	8.064	**0.001**
Maternal						
Maternal caregiver education[*]	7.6 (2.86)	8.2 (2.23)	9.0 (1.81)	8.4 (2.29)	1.746	0.186
Mother's age at delivery	28.6 (7.81)	25.3 (5.44)	27.4 (4.66)	27.3 (5.87)	0.988	0.380
Socio-economic status (SES)[♣]	16.1 (5.73)	20.6 (10.70)	20.8 (8.86)	19.4 (8.66)	1.477	0.239
Blood lead concentration (μg/dl)[c]	10.4 (6.52)	7.5 (4.06)	6.4 (2.06)	7.8 (4.47)	4.096	**0.023**
Maternal substance use during pregnancy[#]						
Absolute alcohol/day (oz)[d]	2.2 (2.79)	1.7 (1.30)	0.002 (0.01)	1.0 (1.87)	9.447	**<0.001**
Absolute alcohol/occasion (oz)[e]	4.7 (2.32)	5.9 (3.79)	0.1 (0.29)	2.7 (3.37)	35.120	**<0.001**
Frequency (days/week)[f]	2.5 (1.93)	2.0 (0.96)	0.01 (0.06)	1.2 (1.60)	26.086	**<0.001**
Cigarettes/day[g]	8.5 (5.79)	10.9 (8.58)	3.7 (8.50)	6.7 (8.28)	3.684	**0.033**

Values are Mean (SD). Bold print denotes significance at $p \leq 0.05$. FAS = fetal alcohol syndrome. PFAS = partial fetal alcohol syndrome. HE = nonsyndromal heavy alcohol exposed. WISC = Wechsler Intelligence Scale for Children. 1 oz absolute alcohol ≈ 2 standard drinks. [*]Of *N*=49, 45 primary caregivers were the biological mothers of the children: 2 (HE) were the fathers, 1 (Control) was the grandmother, and 1 (FAS/PFAS) was another relative. [♣](Hollingshead, 2011)(Hollingshead, 2011)Hollingshead (2011) Four Factor Index of Socio Economic Scale. [#]One mother of a FAS child used Marijuana 0.87 days/month during pregnancy. [a]FAS/PFAS<Controls (p<0.001); [b]FAS/PFAS<Controls (p=0.006); HE<Controls (p=0.005); [c]FAS/PFAS>Controls (p=0.017); [d]FAS/PFAS>Controls (p=0.001), HE>Controls (p=0.013); [e]FAS/PFAS, HE>Controls (p<0.001); [f]FAS/PFAS,HE>Controls (p<0.001); [g]HE>Controls (p=0.040)

Table 4.1 summarises the sample characteristics. Three subjects from the original 52 participants had to be excluded from this study because errors were returned after the recon-all step in the FreeSurfer software (HE *n* = 2 and FAS/PFAS *n* = 1). There were no differences between groups on child sex, child age at scan, maternal education, mother's age at delivery and socioeconomic status. FAS/PFAS children had smaller TIV and higher blood lead concentrations than controls. Children in the exposed groups had lower WISC IQ scores than controls. All the mothers of the control children abstained from drinking except two: one drank 2 standard alcoholic beverages on one occasion, and the other drank 2 standard alcoholic beverages about once every month. Although the mothers of children with FAS/PFAS on average drank fewer drinks per occasion than mothers of children with HE (4.7

standard drinks compared to 5.9), mothers of the FAS/PFAS children drank more frequently (2.5 days per week compared to 2).

4.3.2 Intra-rater reliabilities and comparisons between imaging methods

Table 4.2: Intra-rater reliabilities of manually parcellated ROI volumes for 10 randomly selected participants (*N*=49)

	Pearson	ICC (Consistency)	95% CI	ICC (Absolute agreement)	95% CI
ROI	***r*(*p*)**	***r*(*p*)**		***r*(*p*)**	
Left IPS	0.766 (**0.010**)	0.852 (**0.005**)	0.402 – 0.963	0.860 (**0.005**)	0.439 – 0.965
Right IPS	0.835 (**0.003**)	0.909 (**0.001**)	0.635 – 0.978	0.894 (**0.001**)	0.581 – 0.973

Table 4.3: Comparison between manual and automated methods (*N*=49)

		Left IPS	Right IPS
Manual	**Mean (SD)**	9535.06 (2068.00)	8957.44 (1934.20)
FreeSurfer	**Mean (SD)**	4820.71 (867.63)	5413.00 (981.39)
Paired t-test	***t (p)***	-19.776 (**<0.001**)	-15.681 (**<0.001**)
Pearson correlation	***r (p)***	0.626 (**<0.001**)	0.580 (**<0.001**)
ICC - Consistency	***r (p)***	0.617 (**0.001**)	0.637 (**<0.001**)
95% CI		0.321 – 0.784	0.357 – 0.795
ICC – Absolute agreement	***r (p)***	0.152 (**0.001**)	0.227 (**<0.001**)
95% CI		-0.095 – 0.459	-0.141 – 0.569

The intra-rater reliabilities between the 10 retraced subjects and their original volumes are shown in Table 4.2. The Pearson correlation was significant for both the left- and right IPS volumes. Although ICC was strongly significant for both consistency and absolute agreement, the 95% confidence intervals showed that the reliabilities were only moderate (Koo and Li, 2016). Table 4.3 shows the comparison between manual and automated parcellation methods. Both the left- and right IPS volumes which were manually traced were significantly larger than the volumes measured by FreeSurfer. Similarly to the intra-rater reliabilities, ICC showed significant consistency and absolute agreement between methods, but the 95% confidence intervals for both measures showed only poor to moderate reliability (Koo and Li, 2016).

4.3.3. Relation of IPS volumes with PAE

Table 4.4: Associations of ROI volumes with potential confounders (*N*=49)

	TIV		Imaging Sequence#		Child age		Sex of child#		SES		Cig/Day*		Lead exposure*	
	r	*p*	*r*	*p*	*r*	*p*	*r*	*p*	*r*	*p*	*r*	*p*	*r*	*p*
Manual														
Left IPS	0.369	**0.009**	-0.271	**0.060**	-0.129	0.376	0.166	0.255	0.034	0.814	-0.278	**0.053**	-0.260	**0.071**
Right IPS	0.291	**0.043**	-0.203	0.161	-0.046	0.752	0.048	0.742	-0.030	0.838	-0.009	0.949	-0.111	0.446
FreeSurfer														
Left IPS	0.459	**0.001**	-0.227	0.117	0.016	0.914	-0.081	0.582	0.116	0.426	-0.218	0.131	-0.298	**0.038**
Right IPS	0.375	**0.008**	-0.047	0.748	<0.001	1.000	-0.229	0.113	-0.005	0.974	0.025	0.864	-0.195	0.180

Values are Pearson correlation coefficients. *One outlier recoded to 1 unit above the next highest data point (>3SD beyond the mean). #For categorical variables, point biserial correlation was used.

Table 4.4 shows association of IPS volumes with potential confounders. TIV was related to all IPS volumes for both manual and automated parcellation methods. Imaging sequence and smoking showed association with the manually parcellated left IPS. Lead exposure showed association with both the manually and automated parcellated left IPS.

Table 4.5: Comparison of volumes by FASD diagnosis (*N*=49)

	FAS/PFAS (*n*=14)	HE (*n*=11)	CONTROL (*n*=24)						
	Mean (SD)	Mean (SD)	Mean (SD)	*F*	*P*	F^1	P^1	F^2	P^2
Manual									
Left IPS [a,b,c]	8233.64 (1693.38)	9554.33 (1593.20)	10285.38 (2149.60)	5.095	**0.010**#	2.796	**0.072**	1.539	0.226
Right IPS	8489.24 (1340.67)	8338.66 (2345.16)	9514.16 (1934.44)	2.054	0.140	1.966	0.152	1.234	0.302
FreeSurfer									
Left IPS [c]	4438.79 (928.61)	4618.27 (946.30)	5136.29 (694.25)	3.594	**0.035***	2.131	0.131	0.474	0.626
Right IPS	5189.71 (1098.77)	5106.91 (1022.22)	5683.54 (849.58)	1.875	0.165	1.304	0.281	0.612	0.547

[1]Controlling for [a]Cig/day; [b]Imaging sequence; [c]Lead exposure. [2]Controlling for TIV, in addition to confounders controlled for in F^1. *Post Hocs* (reflecting main effects): #FAS/PFAS<Controls (*p*=0.007); *FAS/PFAS<Controls (*p*=0.040).

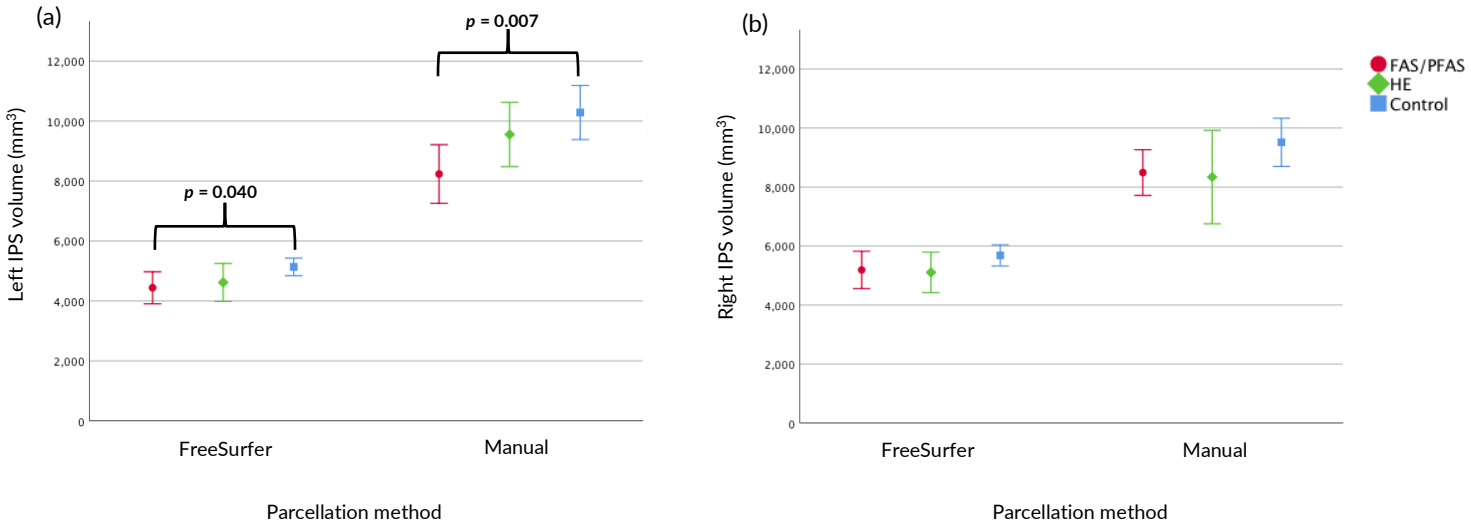

Figure 4.3: The mean and 95% CI by diagnostic group of manual and automated (a) left and (b) right IPS volumes.

The right IPS volume showed no difference between diagnostic groups for either parcellation method (Table 4.5). A significant group difference was observed for the manually parcellated left IPS, which was the result of smaller volumes in the FAS/PFAS children compared to controls. This difference became a trend after controlling for smoking, imaging sequence and lead exposure, but did not survive when TIV was added. The left IPS FreeSurfer volume was similarly smaller in the FAS/PFAS children compared to controls, but this difference did not survive when controlling for confounders. Figure 4.3 shows the mean IPS volumes and 95% confidence intervals.

Table 4.6: Associations of volumes with alcohol measures (*N*=49)

	Absolute alcohol per day (oz)$^{+}$	Absolute alcohol per occasion (oz)	Proportional drinking days*		
	r (p)	*r (p)*	*r (p)*	β^1 *(p)*	β^2 *(p)*
Manual					
Left IPS [a,b,c]	-0.170 (0.242)	-0.079 (0.587)	-0.263 (**0.068**)	-0.201 (0.220)	-0.597 (0.553)
Right IPS	-0.126 (0.388)	-0.151 (0.301)	-0.159 (0.276)	-0.243 (0.157)	-0.140 (0.451)
FreeSurfer					
Left IPS [c]	-0.346 (**0.015**)	-0.215 (0.138)	-0.361 (**0.011**)	-0.294 (**0.046**)	-0.159 (0.285)
Right IPS	-0.333 (**0.019**)	-0.270 (**0.060**)	-0.297 (**0.038**)	-0.261 (**0.087**)	-0.148 (0.351)

r : Pearson correlation. β^1 : Controlling for [a]Cig/day; [b]Imaging sequence; [c]Lead exposure. β^2 : Controlling for TIV, in addition to confounders controlled for in β^1. *2 outliers Winzorised (>3SD beyond the mean); $^{+}$Log transformed

Table 4.6 shows the associations of the IPS volumes with alcohol measures. For the manually parcellated IPS volumes, only the left was associated with proportional drinking days, and this did not survive controlling for potential confounders. The automated parcellated IPS volumes were associated bilaterally with proportional drinking days After controlling for lead exposure, the association remained significant in the left IPS, but became a trend in the right IPS. Neither association survived when TIV was added as a confounder. Figure 2 shows the correlations between the volumes and proportional drinking days for both parcellation methods.

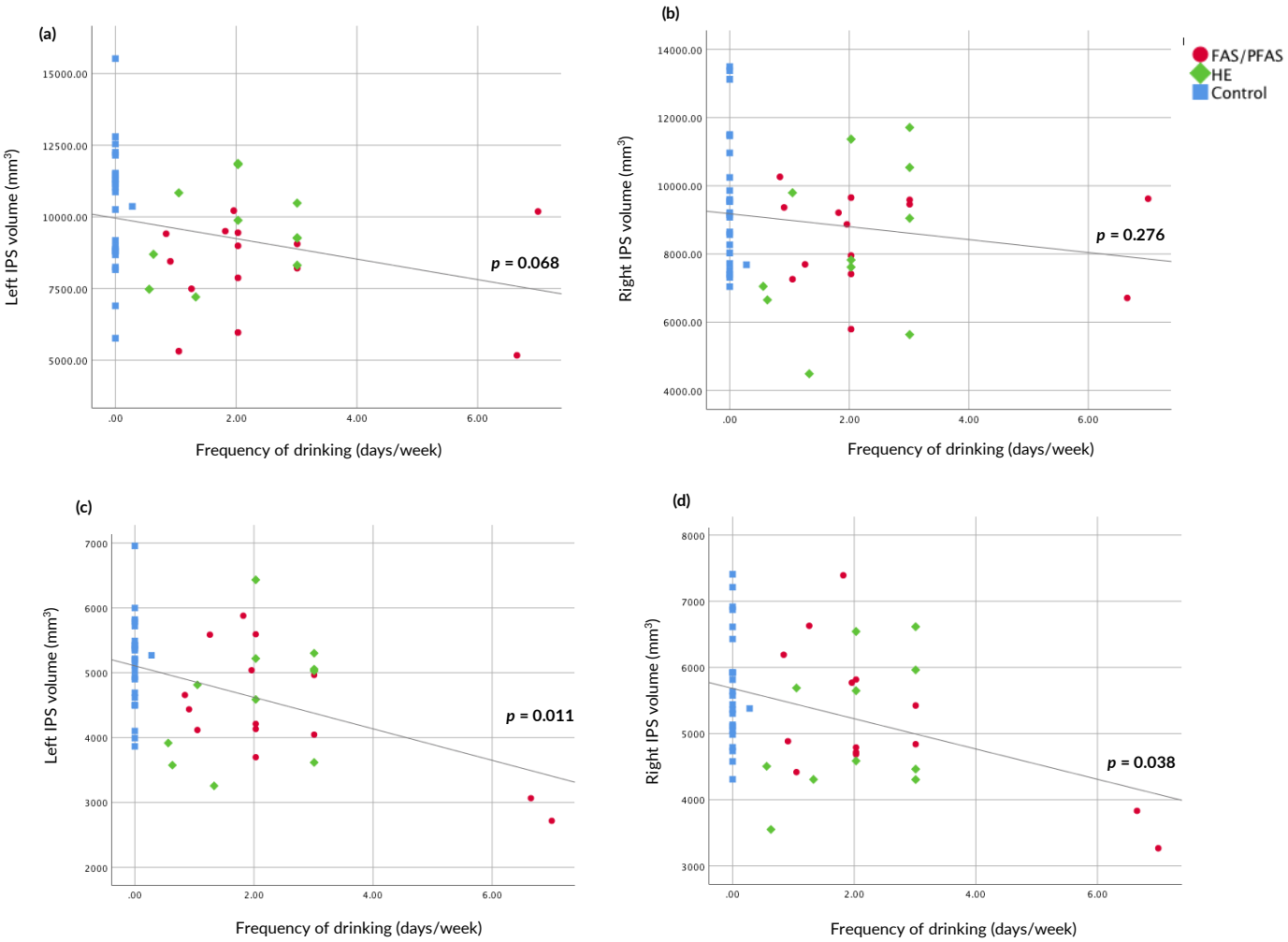

Figure 4.4: The correlation of IPS volume with frequency of drinking (days/week). **(a)** and **(b)** are the manually traced left- and right IPS volumes. **(c)** and **(d)** are the volumes generated from FreeSurfer.

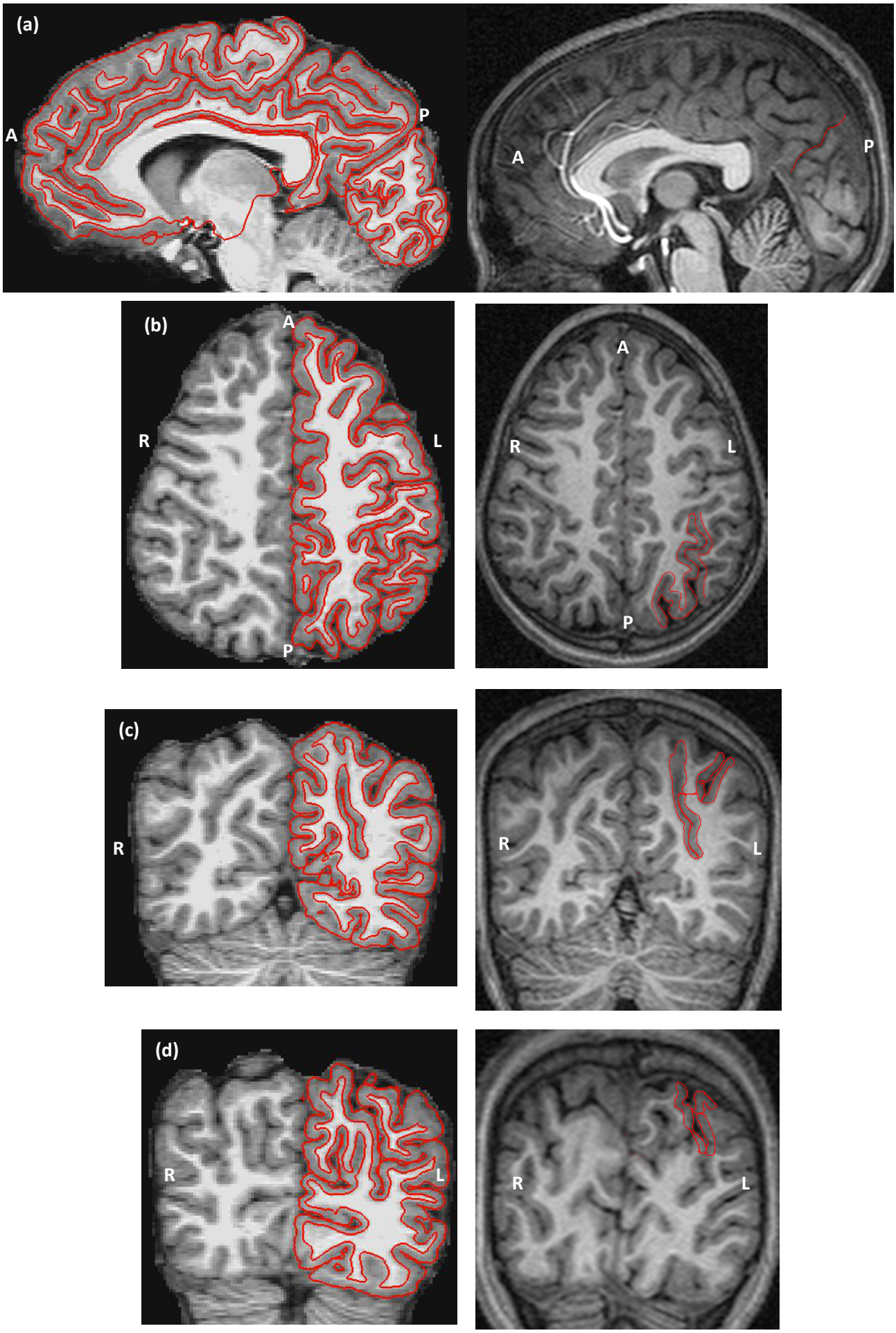

Figure 4.5: Comparison between FreeSurfer (Left) and MultiTracer (Right) tracings on a PFAS subject in the sample. **(a)** On the sagittal planes **(b)** On the horizontal planes **(c)** The coronal planes showing the constant medial branch **(d)** The coronal planes showing the end of the parietal portion of the IPS on the right.

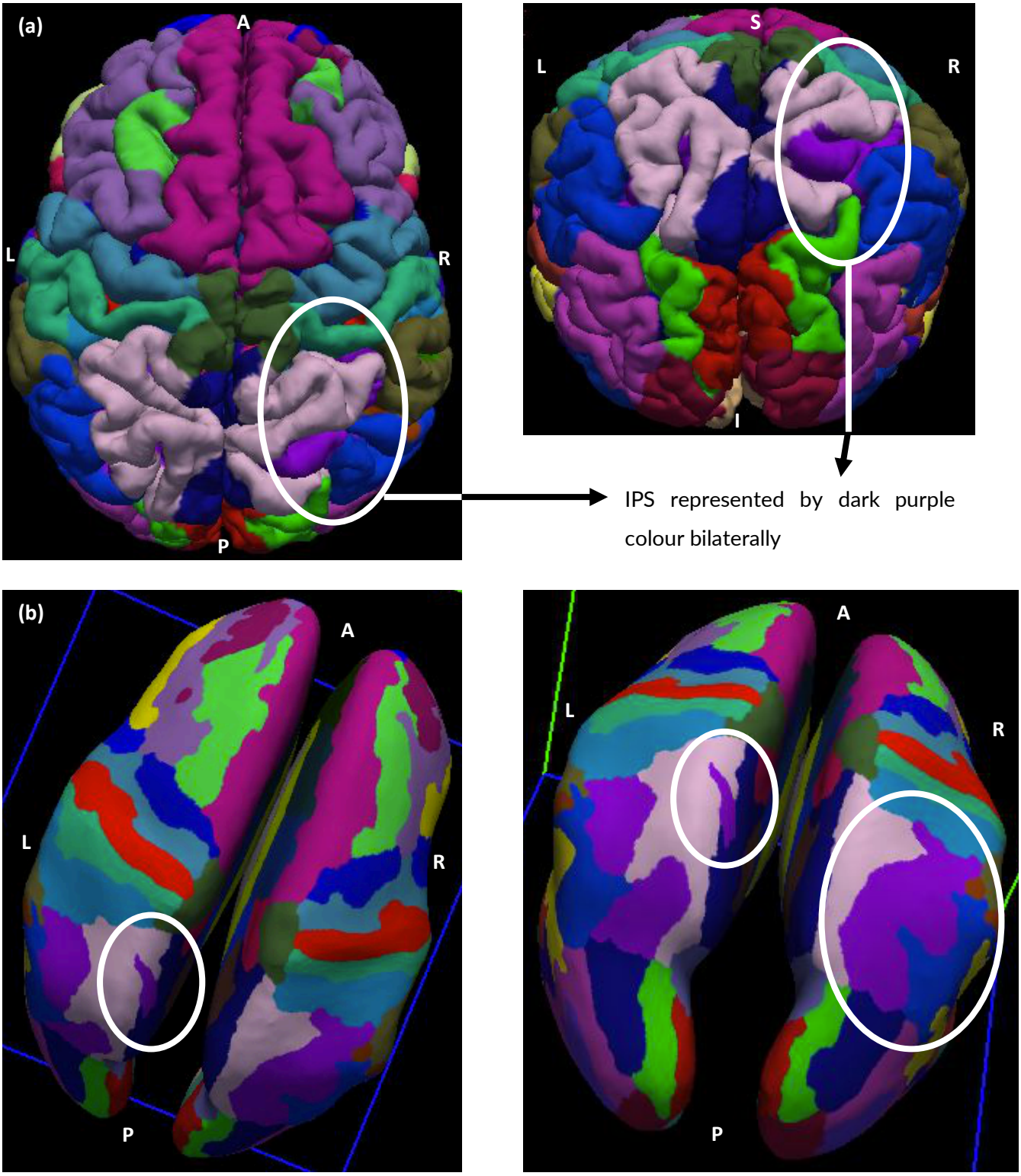

Figure 4.6: The figure shows the Destrieux et al., (2010) atlas parcellation for the same PFAS subject in Figures 4.2 and 4.5. **(a)** The pial view. The image on the left is the horizontal view with the dark purple showing the IPS parcellated by the FreeSurfer atlas. The image on the right is a coronal view. **(b)** These images are the inflated views. The image on the left is a horizontal view showing the inconstant transverse parietal sulcus on the left hemisphere that was sometimes included in the measurement of the IPS. The image on the right is a more coronal/superior-posterior view showing the transverse parietal sulci on the left hemisphere and the continuous IPS on the right hemisphere. Note that the left IPS is not continuous and consists of 2 parts.

4.4 Discussion

This study aimed to compare two different parcellation methods for volume rendering of the IPS. We compared our manually parcellated volumes with volumes calculated by automated software. The results show a consistency between the two methods. The manually parcellated volumes, however, were bilaterally larger than the automated volumes. The automated volumes also had stronger associations with continuous alcohol measures.

Numerous publications exist comparing manual to automated methods for segmenting subcortical structures (Hsu *et al.*, 2002; Bergouignan *et al.*, 2009; Morey *et al.*, 2009; Dewey *et al.*, 2010; Makowski *et al.*, 2018), but none could be found comparing these methods for parcellating cortical structures such as sulci. Mostly, the literature provides evidence that automated measures are reliable alternatives for segmenting brain structures compared to manual methods (Cherbuin *et al.*, 2009; Morey *et al.*, 2009; Cardenas *et al.*, 2014). Automated parcellation is quicker and less labour-intensive than manual parcellation. It is a favourable method for many volumetric studies as it is easy to use, does not require an expert neuroanatomist, and retrieves results for analyses much more quickly, which reduces research time. In the present study, our results also show that comparable parcellation outputs are achieved and is consistent between the two methods, which is consistent with literature stating that FreeSurfer is the most similar to manual tracing (Morey *et al.*, 2009). In addition, we parcellated the medial wall separately from the lateral wall. The automated software was not able to do this, and instead rendered the volume of the entire IPS. By only looking at the entire sulcus, important branching patterns and variability may be missed as the sulcus is not just an orthogonal line running down the parietal lobe from the PCS.

Figures 4.5 and 4.6 show the FreeSurfer and MultiTracer parcellations for the same subject. The delineation of the IPS in Fig. 4.5 looks similar between the manually traced and automated parcellation. The manual parcellation of the left IPS includes an interruption which is also visible in the inflated view of the FreeSurfer parcellation (Figure 4.6). In this parcellation, FreeSurfer also included the medial wall that we consistently included in our manual tracings. In addition, FreeSurfer terminated the IPS at the POS as we did with our tracings.

A clear difference between the two methods, however, is the inconstant 'transverse parietal sulcus' that FreeSurfer included with the IPS measurements and which we excluded. This sulcus is clearly visible when looking at the inflated view (Figure 4.6). It is clear that the sulcus does not branch or join the left IPS, but instead is more medially located. When trying to identify this 'transverse parietal

sulcus' on our image, it is not clear which sulcus they identified and included in the measurement and why it was only included on the left. As it does not form any connection with the IPS itself, this sulcus appears rather to form part of the superior parietal lobule. Further investigation is needed to establish if this 'transverse parietal sulcus' is always more medial and in the superior parietal lobule. A superior-medially located sulcus was observed in a subset of the cohort to join the IPS, but as this was inconsistent it was excluded from the manual tracing protocol. In functional MRI, results are not usually visible in this area (Woods *et al.*, 2015) which is another reason to exclude it from volumetric measurements. The manual parcellation protocol routinely included the medial branch, although its size varied.

Although manual parcellation permits more anatomical accuracy, the smaller volumes produced by the automated method had stronger associations with continuous alcohol measures. The left IPS was the only region that showed associations with alcohol in both parcellation methods, suggesting that this area is most affected by alcohol. This is in agreement with previous research that show the left parietal lobe is a region sensitive to PAE (Sowell *et al.*, 2001). That the automated bilateral IPS volumes yielded stronger relations to alcohol measures may be attributable to the smaller volumes measured in all groups (FAS/PFAS, HE and Controls). The differences between the FAS/PFAS and Control mean volumes are smaller than the difference between the manually parcellated FAS/PFAS and Control mean volumes. The manually parcellated control mean volumes may therefore hide the associations that the PAE children's IPS volumes may have with the continuous alcohol measures.

According to Koo and Li (2016), reliability testing should not just examine the intraclass correlation coefficient (ICC) but also take note of the 95% confidence interval (CI) of the output value. Our 95% CI values were only moderate for intra-rater reliability. Both the ICC (consistency and absolute agreement) 95% CI values for the right IPS were in the moderate to good range, suggesting that the left IPS is more variable in structure. This was also the case when comparing the manual tracings to the automated. In addition, both ICC 95% CI values for the comparison of the tracing modalities were in the poor to moderate range, showing how different these modalities are from each other. This may also explain the difference between the volumetric measures.

The FreeSurfer atlas that is used to compute volumes of cortical structures are based on adult brains with mean ages for females being 25.33 years and for males 21.67 years (Destrieux *et al.*, 2010). This differs considerably from our mean age of 11.2 for both males and females. It is known that the brain changes from childhood to adulthood (Gogtay *et al.*, 2004) and to date, there does not exist an atlas based on children/adolescent brains on this software platform. The importance of atlases for

children's brains has been recognised and several neonatal atlases have been created (for a review see Cabezas *et al*., (2011)). In addition to children's brains being smaller, the PAE children are known to have smaller TIV compared to healthy children (Guerri, Bazinet and Riley, 2009) Therefore, sulcal patterns and volumes of sulci may be different in subjects with PAE.

As mentioned previously, seeing as the IPS volumes of the children in our sample were measured using an atlas based healthy adult brains, this could be a potential limitation as the children in our sample have relatively low IQ's and 14 are prenatally exposed to alcohol. The inconstant adding of a 'transverse parietal sulcus' may hide significant results relating to the IPS and may result in inconsistent volumetric measurements. For these reasons, automated measures are not completely comparable to manual methods, especially when studying variable cortical structures like sulci. Another limitation to the study is that two MRI sequences (MPRAGE for n = 32; and MEMPRAGE for n = 20) were used for the subjects which may have altered the MR images slightly and ultimately have affected the volume results. However, we did account for this by including the imaging sequence as a potential confounder and it did not alter any significant result. The laborious process of manual tracing is subject to small errors that affect results. The intra-rater reliability showed only a moderate 95% CI, suggesting that it is difficult to manually parcellate sulci which are extremely variable.

This study investigated the comparison between manual and automated parcellation of the IPS. Although the results were similar in some respects, clear differences were observed between modalities in terms of volumetric output and delineation of the IPS. This indicates a need for more anatomically defined cortical atlases for automated programmes and especially ones for pediatric brains. Perhaps a semiautomated method which makes use of the anatomical expertise and judgement of expert neuroanatomists along with the precise measuring abilities of automated methods may provide the best way of producing precise results. A potential weakness of manual parcellation of large areas of narrow structures such as cortex is the difficulty of precisely tracing the grey/white matter and grey matter/CSF boundaries which automated methods can do consistently. The equivalent error in manually tracing globular structures would be less as the surface to volume ratios in those structures would be less. The errors and inconsistencies in manual tracings arise from imprecise and inconsistent location of the position of the surfaces. Although our manual tracing protocol did show some errors, it still accounted for more subject specific anatomical variation than the automated method. In conclusion, both modalities have strengths and weaknesses in the measurement of the volumes of cortical sulci. Manual tracing, however, remains the 'gold standard'

as it accounts for individual variation and pathology of cortical structures and provides a more extensive and detailed view of the brain.

Chapter 5

AN FMRI STUDY ON MANUALLY PARCELLATED DIVISIONS OF THE INTRAPARIETAL SULCUS IN CHILDREN PRENATALLY EXPOSED TO ALCOHOL

5.1 Introduction

Proximity judgment (PJ), which refers to the process of deciding which of two numbers is closest to a third (i.e. is 77 or 55 closer to 80?), relies on the ability to evaluate relative quantities and in children has been linked to future arithmetic abilities (Durand *et al.*, 2005; Holloway and Ansari, 2009; Bugden and Ansari, 2011; De Smedt *et al.*, 2013). The parietal lobe and intraparietal sulcus (IPS) have consistently been implicated in numerical magnitude (Dehaene and Cohen, 1995; Dehaene *et al.*, 2003, 2004; Fehr, Code and Herrmann, 2007; Dehaene, 2009; Meintjes *et al.*, 2010a) and functional MRI (fMRI) studies have shown activation of bilateral anterior and posterior IPS when performing magnitude comparison tasks (Pinel *et al.*, 2001; Schultz and Lennert, 2009; Meintjes *et al.*, 2010a). Dehaene *et al*. (2003) identified a parietal network comprising five areas that appear to relate specifically to quantity representation and manipulation – the bilateral anterior IPS is involved in representing semantic information about magnitude, the left angular gyrus in retrieval of number processing facts from long term memory, and the posterior superior parietal lobule (PSPL) bilaterally in supporting the engagement of attention. The IPS is an anatomical landmark that runs horizontally across the parietal lobe from the postcentral sulcus (PCS) into the occipital lobe (Cunningham, 1890), dividing the lobe into superior and inferior lobules.

Fetal alcohol spectrum disorders (FASD) is an umbrella term referring to the range of disorders found in individuals who were prenatally exposed to alcohol, including fetal alcohol syndrome (FAS), partial FAS (PFAS), alcohol-related neurodevelopmental disorder (ARND) and alcohol-related birth defects (ARBD) (Bertrand *et al.*, 2005; Hoyme, 2005). Prenatal alcohol exposure (PAE) is known to have widespread effects on cognitive functioning (Mattson and Riley, 1998), including deficits in arithmetic (Kopera-Frye, Dehaene and Streissguth, 1996; Rasmussen and Bisanz, 2009; Santhanam *et al.*, 2009; Jacobson *et al.*, 2011), and has been linked to altered parietal activation during magnitude comparison (Meintjes *et al.*, 2010; Woods *et al.*, 2015). When examining activation during PJ and exact addition in spherical regions-of-interest (ROIs) placed within each of the five key parietal regions proposed by Dehaene and associates (2003), Woods et al. (2015) found PAE-related decreases in the ROI placed in the right anterior IPS.

Since functional MRI analyses typically involve co-registration of individual brains to a standard template, thereby reducing anatomical specificity of the BOLD signal, the question arises as to whether the specific cortical areas within the IPS involved in number processing could be identified more precisely if anatomical variability between individuals could be accounted for. As part of earlier work examining the effects of PAE on the volume and asymmetry of the IPS, we manually traced this

region on MR images acquired in children from our cross-sectional cohort, all of whom also completed fMRI during administration of a PJ task. In this study we investigate whether extracting subject-specific BOLD signals in manually-traced anatomically-defined subregions of the IPS can improve localisation of regions showing PAE-related alterations during PJ. To our knowledge no previous study has used an anatomical approach such as the one proposed here to investigate IPS activation during number processing.

5.2 Methods

5.2.1 Participants

Participants were children from our cross-sectional cohort who were recruited to investigate the effects of prenatal alcohol exposure on brain structure and function during number processing (Dodge *et al.*, 2009; Meintjes *et al.*, 2010). Children were from the same community in Cape Town, South Africa and were identified by screening children from an elementary school in a rural section of Cape Town where alcohol abuse among local farm workers is high (Jacobson *et al.*, 2011). Two groups of children were recruited: (1) children whose mothers were heavy drinkers, consuming at least 14 standard drinks per week (1.0 oz AA/day) on average or engaging in binge drinking (5 or more drinks/occasion) during pregnancy and (2) controls whose mothers abstained or drank only minimally during pregnancy (≤2 drinks per occasion). Within the sample of 24 children, 6 had been diagnosed with FAS/PFAS, 6 were heavily exposed but non-syndromal (HE) and 12 were non- or minimally exposed controls. Due to the small sample size, children with FAS, PFAS or HE were grouped together in a PAE group.

5.2.2 Procedure

Mothers and children were transported to the Child Development Research Laboratory (CDRL) at the Faculty of Health Sciences campus of the University of Cape Town (UCT) by our driver, and on a separate day to the Cape Universities Brain Imaging Centre (CUBIC) at Tygerberg Hospital for neuroimaging. Each mother completed a written informed consent and each child a written assent. Breakfast, lunch and snacks were provided for the mothers and children at each of their study visits. Each mother received monetary compensation for every visit and each child a small gift. Neuropsychological and neuroimaging assessments were administered to each child by examiners who were blind regarding the FASD diagnoses, except in a small subset of the cases where the FAS diagnosis was obvious from facial features. Ethics approval for the study was obtained from the Wayne State University Human Investigation committee and the UCT Faculty of Health Sciences Human Research Ethics Committee.

5.2.3 Neuropsychological assessment

During their visit to the CDRL, each child was administered a computer-based number processing test designed by Dehaene (Kopera-Frye, Dehaene and Streissguth, 1996) and adapted by Jacobson *et al.*, 2011, that included a 32-problem Proximity Judgement (PJ) subtest. During this test, a number appeared at the top of the screen with two numbers below it, and the participant used the mouse to

indicate which number was closer to the number at the top. IQ was estimated from 7 of the 10 subtests from the Wechsler Intelligence Scale for Children, Third Edition (WISC-III)—Similarities, Arithmetic, Digit Span, Symbol Search, Coding, Block Design and Picture Completion—and Matrix Reasoning from the WISC-IV. Sattler's (1992) formula for computing Short Form IQ was used to estimate the IQ of the children using the aforementioned subtests. Handedness was assessed using the Annett (1970) Behavioral Handedness Inventory.

5.2.4 Neuroimaging assessment

Magnetic resonance imaging protocol

All children received neuroimaging on a 3 T Allegra MRI scanner (Siemens Medical Systems, Erlangen, Germany) using the single channel head coil. High-resolution anatomical images for the 24 participants were acquired in the sagittal plane using a magnetization prepared rapid gradient echo (MPRAGE) sequence (TR 2300 ms, TE 3.93 ms, TI 1100 ms, 160 slices, flip angle 12°, $1.3 \times 1.0 \times 1.0$ mm^3, 6.03 min). For the fMRI protocol, 154 functional volumes sensitive to blood oxygen level dependent contrast were acquired with a T2*-weighted gradient echo, echo planar imaging sequence (TR 2000 ms, TE 30 ms, 34 interleaved slices, 3 mm thick, gap 0.9 mm, 200 mm field of view, resolution 3.125 x 3.125 x 3 mm^3, 5.13 min).

Functional MRI experimental task

The computer-based PJ task explained in section 5.2.3 was simplified and administered inside the scanner. The reason for simplifying the task was to ensure that the exposed children could achieve acceptable scores inside the scanner. A mock scanner was built to introduce participants to the scanning environment and reduce anxiety. Each child first practiced the task in the mock scanner. E-Prime software (Psychology Software Tools, Inc., Pittsburg, PA) was used to program the experimental task which was presented using a data projector and a rear projection screen mounted at the head of the MRI bore. The child held a Lumitouch response system (Photon Control Inc., Burnaby, Canada) in his/her right hand and responded to the task with his/her right index and middle fingers. The children were able to talk to the examiner over the intercom that is built into the scanner and could stop the scan at any time by squeezing a ball held in their left hand. The task was administered using a self-paced block design, in which the child completed as many problems as possible during each 40s block. In the active blocks, a fixation square was displayed for 500ms prior to each trial. In the task blocks, a single number – the "target" – was displayed at the top of the screen for 1000ms, and the child was instructed to select from two numbers displayed horizontally below it the number numerically closer to the target. Problems were selected randomly from a list of 1-digit and 2-digit numbers. In the control blocks, the target consisted of a single Greek symbol, followed

by two Greek symbols displayed horizontally below it. The child pressed the button on the same side as the symbol that was identical to the target. Each block was repeated three times in the order PJ, PJ control (PJ_CTL), rest, PJ, PJ_CTL, rest, PJ_CTL, PJ and rest, with the fixation square displayed for 20s during the rest blocks, for a total task duration of 5 min.

Behavioral performance

The responses for the PJ task in the scanner were recorded on a computer. Number of trials attempted, number of trials correct, and accuracy (% correct) were computed for the task. Functional data were excluded for children with poor task performance (<66% correct) to ensure that all those included in the analysis had been mentally engaged in the task. Imaging data for one alcohol exposed child were excluded due to corrupted fMRI images that could not be pre-processed or analysed.

5.2.5 fMRI analysis

FMRI analyses were performed using BrainVoyager QX (Brain Innovation, Maastricht, the Netherlands) (Goebel, 2012). Four dummy images acquired in each run were excluded from all analyses. Images were motion corrected relative to their first volume with trilinear/sinc interpolation, corrected for different slice acquisition times and linear trends, and temporally smoothed with a high pass filter of 2 cycles/point. For each child, the largest segment of data with no movement greater than 3 mm displacement or 3.0° rotation was analysed. Each child's functional data were co-registered to their high-resolution anatomical MRI, rotated into the AC-PC plane and normalized to Talairach space using a linear transform calculated on the anatomical images. The 3.125 mm x 3.125 mm x 3 mm fMRI voxels were interpolated during Talairach normalization to 3 mm x 3 mm x 3 mm.

For each subject, the left and right IPS were manually drawn in Brain Voyager on the Talairach-normalised structural images (figure 5.1) and subdivided into five areas (i.e. 10 ROIs per subject):
The medial wall was divided into 3 areas. These were the:-
(1) Superior medial wall of the IPS (MIPS) – the anterior superior part of the medial wall ending at the point where the medial branch arose from the IPS.
(2) Medial branch of the MIPS - a branch projecting medially from the posterior IPS a short distance anterior to the parieto-occipital sulcus.
(3) Inferior MIPS representing the portion of the medial wall posteroinferior to the medial branch.

The lateral wall was divided into 2 areas namely the:-
(4) Superior lateral wall of the IPS (LIPS) - being the anterosuperior part of the lateral wall. The posterior limit of this was the same as that of the superior medial wall.

(5) Inferior LIPS – the lateral wall of the IPS posterior to the region.

The reason for using 'superior' and 'inferior' instead of 'anterior' and 'posterior', was to eliminate confusion with the functional areas of the IPS which include a posterior and anterior area. The average BOLD signal time course within each ROI was then extracted for each subject and separate subject analyses performed using the general linear model with predictors based on the known experimental blocks convolved by the standard hemodynamic function. The six z-transformed motion correction parameters were added as predictors of no interest. The beta values from this analysis, which reflect the percent signal change during each experimental condition relative to rest for each subject, were used to compute the percent signal change (i.e. the difference) between the PJ and control conditions in each ROI for each subject.

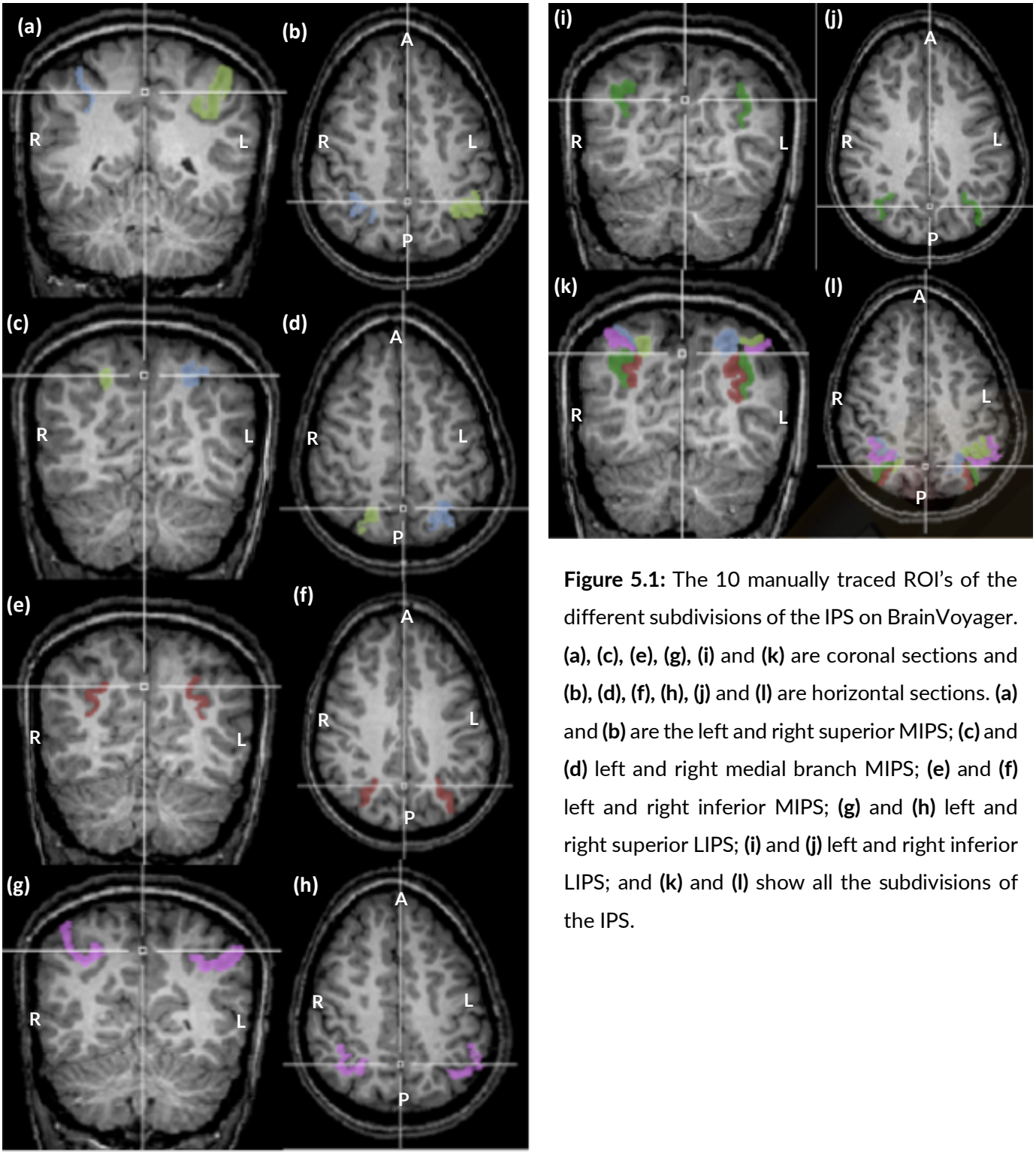

Figure 5.1: The 10 manually traced ROI's of the different subdivisions of the IPS on BrainVoyager. **(a), (c), (e), (g), (i)** and **(k)** are coronal sections and **(b), (d), (f), (h), (j)** and **(l)** are horizontal sections. **(a)** and **(b)** are the left and right superior MIPS; **(c)** and **(d)** left and right medial branch MIPS; **(e)** and **(f)** left and right inferior MIPS; **(g)** and **(h)** left and right superior LIPS; **(i)** and **(j)** left and right inferior LIPS; and **(k)** and **(l)** show all the subdivisions of the IPS.

5.2.6 Statistical analyses

Statistical analyses were performed using SPSS (version 25, IBM). All variables were normally distributed. The following variables had outliers >3 SD beyond the mean and were subsequently recoded to one unit higher than the next highest value (Winer, 1971): cigarettes per day (*n*=1, HE), proportional drinking days (*n*=2, FAS/PFAS; Control) and percent signal change in the right superior MIPS (*n*=1, Control). AA/day was positively skewed and was log transformed.

Seven control variables were considered and assessed as potential confounders: total intracranial volume (TIV; mm^3), age at scan (yr), sex of child, socioeconomic status, lead exposure, maternal cigarette use during pregnancy (number of cigarettes smoked per day) and WISC IQ.

The outcome measures (number of trials attempted, number of trials correct, accuracy (% correct) and % signal change on PJ relative to the control task for each ROI) were compared by diagnostic groups (PAE and controls) with an independent sample t-test. Associations of the outcome measures with the level of prenatal alcohol exposure were assessed in the PAE (*n*=12) group only with Pearson correlations. Multiple regression was used to control for potential confounders that were related to outcome variables at $p \leq 0.1$.

5.3 Results

5.3.1 Sample characteristics

Table 5.1: Sample characteristics

	Prenatally Alcohol Exposed	Control	Total	*t* or χ2	*p*
	(*n*=12)	(*n*=12)	(*N*=24)		
Demographic background					
Child					
Sex: *n* = Male (%)	25	42	33	0.750	0.386
Child age (yr) at scan	11.9 (1.1)	11.8 (1.2)	11.9 (1.2)	0.205	0.839
Total Intracranial Volume (TIV) (x 10^6 mm^3)	1.4 (2.0)	1.5 (1.4)	1.5 (1.8)	-1.951	0.064
WISC IQ	62.32 (9.5)	76.6 (13.4)	69.4 (13.4)	-3.041	**0.006**
Maternal					
Primary caregiver education*	7.0 (2.8)	8.4 (2.2)	7.7 (2.6)	-1.468	0.156
Mother's age at delivery	25.6 (4.5)	25.7 (3.4)	25.4 (4.0)	0.250	0.805
Socio-economic status (SES)♣	17.2 (7.2)	20.7 (10.5)	19.0 (9.0)	-0.955	0.350
Blood lead concentration (µg/dl)	6.0 (2.6)	5.8 (2.0)	6.0 (2.2)	0.268	0.791
Maternal Substance use during pregnancy					
Absolute alcohol/day (oz)	2.8 (2.4)	0.004 (0.01)	1.4 (2.2)	4.047	**0.001**
Absolute alcohol/occasion (oz)	6.6 (3.4)	0.2 (0.4)	3.4 (4.1)	6.479	**<0.001**
Frequency (days/week)	3.0 (1.4)	0.02 (0.1)	1.4 (1.7)	7.017	**<0.001**
Cigarettes/day	7.7 (7.5)	3.4 (4.4)	5.5 (6.4)	1.691	0.105

Values are Mean (SD). Bold print denotes significance at $p \leq 0.05$. WISC = Wechsler Intelligence Scale for Children. 1 oz absolute alcohol ≈ 2 standard drinks. *Of *N*=24, 23 primary caregivers were the biological mothers of the children, 1 (Control) was the grandmother. ♣(Hollingshead, 2011)(Hollingshead, 2011)Four Factor Index of Socio Economic Scale.

The sample characteristics are displayed in Table 5.1. There were no differences between the PAE and control groups for child sex, child age, primary caregiver education, mother's age at delivery, socio-economic status (SES), blood lead concentration (µg/dl) or the number of cigarettes smoked by the mother per day during pregnancy. Although below conventional levels of significance, total intracranial volume (TIV) tended to be smaller in the PAE children than controls. Children in the PAE group had lower IQ scores compared to controls and the mothers of these children on average drank more alcohol per day during pregnancy, both in terms of frequency and drinks per occasion. All but two mothers of the control children abstained from drinking: one drank 2 standard alcoholic beverages on one occasion, and the other drank 2 standard alcoholic beverages about once every month.

5.3.2 Association of the PJ task with % signal change

Table 5.2: Associations of the PJ task outcomes and % signal change in each ROI with potential confounders (*N* = 24)

	TIV		Child age		Sex of child[#]		SES		Cig/Day[*]		Lead exposure		WISC IQ	
	r	*p*	*r*	*p*	*r*	*p*	*r*	*p*	*r*	*p*	*r*	*p*	*r*	*p*
Trials attempted	0.420	**0.041**	0.344	**0.100**	-0.126	0.558	0.336	0.109	-0.232	0.275	-0.216	0.312	0.397	**0.055**
Trials correct	0.173	0.419	0.433	**0.035**	-0.296	0.160	0.456	**0.025**	0.310	0.141	-0.273	0.197	0.006	0.977
Accuracy (%)	-0.157	0.465	0.152	0.479	-0.191	0.370	0.200	0.349	0.486	**0.016**	-0.100	0.641	-0.295	0.161
Left IPS														
Sup. MIPS	0.025	0.906	-0.198	0.366	-0.136	0.527	0.160	0.455	-0.226	0.289	-0.021	0.923	0.449	**0.028**
Med. Branch MIPS	0.125	0.559	-0.164	0.443	-0.366	**0.079**	-0.017	0.937	-0.259	0.222	0.057	0.790	0.425	**0.038**
Inf. MIPS	0.356	**0.088**	0.091	0.674	-0.070	0.744	0.153	0.474	-0.202	0.344	-0.045	0.836	0.350	**0.094**
Sup. LIPS	0.178	0.406	-0.135	0.529	-0.167	0.434	0.137	0.522	-0.166	0.437	0.009	0.966	0.327	0.119
Inf. LIPS	0.316	0.133	-0.132	0.538	-0.135	0.530	0.152	0.480	-0.023	0.914	-0.063	0.769	0.323	0.123
Right IPS														
Sup. MIPS[*]	0.003	0.987	-0.181	0.398	-0.112	0.603	0.164	0.445	-0.078	0.716	-0.122	0.571	0.239	0.260
Med. Branch MIPS	-0.050	0.816	-0.268	0.205	-0.024	0.912	0.120	0.577	-0.273	0.197	-0.012	0.957	0.445	**0.029**
Inf. MIPS	0.241	0.257	-0.141	0.511	0.086	0.691	0.251	0.237	-0.011	0.959	-0.081	0.705	0.218	0.305
Sup. LIPS	0.042	0.845	-0.336	0.108	-0.043	0.841	0.095	0.657	-0.219	0.305	0.019	0.930	0.238	0.263
Inf. LIPS	0.113	0.600	-0.177	0.407	0.002	0.994	0.331	0.114	-0.176	0.409	0.040	0.853	0.021	0.921

Values are Pearson correlation coefficients; bold print denotes $p \leq 0.1$.

[*]One outlier recoded to one unit higher than next highest value (>3SD beyond the mean).

[#]For categorical variables, point biserial correlation was used.

Table 5.2 shows Pearson correlations of the outcome variables with potential confounders. Lead exposure was not associated with any of the outcome measures. Trials attempted and correct both showed association with child age. SES was only correlated with trials correct, sex with % signal change in the left medial branch of the MIPS, and cigarettes per day with accuracy. WISC IQ was associated with trials attempted and % signal change in various regions, specifically the left superior MIPS, left medial branch MIPS, left inferior MIPS and right medial branch MIPS, but not with trials correct or accuracy. TIV showed association with trials attempted and % signal change in left inferior MIPS.

Table 5.3: Comparison of the PJ task outcomes and % signal change in each ROI by diagnostic group (*N* = 24)

	EXPOSED (*n*=12)	CONTROL (*n*=12)		
	Mean (SD)	Mean (SD)	*t*	*p*
Trials attempted	46.1 (6.7)	49.6 (4.8)	-1.470	0.156
Trials correct	35.3 (4.7)	37.1 (6.4)	-0.759	0.456
Accuracy (%)	77.5 (10.8)	75.1 (12.8)	0.494	0.626
Left IPS				
Sup. MIPS	0.05 (0.27)	0.12 (0.22)	-0.709	0.486
Med. Branch MIPS	0.01 (0.27)	0.21 (0.38)	-1.489	0.151
Inf. MIPS	0.10 (0.20)	0.90 (0.21)	-1.021	0.319
Sup. LIPS	0.12 (0.23)	0.14 (0.16)	-0.219	0.829
Inf. LIPS	0.17 (0.23)	0.21 (0.20)	-0.351	0.729
Right IPS				
Sup. MIPS*	0.04 (0.23)	0.05 (0.16)	-0.147	0.884
Med. Branch MIPS	0.0002 (0.32)	0.20 (0.36)	-1.439	0.164
Inf. MIPS	0.07 (0.22)	0.12 (0.14)	-0.706	0.488
Sup. LIPS	0.12 (0.26)	0.14 (0.22)	-0.267	0.792
Inf. LIPS	0.17 (0.24)	0.15 (0.16)	0.176	0.862

*One outlier recoded to one unit higher than next highest value (>3 SD beyond the mean).

We did not find group differences on any of the outcome variables examined (Table 5.3, Figures 5.2-5.4). Within the PAE group, more frequent maternal drinking was associated with poorer accuracy on the PJ task, an effect that did not survive after adjustment for smoking (Table 5.4), and heavier maternal drinking per occasion with increasing activation during PJ in all the regions on the left and right medial walls of the IPS (Table 5.5, Figure 5.5). These associations got stronger after adjustment for IQ and other confounders. Averaged daily alcohol consumption (absolute alcohol (AA)/day) demonstrated similar associations with % signal change in a subset of the same regions, specifically bilateral medial branch of the MIPS and left superior MIPS (Figure 5.6). Although below conventional levels of significance, heavier alcohol consumption per occasion was also related to greater activation bilaterally in the superior lateral wall and right inferior lateral wall.

Table 5.4: Associations of PJ task outcomes with the level of prenatal alcohol exposure (*n* = 12)

	Absolute alcohol per day (oz AA/day)+	Absolute alcohol per occasion (oz AA/occasion)	Frequency of drinking (days/week)*	
	r (p)	*r (p)*	*r (p)*	*β^1 (p)*
Trials attempted [a, b, c]	0.179 (0.577)	0.238 (0.456)	0.270 (0.396)	0.157 (0.453)
Trials correct [b,d]	-0.011 (0.973)	0.355 (0.257)	-0.304 (0.336)	-0.171 (0.348)
Accuracy (%) [e]	-0.219 (0.493)	0.085 (0.793)	**-0.583 (0.047)**	-0.147 (0.446)

*2 outliers recoded to one unit higher than next highest value (>3SD beyond the mean); +Log transformed
r : Pearson correlation
β^1 : Controlling for [a]TIV; [b]Child age; [c]IQ; [d]SES, [e]Cig/day

Table 5.5: Associations of % signal change in each ROI with continuous measures of prenatal alcohol exposure (*n* = 12)

	Absolute alcohol per day (oz AA/day)+			Absolute alcohol per occasion (oz AA/occasion)		
	r (p)	*β^1 (p)*	*β^2 (p)*	*r (p)*	*β^1 (p)*	*β^2 (p)*
Left IPS						
Sup. MIPS	**0.589 (0.044)**	**0.661 (0.021)**	**0.626 (0.029)**	0.565 (0.056)	**0.629 (0.031)**	**0.691 (0.011)**
Med. Branch MIPS [a]	0.512 (0.089)	**0.587 (0.047)**	**0.693 (0.015)**	0.496 (0.101)	0.563 (0.058)	**0.686 (0.017)**
Inf. MIPS	0.122 (0.706)	0.228 (0.421)	0.281 (0.300)	0.490 (0.106)	**0.596 (0.014)**	**0.558 (0.018)**
Sup. LIPS	0.491 (0.105)	0.525 (0.102)	0.543 (0.113)	0.546 (0.066)	0.577 (0.066)	0.580 (0.085)
Inf. LIPS	-0.003 (0.994)	0.040 (0.906)	0.087 (0.799)	0.367 (0.241)	0.416 (0.196)	0.377 (0.249)
Right IPS						
Sup. MIPS*	0.404 (0.193)	0.461 (0.147)	0.466 (0.172)	**0.621 (0.031)**	**0.678 (0.019)**	**0.695 (0.024)**
Med. Branch MIPS	**0.695 (0.012)**	**0.772 (0.003)**	**0.749 (0.006)**	**0.617 (0.033)**	**0.684 (0.015)**	**0.735 (0.007)**
Inf. MIPS	0.454 (0.138)	0.485 (0.136)	0.525 (0.118)	**0.806 (0.002)**	**0.842 (0.001)**	**0.828 (0.003)**
Sup. LIPS	0.400 (0.198)	0.431 (0.191)	0.447 (0.205)	0.556 (0.061)	0.588 (0.060)	0.591 (0.078)
Inf. LIPS	0.458 (0.134)	0.447 (0.171)	0.487 (0.148)	**0.601 (0.039)**	0.593 (0.055)	0.573 (0.079)

*2 outliers recoded to one unit higher than next highest value (>3SD beyond the mean); +Log transformed; bold denotes significance at $p \leq 0.05$.
r : Pearson correlation
β^1 : Controlling for IQ
β^2 : Controlling for IQ and [a]Sex of child; TIV

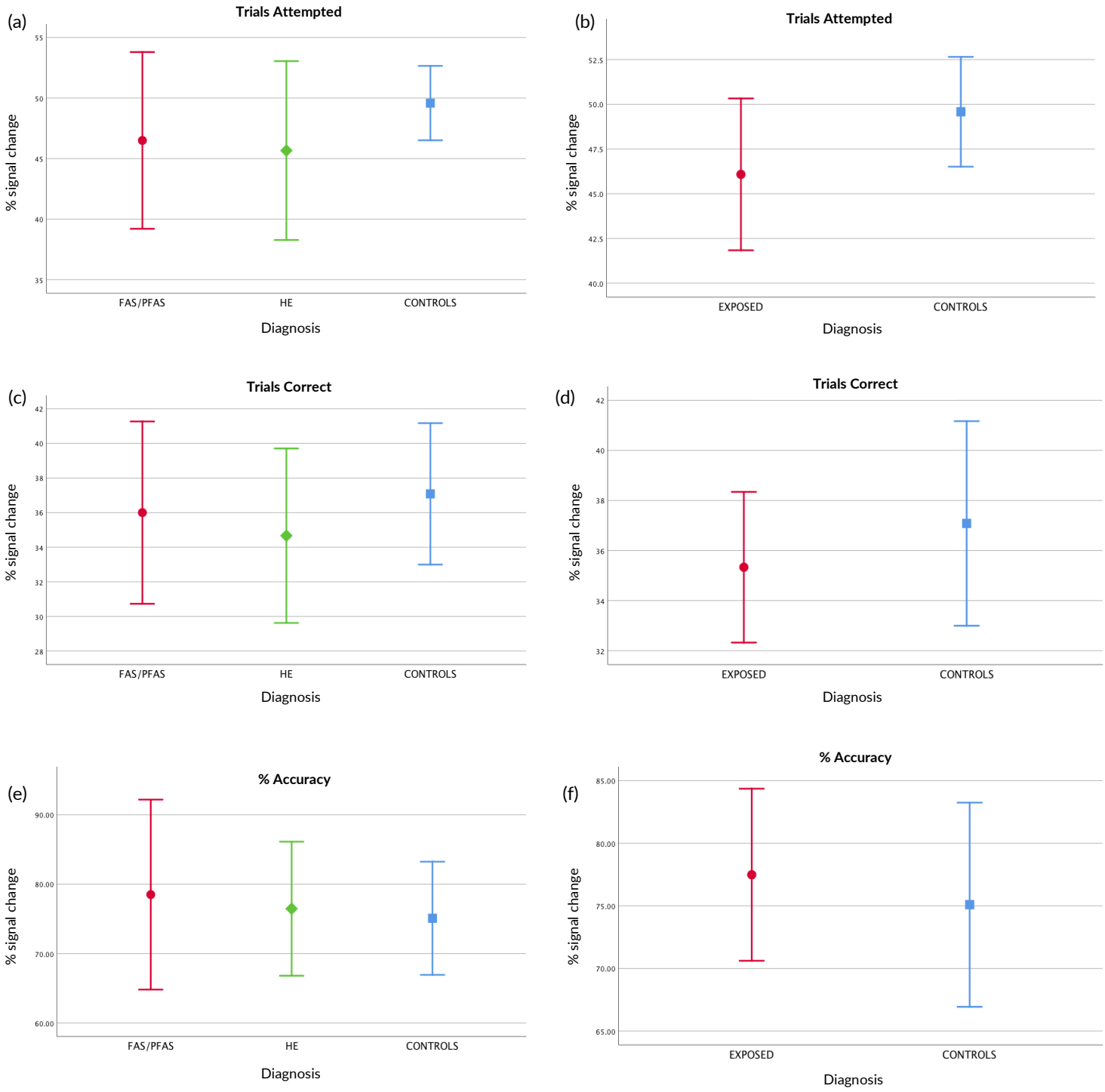

Figure 5.2: Mean and 95% CI's of PJ task outcomes by diagnosis. (a) and (b) Trials attempted; (c) and (d) Trials correct; and (e) and (f) % Accuracy. Plots in the left column show the data by diagnostic groups and plots on the right with FAS/PFAS and HE children combined into a single group.

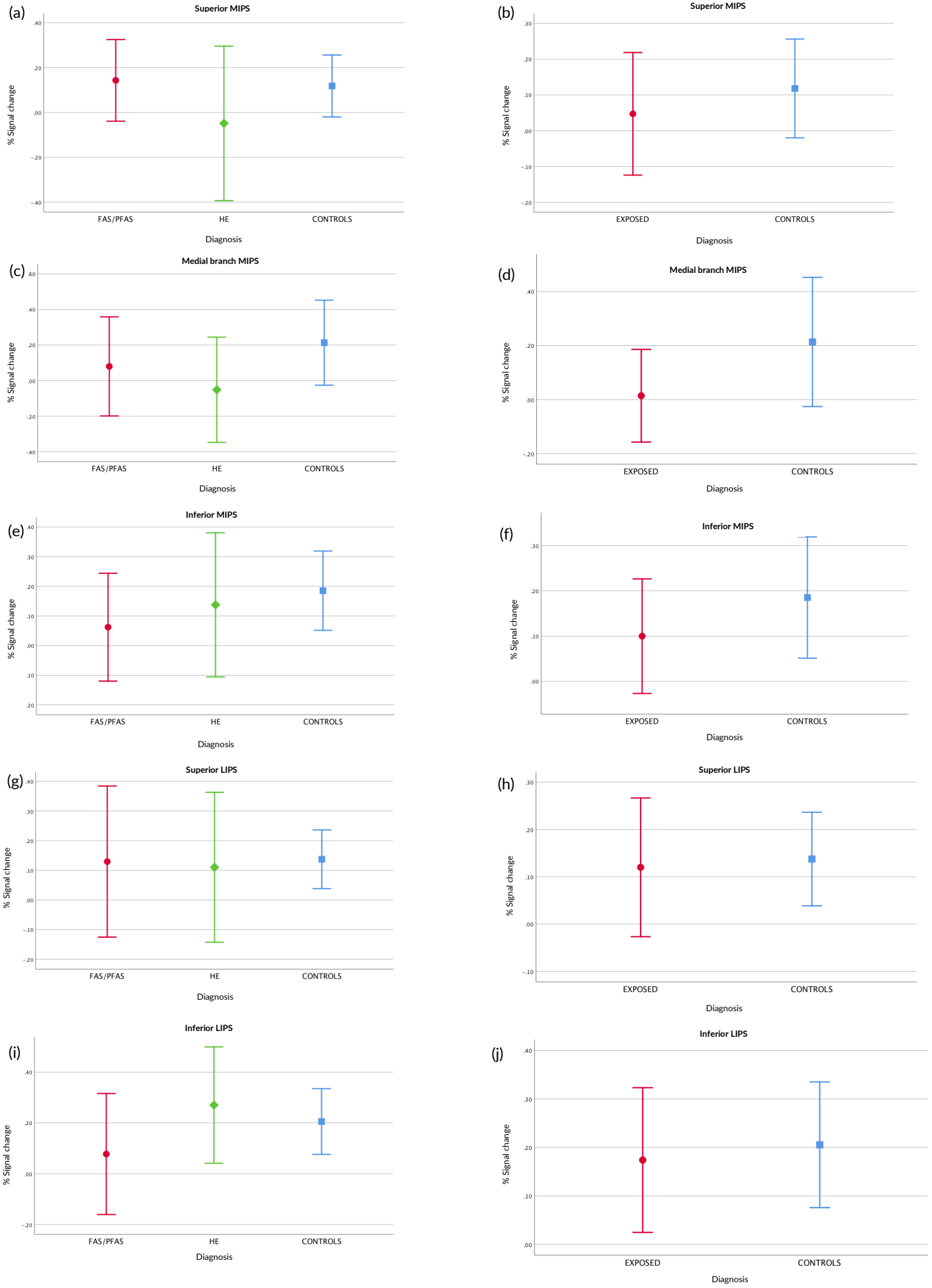

Figure 5.3: Mean and 95% CI's of % signal change during PJ (relative to a control condition) in each ROI in the left hemisphere. (a) and (b) Superior MIPS ; (c) and (d) Medial branch MIPS; (e) and (f) Inferior MIPS; (g) and (h) Superior LIPS; (i) and (j) Inferior LIPS. Plots in the left column show the data by diagnostic groups and plots on the right with FAS/PFAS and HE children combined into a single group.

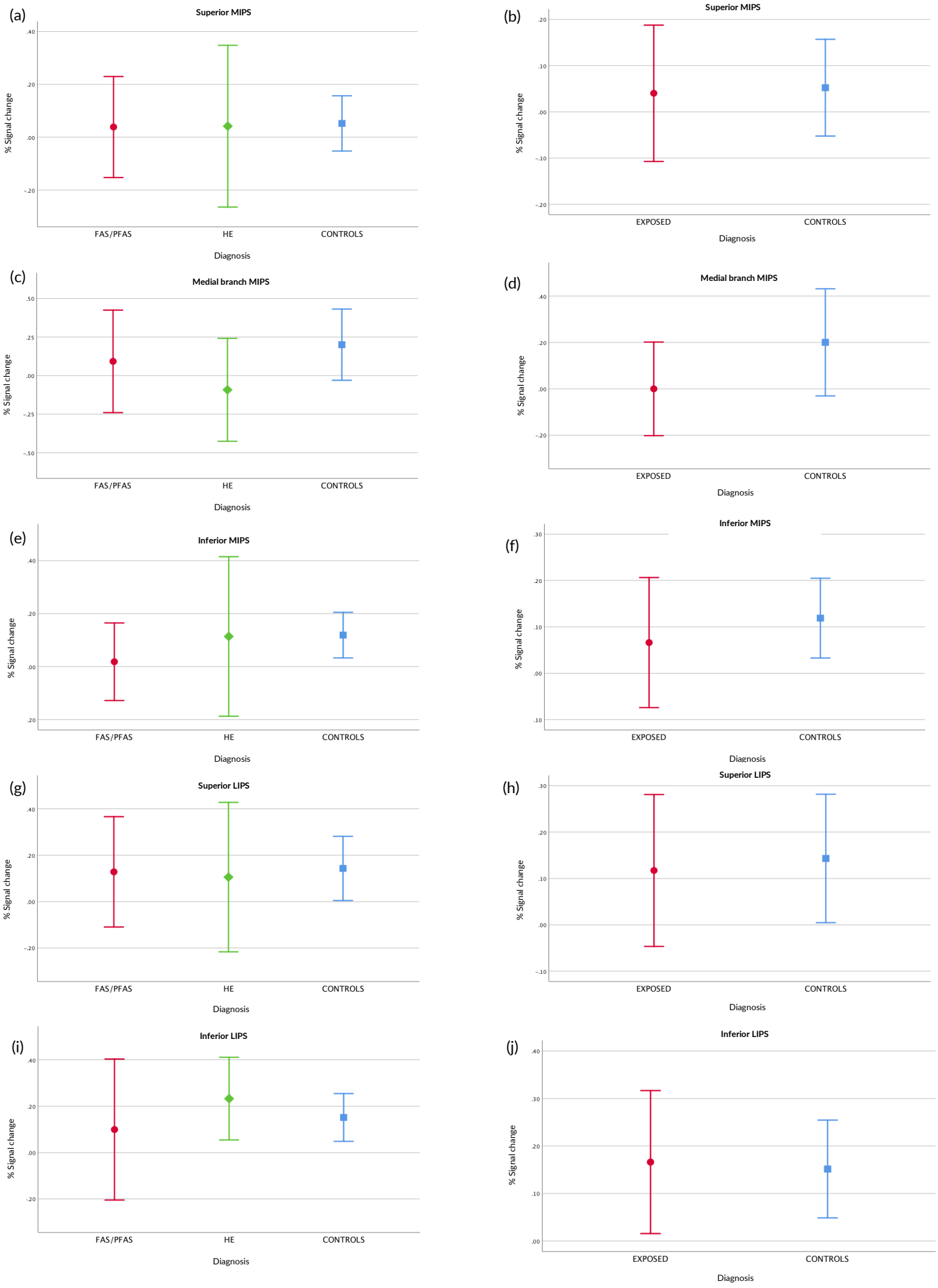

Figure 5.4: Mean and 95% CI's of % signal change during PJ (relative to a control condition) in each ROI in the right hemisphere. (a) and (b) Superior MIPS ; (c) and (d) Medial branch MIPS; (e) and (f) Inferior MIPS; (g) and (h) Superior LIPS; (i) and (j) Inferior LIPS. Plots in the left column show the data by diagnostic groups and plots on the right with FAS/PFAS and HE children combined into a single group.

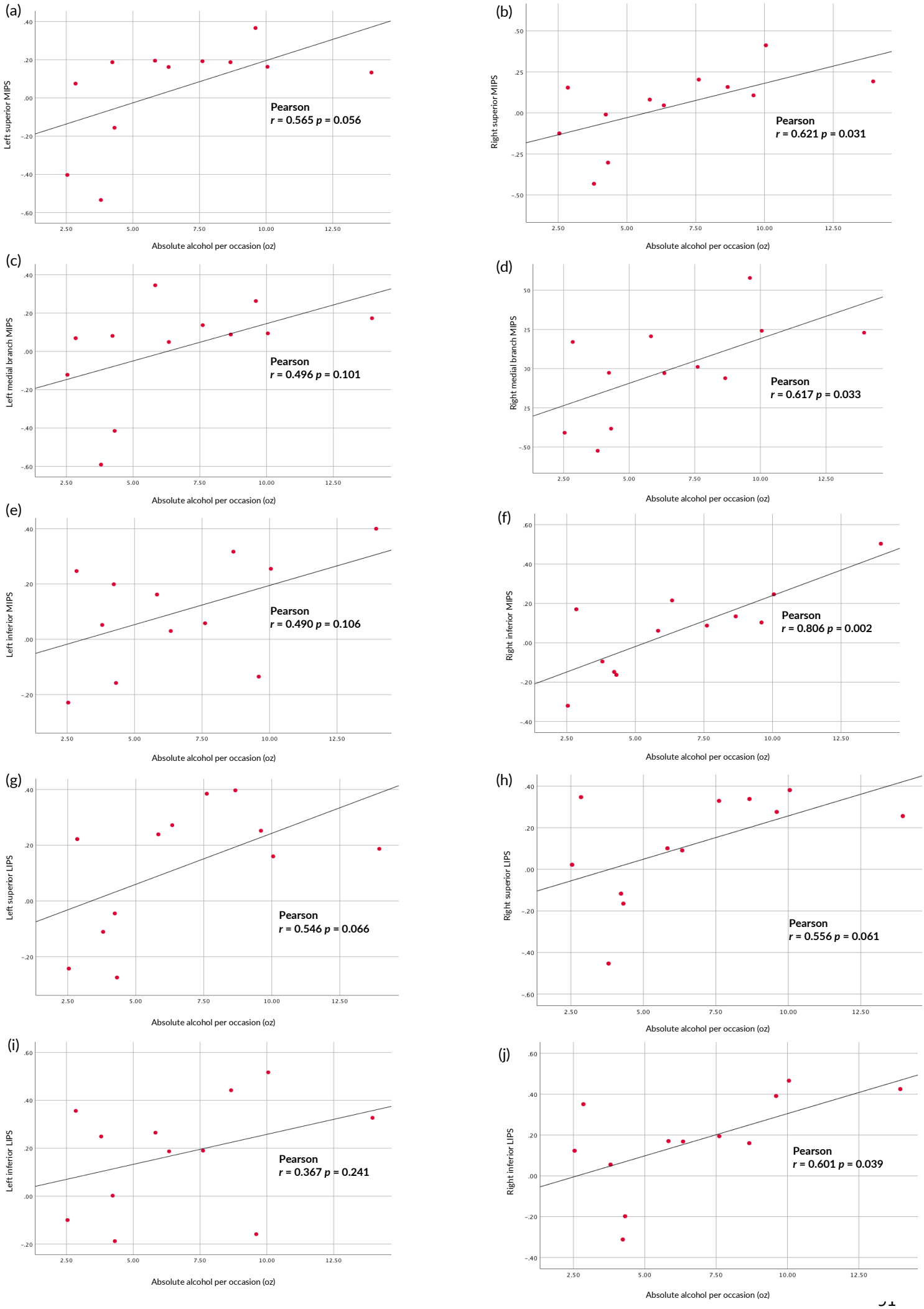

Figure 5.5: Plots showing % signal change during proximity judgement (relative to a control condition) in each ROI as a function of the amount of alcohol the mother consumed per drinking occasion during pregnancy.

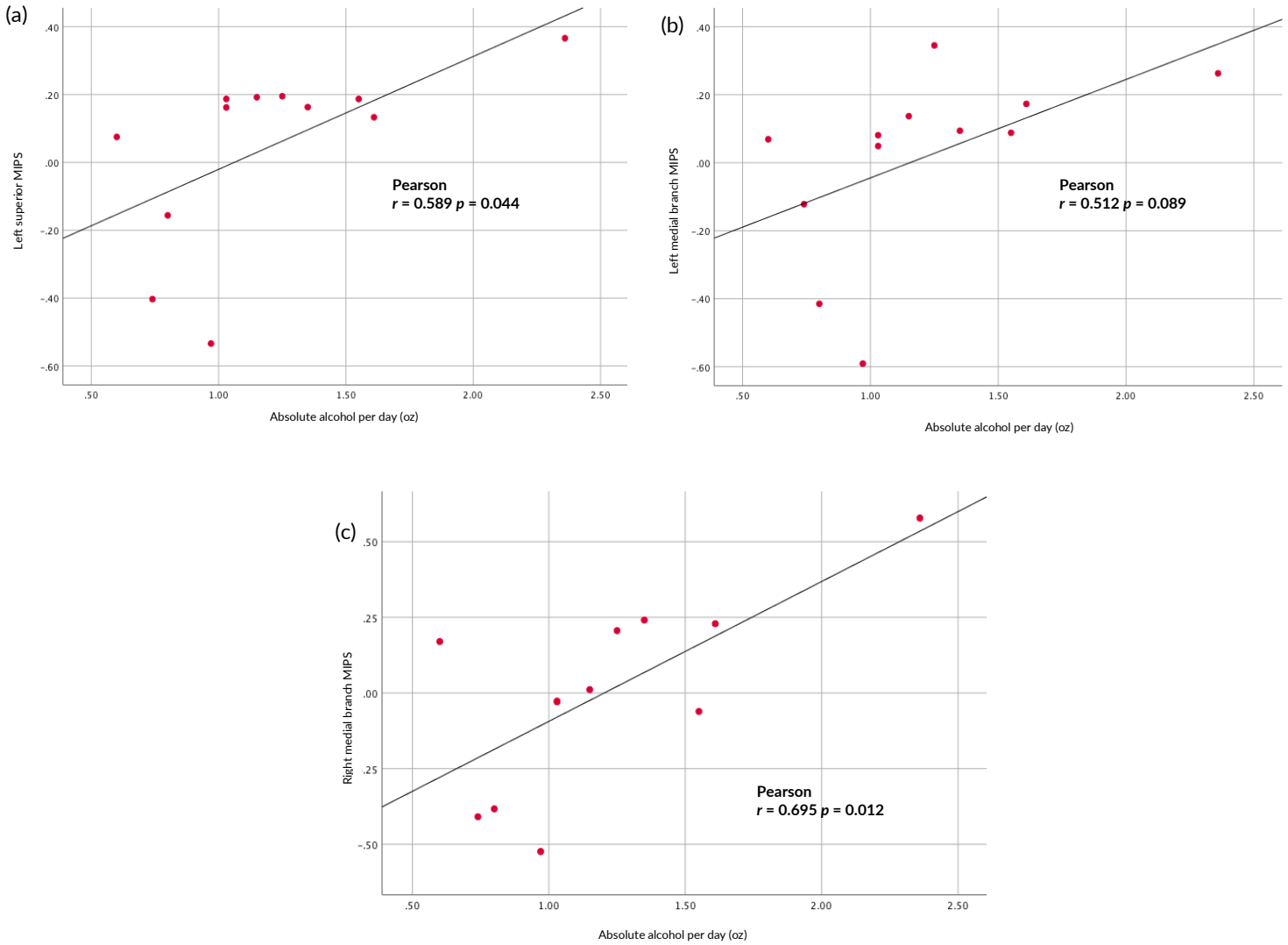

Figure 6.6: Plots showing % signal change during proximity judgment (relative to a control condition) in the (a) Left superior MIPS, (b) Left medial branch of the MIPS, and (c) Right medial branch of the MIPS as a function of the amount of alcohol the mother consumed per day during pregnancy.

5.4 Discussion

In this study, we examined effects of PAE on brain activation during proximity judgement separately in subsections of the medial and lateral walls of the IPS cortex that were defined anatomically in each subject, thereby reducing effects of inter-subject anatomical variability. Despite the absence of group differences in performance or activation in any of the regions, we found within the PAE children that heavier maternal drinking per occasion during pregnancy was related to increased activation in all the subsections of both the left and right medial walls, including the medial branch.

The lack of differences in the PJ task outcomes were not surprising as the task had purposefully been made simple to ensure that the exposed children were able to complete it and achieve acceptable scores (Meintjes *et al.*, 2010b).

Previously we observed both PAE-related activation increases and decreases in the IPS during number processing in children from the same cohort. In a voxelwise analysis, we found greater activation during PJ in the left anterior IPS in children with FAS/PFAS compared to controls, but lower activation in the right posterior IPS (Meintjes *et al.*, 2010b), while region-of-interest analyses showed PAE-related activation decreases of the ROI within the right anterior IPS during exact addition, PJ (Woods *et al.*, 2015) and non-symbolic number comparison (Woods *et al.*, 2018). It is difficult to directly compare the current findings of PAE-related activation increases during PJ on the medial walls of the IPS, as the anatomical subdivisions used here are very different to the anterior and posterior regions where changes were previously observed. It is possible that activation decreases may be present in anterior regions and increases in posterior regions, which would not be detectable here as time courses were averaged along the entire length of the subdivisions. It is striking, however, that PAE effects were evident bilaterally here, while the right IPS appeared to show more effects of PAE on earlier studies.

Activation increases have been attributed to blood flow abnormalities (Tapert *et al.*, 2004) and compensatory mechanisms. FAS/PFAS individuals, for example, recruited more parietal areas when performing the same PJ task than healthy individuals who chiefly recruited the anterior portion of the IPS (Meintjes *et al.*, 2010b). The activation increases observed in the present study may, therefore, be due to more diffuse and widespread activation of the IPS, which would not have been evident in the analysis where activation was examined only within a spherical ROI (radius 6 mm) placed in the anterior IPS. Although not prenatally exposed, chronic heavy drinkers have also been

shown to use compensatory methods when performing cognitive processes (Pfefferbaum *et al.*, 2001).

In the present study activation in more regions showed association with the amount of alcohol the mother consumed per occasion during pregnancy, than averaged daily consumption. Binge drinking is known to be particularly prevalent in the communities from which the children in this study were recruited, with social weekend drinking being the norm (May *et al.*, 2007). The current findings suggest that binge drinking may be particularly harmful to the developing fetus. Myelin damage has been observed in the pups of pregnant binge-drinking rats (Cantacorps *et al.*, 2017). Myelin damage may play a role here, affecting connections between regions required during number processing, and leading to compensatory activation increases.

Interestingly, the medial branch off the MIPS bilaterally showed association with both averaged daily alcohol consumption and consumption per occasion, effects that survived after controlling for IQ and other potential confounders. This finding suggests that this region is sensitive to PAE, irrespective of whether the exposure occurs periodically in high doses or continuously during gestation. The posterior superior parietal lobules, which form part of the parietal number processing circuit identified by Dehaene *et al.*, (2003), appears to partly overlap with our traced medial branch of the MIPS. Because this area supports the maintenance of attention during number processing, greater activation of this region suggests that PAE children need to engage more attentional resources to complete the PJ task.

Although the small sample size is a limitation of the current study, the anatomical approach used here may increase sensitivity by accounting for inter-subject anatomical variability. The children in the sample also come from a socioeconomically disadvantaged community and may not be comparable with children from other less disadvantaged communities.

This study extends the existing literature on the effects of PAE on IPS function during number processing, by revealing that medial wall function is particularly affected, and that binge drinking appears to be more harmful to the IPS.

Chapter 6

DISCUSSION AND CONCLUSION

Prenatal alcohol exposure (PAE) has long been a problem in the Western Cape region of South Africa. Fetal alcohol spectrum disorders (FASD) are preventable but factors such as socio-economic status (SES) and family life can influence mothers to consume copious amounts of alcohol while pregnant. That alcohol has teratogenic effects on the brain is well established, and research is still ongoing. Effects of PAE have been observed in the parietal lobe, including the intraparietal sulcus (IPS) cortex and its functions. The IPS plays a role in visuospatial functions which have been linked to basic arithmetic in children and adults, and PAE has been shown to exert effects on this functioning of the sulcus.

The first study examined the morphology of the IPS and designed a novel manual parcellation method for the sulcal cortex for volume rendering. The IPS shows between-subject variability in addition to inter-hemispheric variability. In cognisance of the variation, a consistent protocol for manual tracing was designed and used to examine sulcal volume and morphology in PAE children and control subjects. Only the volume of the left lateral wall of the IPS (LIPS) was associated with PAE, while the medial walls of the sulcus (MIPS) bilaterally were associated with WISC arithmetic scaled scores. These findings agree with previous literature showing reduced regional brain volumes in children with PAE, but suggest that the observed effects of PAE on math ability are not moderated by sulcal volume.

The second study compared an automated method, FreeSurfer, and the custom-designed manual method mentioned above for parcellating the IPS. Automated programmes like FreeSurfer are widely used for volumetric measurements of cortical and subcortical structures in the brain using atlases based on the brains of healthy individuals. Manual tracing is generally regarded as the 'gold-standard' because expert neuroanatomists meticulously perform the parcellation slice by slice. FreeSurfer produces a single volume output for the entire IPS cortex whereas the manual protocol used here was able to measure the walls of the sulcus (LIPS and MIPS) separately. The manual method showed a moderate level of reproducibility, indicating a need for some refining of the protocol. The way the sulcus was parcellated by each method was different as FreeSurfer's atlas included a inconstant 'transverse parietal sulcus' which was not included in the manual protocol. Although the two methods are not anatomically identical, the association of volume with PAE was observed using both methods, suggesting that either method would be suitable for examining the volume of the IPS. Manual parcellation, however, provides an advantage over the automated method in that it permits subdivision of the sulcus into anatomical regions of interest (ROI) which may provide more sensitive results.

The final study used fMRI to analyse the effects of PAE on activation of the IPS cortex in the performance of a Proximity Judgement (PJ) task. Using the previous manual parcellation of the MIPS and LIPS, each wall was subdivided into smaller ROIs bilaterally, namely: (1) the superior MIPS, (2) the medial branch of the MIPS, (3) the inferior MIPS, (4) the superior LIPS, and (5) the inferior LIPS. Activation of the IPS in performance of the PJ task was observed to be affected by PAE. The findings were, however, contrary to what was expected in that increased PAE was associated with greater activation of the bilateral IPS. This observation suggests that compensation may occur in the IPS in PAE individuals, .

The complicated love triangle in the IPS cortex: anatomy, visuo-spatiality and arithmetic

The IPS cortex is a small part of the entire cortex, but exhibits an impressive intricacy of function and anatomical morphology. This sulcus is responsible for a range of visuospatial functions, from grasping to object location and visual signals (Clark, Boutros and Mendez, 2010). All three studies suggest that the PAE may exert a stronger effect on left than right IPS volume. By contrast, PAE was associated with altered activation of the right IPS when performing magnitude comparison tasks, while this sensitivity was not observed on the left hemisphere. In the medial branch of the MIPS included in our manual tracing both volume and activation were observed to be associated with mathematical performance.

Little previous research has focused in detail on the volume of the cortex of the IPS. Investigation of grey matter abnormalities in children with PAE found these predominantly in the left hemisphere (Sowell *et al.*, 2001). The left IPS has been implicated as a crucial area that is activated during number processing (Vogel *et al.*, 2017) and it has been shown to become more skilled at certain arithmetic tasks as age progresses (Matejko, Hutchison and Ansari, 2019). It is interesting then that the volumetric changes found in left LIPS were not associated with the numerical functioning of the PAE children. Although the left cortical volume may be sensitive to PAE, the mathematical function on the left was not observed to be similarly affected. We investigated only one of the many functions of the IPS. Therefore, the volumetric morphology may have an effect on a visuospatial function other than the mathematical one. The left LIPS contains the cortical areas responsible for control of grasping, and PAE children have been shown to have deficits when conducting these fine-motor movements (Simmons *et al.*, 2012). It is possible that these deficits are moderated by altered anatomical morphology.

Despite no significant morphological change in the right IPS, altered activation of this region was observed in children with PAE when they performed a proximity judgement (PJ) task. This sensitivity is in accordance with previous fMRI studies of children with PAE during number processing (Meintjes *et al.*, 2010; Woods *et al.*, 2015, 2018). In agreement with our results, the right IPS has also been implicated specifically when performing magnitude comparison tasks (Dehaene *et al.*, 2003). The current results, however, are in contrast to previous research in that greater PAE was associated with increased activation. A possible explanation for this is that the IPS may have a compensatory mechanism by recruiting more neurons for numerical tasks as FAS/PFAS individuals have been shown to also recruit more parietal areas in this instance (Meintjes *et al.*, 2010).

The medial branch of the MIPS that we included in our tracing protocol yielded interesting findings. This medial branch may form part of the area that Dehaene *et al.*, (2003) mentioned as the posterior superior parietal lobule (PSPL) in their parietal circuit for number processing. Larger MIPS volumes bilaterally were associated with higher arithmetic scores and increase in activation of the medial branch of the MIPS was strongly associated with PAE when subjects performed a PJ task. These results suggest that the consistently present medial branch may be the most sensitive of the IPS subdivisions to PAE. Number processing in this region, however, does not appear to be affected. Although larger volumes were associated with better scores, the smaller volume of this area in the PAE children was not associated with weaker activation. This supports the conclusion that IPS volume does not moderate the effects of PAE on arithmetic function.

From Turner to present: how knowledge of the anatomy of the IPS has changed

The manual parcellation protocol used in these studies was designed following extensive examination of the anatomy of the sulcus, and attempted to consistently trace the same regions of the sulcus for all subjects. To the author's knowledge, no previous studies have used a similar protocol. Previous studies using manual segmentation for volumetric measurements have typically only looked at subcortical structures (Randall *et al.*, 2017; Biffen *et al.*, 2018; Warton *et al.*, 2018). It was therefore difficult to design a protocol for manually parcellating an extremely variable structure such as a sulcus. In this the extensive work of past anatomists proved invaluable (Turner, 1866; Cunningham, 1890). Although the postcentral sulcus (PCS) is no longer considered to form part of the IPS, as previously described by Cunningham and Turner, Cunningham's classifications of the variations of the IPS are still essentially valid today. For obvious reasons, Cunningham and Turner were not able to use imaging and relied on examining the surface cortex in the dissections of cadaver brains. MRI now allows us to examine brain structures and their exact morphology in greater depth.

Researchers in a range of fields use imaging modalities to draw conclusions on brain function and structure. It is now possible to investigate brain structure without expertise in neuroanatomy. The current studies, however, reinforce the importance of expert neuroanatomists in imaging research and especially in studies that involve the manual parcellation of structures.

The comparison between manual and automated segmentation demonstrated a marked variation in how different atlases and researchers delineate structures in the brain. In the adult atlas used for the current study, the authors included a sulcal branch that is not consistently present in all subjects, and that may affect volumetric measurements (Destrieux *et al.*, 2010). It is also essential that more reliable pediatric atlases be developed, that account for the differences between adult and developing brains, as well as for pathologies that may alter brain morphology.

The aim of this project was to use neuroimaging data acquired from an ongoing study of children prenatally exposed to alcohol to investigate alterations in cortical volume of the IPS, and to assess the potential role of these alterations on number processing. PAE is a world-wide problem with a particularly high incidence in the Western Cape province of South Africa (Jacobson *et al.*, 2006, 2008). From its first formal description in 1973 (Jones and Smith, 1973), understanding of the neurological correlates of FASD has grown extensively. The current findings, in agreement with previous studies, demonstrate that PAE is associated with both structural and functional changes in the brain. While the morphology of the IPS may not moderate the effects of PAE on arithmetic function, some cortical volumes within the IPS were sensitive to PAE. Moreover, altered activation of the IPS in the performance of magnitude comparison tasks was strongly associated with PAE. The IPS is an extremely variable structure whose anatomy is often misunderstood, which emphasises the importance of anatomical knowledge for imaging studies. Future research will refine the protocol for manual tracing of the IPS, which may lead to greater understanding of the functions of the different areas. It is to be hoped that these findings will give more insight into understanding the functioning of children and adults with FASDs and contribute to more effective therapeutic interventions for these individuals.

References

Anonymous (1909) 'DANIEL JOHN CUNNINGHAM, M.D., F.R.S', *British Medical Journal*, 2(2531), pp. 1–57. doi: 10.1136/bmj.2.2531.1.

Amaro, E. and Barker, G. J. (2006) 'Study design in fMRI: Basic principles', *Brain and Cognition*, 60(3), pp. 220–232. doi: 10.1016/j.bandc.2005.11.009.

Andersen, R. A. (1997) 'Multimodal integration for the representation of space in the posterior parietal cortex', *Philosophical Transactions of the Royal Society B: Biological Sciences*, 352(1360), pp. 1421–1428. doi: 10.1098/rstb.1997.0128.

Annett, M. (1970) 'A classification of hand preference by association analysis.', *British journal of psychology (London, England : 1953)*, 61(3), pp. 303–21. Available at: http://www.ncbi.nlm.nih.gov/pubmed/5457503.

Archibald, S. L., Fennema-Notestine, C., Gamst, a, Riley, E. P., *et al.* (2001) 'Brain dysmorphology in individuals with severe prenatal alcohol exposure.', *Developmental medicine and child neurology*, 43(3), pp. 148–154. doi: 10.1097/00004703-200110000-00024.

Ashkenazi, S., Henik, A., Ifergane, G. and Shelef, I. (2008) 'Basic numerical processing in left intraparietal sulcus (IPS) acalculia.', *Cortex; a journal devoted to the study of the nervous system and behavior*, 44(4), pp. 439–48. doi: 10.1016/j.cortex.2007.08.008.

Beck, B., Bertini, C., Haggard, P. and Làdavas, E. (2015) 'Dissociable routes for personal and interpersonal visual enhancement of touch', *Cortex*, 73, pp. 289–297. doi: 10.1016/j.cortex.2015.09.008.

Bergouignan, L., Chupin, M., Czechowska, Y., Kinkingnéhun, S., *et al.* (2009) 'Can voxel based morphometry, manual segmentation and automated segmentation equally detect hippocampal volume differences in acute depression?', *NeuroImage*, 45(1), pp. 29–37. doi: 10.1016/j.neuroimage.2008.11.006.

Bertrand, J., Floyd, L. L., Weber, M. K. and Fetal Alcohol Syndrome Prevention Team, Division of Birth Defects and Developmental Disabilities, National Center on Birth Defects and Developmental Disabilities, C. for D. C. and P. (CDC) (2005) 'Guidelines for identifying and referring persons with fetal alcohol syndrome.', *MMWR. Recommendations and reports : Morbidity and mortality weekly report. Recommendations and reports*, 54(RR-11), pp. 1–14. Available at: http://www.ncbi.nlm.nih.gov/pubmed/16251866.

Biffen, S. C., Warton, C. M. R., Lindinger, N. M., Randall, S. R., *et al.* (2018) 'Reductions in Corpus Callosum Volume Partially Mediate Effects of Prenatal Alcohol Exposure on IQ', *Frontiers in Neuroanatomy*, 11(January), pp. 1–12. doi: 10.3389/fnana.2017.00132.

Bigler, E. D., Abildskov, T. J., Wilde, E. A., McCauley, S. R., *et al.* (2010) 'Diffuse damage in pediatric traumatic brain injury: A comparison of automated versus operator-controlled quantification methods', *NeuroImage*. Elsevier Inc., 50(3), pp. 1017–1026. doi: 10.1016/j.neuroimage.2010.01.003.

Binkofski, F. C., Klann, J. and Caspers, S. (2016) 'On the Neuroanatomy and Functional Role of the Inferior Parietal Lobule and Intraparietal Sulcus', in *Neurobiology of Language*. Elsevier, pp. 35–47. doi: 10.1016/B978-0-12-407794-2.00004-3.

Blair, P. and O'Connor, M. J. (2007) 'Neurocognitive and neurobehavioural impairments in individuals with fetal alcohol spectrum disorders: Recognition and assessment', pp. 127–142.

Bowman, R. S., Stein, L. I. and Newton, J. R. (1975) 'Measurement and interpretation of drinking behavior. I. On measuring patterns of alcohol consumption. II. Relationships between drinking behavior and social adjustment in a sample of problem drinkers.', *Journal of Studies on Alcohol*, 36(9), pp. 1154–1172. doi: 10.15288/jsa.1975.36.1154.

Bremmer, F. (2005) 'Navigation in space - The role of the macaque ventral intraparietal area', *Journal of Physiology*, 566(1), pp. 29–35. doi: 10.1113/jphysiol.2005.082552.

Bremmer, F., Schlack, A., Shah, N. J., Zafiris, O., *et al.* (2001) 'Polymodal Motion Processing in Posterior Parietal and Premotor Cortex', *Neuron*, 29(1), pp. 287–296. doi: 10.1016/S0896-6273(01)00198-2.

Bugden, S. and Ansari, D. (2011) 'Individual differences in children's mathematical competence are related to the intentional but not automatic processing of Arabic numerals', *Cognition*, 118(1), pp. 32–44. doi: 10.1016/j.cognition.2010.09.005.

Bugden, S., Price, G. R., McLean, D. A. and Ansari, D. (2012) 'The role of the left intraparietal sulcus in the relationship between symbolic number processing and children's arithmetic competence', *Developmental Cognitive Neuroscience*, 2(4), pp. 448–457. doi: 10.1016/j.dcn.2012.04.001.

Burden, M. J., Jacobson, S. W., Sokol, R. J. and Jacobson, J. L. (2005) 'Effects of prenatal alcohol exposure on attention and working memory at 7.5 years of age', *Alcohol Clin Exp Res*, 29(3), pp. 443–452. doi: 00000374-200503000-00020 [pii].

Buxbaum, L. J., Kyle, K., Grossman, M. and Coslett, H. B. (2007) 'Left inferior parietal representations for skilled hand-object interactions: Evidence from stroke and corticobasal degeneration', *Cortex*, 43(3), pp. 411–423. doi: 10.1016/S0010-9452(08)70466-0.

Cantacorps, L., Alfonso-Loeches, S., Moscoso-Castro, M., Cuitavi, J., *et al.* (2017) 'Maternal alcohol binge drinking induces persistent neuroinflammation associated with myelin damage and behavioural dysfunctions in offspring mice', *Neuropharmacology*, 123, pp. 368–384. doi: 10.1016/j.neuropharm.2017.05.034.

Cardenas, V. A., Price, M., Infante, M. A., Moore, E. M., *et al.* (2014) 'Automated cerebellar segmentation: Validation and application to detect smaller volumes in children prenatally exposed to alcohol', *NeuroImage: Clinical*, 4, pp. 295–301. doi: 10.1016/j.nicl.2014.01.002.

Caspers, S. and Zilles, K. (2018) 'Microarchitecture and connectivity of the parietal lobe', in *Handbook of Clinical Neurology*. Vol. 151, pp. 53–72. doi: 10.1016/B978-0-444-63622-5.00003-6.

Cherbuin, N., Anstey, K. J., Réglade-Meslin, C. and Sachdev, P. S. (2009) 'In Vivo Hippocampal Measurement and Memory: A Comparison of Manual Tracing and Automated Segmentation in a Large Community-Based Sample', *PLoS ONE*. Edited by M. W. Greenlee, 4(4), p. e5265. doi: 10.1371/journal.pone.0005265.

Chiodo, L. M., Jacobson, S. W. and Jacobson, J. L. (2004) 'Neurodevelopmental effects of postnatal lead exposure at very low levels', *Neurotoxicology and Teratology*, 26(3), pp. 359–371. doi: 10.1016/j.ntt.2004.01.010.

Clark, D. L., Boutros, N. N. and Mendez, M. F. (2010) *The Brain and Behavior: An Introduction to Behavioral Neuroanatomy*, *American Journal of Psychiatry*. New York: Cambridge University Press. Available at: http://ajp.psychiatryonline.org/article.aspx?articleID=98964 (Accessed: 14 June 2013).

Clarren, S. K. and Smith, D. W. (1978) 'The fetal alcohol syndrome.', *The Lamp*, 35(10), pp. 4–7. Available at: http://www.ncbi.nlm.nih.gov/pubmed/251812.

Cohen, L. and Dehaene, S. (1995) 'Number processing in pure alexia: The effect of hemispheric asymmetries and task demands', *Neurocase*, 1(2), pp. 121–137. doi: 10.1080/13554799508402356.

Coles, C. D. and Li, Z. (2011) 'Functional Neuroimaging in the Examination of Effects of Prenatal Alcohol Exposure', *Neuropsychology Review*, 21(2), pp. 119–132. doi: 10.1007/s11065-011-9165-y.

Connolly, J. D., Andersen, R. A. and Goodale, M. A. (2003) 'FMRI evidence for a "parietal reach region" in the human brain', *Experimental Brain Research*, 153(2), pp. 140–145. doi: 10.1007/s00221-003-1587-1.

Cooke, D. F., Taylor, C. S. R., Moore, T. and Graziano, M. S. A. (2003) 'Complex movements evoked by microstimulation of the ventral intraparietal area', *Proceedings of the National Academy of Sciences*, 100(10), pp. 6163–6168. doi: 10.1073/pnas.1031751100.

Coull, J. T. and Frith, C. D. (1998) 'Differential activation of right superior parietal cortex and intraparietal sulcus by spatial and nonspatial attention.', *NeuroImage*, 8(2), pp. 176–87. doi: 10.1006/nimg.1998.0354.

Crossman, A. and Neary, D. (2014) *Neuroanatomy: an Illustrated Colour Text*. Elsevier.

Croxford, J. and Viljoen, D. (1999) 'Alcohol consumption by pregnant women in the Western Cape', *South African Medical Journal*, 89(9), pp. 962–965. doi: 10.1046/j.1464-5491.1999.00150.x.

Culham, J. C. and Kanwisher, N. G. (2001) 'Neuroimaging of cognitive functions in human parietal cortex', pp. 157–163.

Culham, J. C. and Valyear, K. F. (2006) 'Human parietal cortex in action', pp. 205–212. doi: 10.1016/j.conb.2006.03.005.

Cunningham, D. J. (1890) 'Intraparietal Sulcus of the Brain.', *Journal of anatomy and physiology*, 24(Pt 2), pp. 135–55. Available at: http://www.ncbi.nlm.nih.gov/pubmed/1328036 (Accessed: 26 August 2014).

Cunningham, D. J. (1892) 'Contribution to the Surface Anatomy of the Cerebral Hemispheres', *Royal Irish Academy*, 30(7), p. 372. Available at: http://www.pubmedcentral.nih.gov/articlerender.fcgi?artid=265531&tool=pmcentrez&rendertype=abstract (Accessed: 2 November 2014).

Darnell, D. and Gilbert, S. F. (2017) 'Neuroembryology', *Wiley Interdisciplinary Reviews: Developmental Biology*, 6(1), p. e215. doi: 10.1002/wdev.215.

De Smedt, B., Noël, M.-P., Gilmore, C. and Ansari, D. (2013) 'How do symbolic and non-symbolic numerical magnitude processing skills relate to individual differences in children's mathematical skills? A review of evidence from brain and behavior', *Trends in Neuroscience and Education*, 2(2), pp. 48–55. doi: 10.1016/j.tine.2013.06.001.

Dehaene, S. (2009) 'Origins of Mathematical Intuitions', *Annals of the New York Academy of Sciences*, 1156(1), pp. 232–259. doi: 10.1111/j.1749-6632.2009.04469.x.

Dehaene, S. and Cohen, L. (1995) 'Towards an anatomical and functional model of number processing', *Mathematical Cognition*, pp. 83–120.

Dehaene, S., Molko, N., Cohen, L. and Wilson, A. J. (2004) 'Arithmetic and the brain', *Current Opinion in Neurobiology*, 14(2), pp. 218–224. doi: 10.1016/j.conb.2004.03.008.

Dehaene, S., Piazza, M., Pinel, P. and Cohen, L. (2003) 'Three parietal circuits for number processing.', *Cognitive neuropsychology*, 20(3), pp. 487–506. doi: 10.1080/02643290244000239.

Delazer, M., Domahs, F., Bartha, L., Brenneis, C., *et al.* (2003) 'Learning complex arithmetic - An fMRI study', *Cognitive Brain Research*, 18(1), pp. 76–88. doi: 10.1016/j.cogbrainres.2003.09.005.

Desikan, R. S., Ségonne, F., Fischl, B., Quinn, B. T., *et al.* (2006) 'An automated labeling system for subdividing the human cerebral cortex on MRI scans into gyral based regions of interest', *NeuroImage*, 31(3), pp. 968–980. doi: 10.1016/j.neuroimage.2006.01.021.

Destrieux, C., Fischl, B., Dale, A. and Halgren, E. (2010) 'Automatic parcellation of human cortical gyri and sulci using standard anatomical nomenclature', *NeuroImage*, 53(1), pp. 1–15. doi: 10.1016/j.neuroimage.2010.06.010.

Dewey, J., Hana, G., Russell, T., Price, J., *et al.* (2010) 'Reliability and validity of MRI-based automated volumetry software relative to auto-assisted manual measurement of subcortical structures in HIV-infected patients from a multisite study', *NeuroImage*, 51(4), pp. 1334–1344. doi: 10.1016/j.neuroimage.2010.03.033.

Dodge, N. C., Jacobson, J. L., Molteno, C. D., Meintjes, E. M., *et al.* (2009) 'Prenatal Alcohol Exposure and Interhemispheric Transfer of Tactile Information: Detroit and Cape Town Findings', *Alcoholism: Clinical and Experimental Research*, 33(9), pp. 1628–1637. doi: 10.1111/j.1530-0277.2009.00994.x.

Durand, M., Hulme, C., Larkin, R. and Snowling, M. (2005) 'The cognitive foundations of reading and arithmetic skills in 7- to 10-year-olds', *Journal of Experimental Child Psychology*, 91(2), pp. 113–136. doi: 10.1016/j.jecp.2005.01.003.

Duvernoy, H. M. (1999) *The Human Brain*. Vienna: Springer Vienna. doi: 10.1007/978-3-7091-6792-2.

Ekblad, M., Korkeila, J., Parkkola, R., Lapinleimu, H., *et al.* (2010) 'Maternal Smoking during Pregnancy and Regional Brain Volumes in Preterm Infants', *Journal of Pediatrics*, 156(2). doi: 10.1016/j.jpeds.2009.07.061.

Fehr, T., Code, C. and Herrmann, M. (2007) 'Common brain regions underlying different arithmetic operations as revealed by conjunct fMRI–BOLD activation', *Brain Research*, 1172, pp. 93–102. doi: 10.1016/j.brainres.2007.07.043.

Fias, W., Lammertyn, J., Caessens, B. and Orban, G. A. (2007) 'Processing of Abstract Ordinal Knowledge in the Horizontal Segment of the Intraparietal Sulcus', *Journal of Neuroscience*, 27(33), pp. 8952–8956. doi: 10.1523/JNEUROSCI.2076-07.2007.

Fischl, B., Van Der Kouwe, A., Destrieux, C., Halgren, E., *et al.* (2004) 'Automatically Parcellating the Human Cerebral Cortex', *Cerebral Cortex*, 14(1), pp. 11–22. doi: 10.1093/cercor/bhg087.

Ghosh, S. S., Kakunoori, S., Augustinack, J., Nieto-Castanon, A., *et al.* (2010) 'Evaluating the validity of volume-based and surface-based brain image registration for developmental cognitive neuroscience studies in children 4 to 11years of age', *NeuroImage*. Elsevier Inc., 53(1), pp. 85–93. doi: 10.1016/j.neuroimage.2010.05.075.

Goebel, R. (2012) 'BrainVoyager — Past, present, future', *NeuroImage*, 62(2), pp. 748–756. doi: 10.1016/j.neuroimage.2012.01.083.

Gogtay, N., Giedd, J. N., Lusk, L., Hayashi, K. M., *et al.* (2004) 'Dynamic mapping of human cortical development during childhood through early adulthood', *Proceedings of the National Academy of Sciences*, 101(21), pp. 8174–8179. doi: 10.1073/pnas.0402680101.

Gore, J. C. (2003) 'Principles and practice of functional MRI of the human brain.', *The Journal of clinical investigation*, 112(1), pp. 4–9. doi: 10.1172/JCI19010.

Graziano, M. S. A. and Cooke, D. F. (2006) 'Parieto-frontal interactions, personal space, and defensive behavior (DOI:10.1016/j.neuropsychologia.2005.09.009)', *Neuropsychologia*, 44(13), pp. 2621–2635. doi: 10.1016/j.neuropsychologia.2005.09.011.

Grefkes, C. and Fink, G. R. (2005) 'The functional organization of the intraparietal sulcus in humans and monkeys.', *Journal of anatomy*, 207(1), pp. 3–17. doi: 10.1111/j.1469-7580.2005.00426.x.

Guerri, C. and Pascual, M. (2017) 'Effects of Alcohol on Embryo/Fetal Development', in *Reproductive and Developmental Toxicology*. Elsevier, pp. 431–445. doi: 10.1016/B978-0-12-804239-7.00024-X.

Hall, J. E. (2016) *Guyton and Hall Textbook of Medical Physiology*. 13th edn. Elsevier.
Hamilton, D. A., Kodituwakku, P., Sutherland, R. J. and Savage, D. D. (2003) 'Children with Fetal Alcohol Syndrome are impaired at place learning but not cued-navigation in a virtual Morris water task', *Behavioural Brain Research*, 143(1), pp. 85–94. doi: 10.1016/S0166-4328(03)00028-7.

Harding-Forrester, S. and Feldman, D. E. (2018) 'Somatosensory maps', in, pp. 73–102. doi: 10.1016/B978-0-444-63622-5.00004-8.

Harvey, B. M., Ferri, S. and Orban, G. A. (2017) 'Comparing Parietal Quantity-Processing Mechanisms between Humans and Macaques', *Trends in Cognitive Sciences*, 21(10), pp. 779–793. doi: 10.1016/j.tics.2017.07.002.

Hashemi, R. H. and Bradley, W. G. (2010) *MRI: The Basics*. 3rd edn. Lippincott Williams and Wilkins.

Hendelman, W. J. (2015) *Atlas of Functional Neuroanatomy*. 3rd edn. CRC Press.

Himmelbach, M., Karnath, H. O., Perenin, M. T., Franz, V. H., *et al.* (2006) 'A general deficit of the "automatic pilot" with posterior parietal cortex lesions?', *Neuropsychologia*, 44(13), pp. 2749–2756. doi: 10.1016/j.neuropsychologia.2006.04.030.

Hollingshead, A. B. (2011) 'Yale journal of sociology', *Yale Journal of Sociology*, 8, pp. 21–51.

Hsu, Y.-Y., Schuff, N., Du, A.-T., Mark, K., *et al.* (2002) 'Comparison of automated and manual MRI volumetry of hippocampus in normal aging and dementia', *Journal of Magnetic Resonance Imaging*, 16(3), pp. 305–310. doi: 10.1002/jmri.10163.

Holloway, I. D. and Ansari, D. (2009) 'Mapping numerical magnitudes onto symbols: The numerical distance effect and individual differences in children's mathematics achievement', *Journal of Experimental Child Psychology*, 103(1), pp. 17–29. doi: 10.1016/j.jecp.2008.04.001.

Howell, K., Lynch Ellen, M., Platzman, A., Smith Harold, G., *et al.* (2006) 'Prenatal alcohol exposure and ability, academic achievement, and school functioning in adolescence: a longitudinal follow-up.', *Journal of pediatric psychology*, 31(1), p. 116.

Hoyme, H. E. (2005) 'A Practical Clinical Approach to Diagnosis of Fetal Alcohol Spectrum Disorders: Clarification of the 1996 Institute of Medicine Criteria: In Reply', *PEDIATRICS*, 115(6), pp. 1787–1788. doi: 10.1542/peds.2005-0702.

Hoyme, H. E., Kalberg, W. O., Elliott, A. J., Blankenship, J., *et al.* (2016) 'Updated Clinical Guidelines for Diagnosing Fetal Alcohol Spectrum Disorders', *Pediatrics*, 138(2), p. e20154256. doi: 10.1542/peds.2015-4256.

Husain, M. and Nachev, P. (2007) 'Space and the parietal cortex', *Trends in Cognitive Sciences*, 11(1), pp. 30–36. doi: 10.1016/j.tics.2006.10.011.

Huttenlocher, P. R. (2002) *Neural Plasticity: The Effects of Environment on the Development of the Cerebral Cortex*. Harvard University Press.

Infante, M. A., Moore, E. M., Bischoff-Grethe, A., Tapert, S. F., *et al.* (2017) 'Altered functional connectivity during spatial working memory in children with heavy prenatal alcohol exposure', *Alcohol*, 64, pp. 11–21. doi: 10.1016/j.alcohol.2017.05.002.

Ipata, A. E. (2006) 'Activity in the Lateral Intraparietal Area Predicts the Goal and Latency of Saccades in a Free-Viewing Visual Search Task', *Journal of Neuroscience*, 26(14), pp. 3656–3661. doi: 10.1523/JNEUROSCI.5074-05.2006.

Isaacs, E. B., Edmonds, C. J., Lucas, A. and Gadian, D. G. (2001) 'Calculation difficulties in children of very low birthweight: A neural correlate', *Brain*, 124(9), pp. 1701–1707. doi: 10.1093/brain/124.9.1701.

Jacobson, J. L., Dodge, N. C., Burden, M. J., Klorman, R., *et al.* (2011) 'Number Processing in Adolescents With Prenatal Alcohol Exposure and ADHD: Differences in the Neurobehavioral Phenotype', *Alcoholism: Clinical and Experimental Research*, 35(3), pp. 431–442. doi: 10.1111/j.1530-0277.2010.01360.x.

Jacobson, S. W., Carr, L. G., Croxford, J., Sokol, R. J., *et al.* (2006) 'Protective effects of the alcohol dehydrogenase-ADH1B allele in children exposed to alcohol during pregnancy', *Journal of Pediatrics*, 148(1), pp. 30–37. doi: 10.1016/j.jpeds.2005.08.023.

Jacobson, S. W., Chiodo, L. M., Sokol, R. J. and Jacobson, J. L. (2002) 'Validity of maternal report of prenatal alcohol, cocaine, and smoking in relation to neurobehavioral outcome.', *Pediatrics*, 109(5), pp. 815–825. doi: 10.1542/peds.109.5.815.

Jacobson, S. W., Stanton, M. E., Dodge, N. C., Pienaar, M., *et al.* (2011) 'Impaired Delay and Trace Eyeblink Conditioning in School-Age Children With Fetal Alcohol Syndrome', *Alcoholism: Clinical and Experimental Research*, 35(2), pp. 250–264. doi: 10.1111/j.1530-0277.2010.01341.x.

Jacobson, S. W., Stanton, M. E., Molteno, C. D., Burden, M. J., *et al.* (2008) 'Impaired eyeblink conditioning in children with fetal alcohol syndrome', *Alcoholism: Clinical and Experimental Research*, 32(2), pp. 365–372. doi: 10.1111/j.1530-0277.2007.00585.x.

Jezzard, P., Matthews, P. M. and Smith, S. M. (2003) *Functional MRI: An introduction to methods*. Oxford University Press. doi: 10.1002/jmri.10284.

Jones, K. and Smith, D. (1973) 'RECOGNITION OF THE FETAL ALCOHOL SYNDROME IN EARLY INFANCY', *The Lancet*, 302(7836), pp. 999–1001. doi: 10.1016/S0140-6736(73)91092-1.

Kalberg, W. O., Provost, B., Tollison, S. J., Tabachnick, B. G., *et al.* (2006) 'Comparison of motor delays in young children with fetal alcohol syndrome to those with prenatal alcohol exposure and with no prenatal alcohol exposure', *Alcoholism: Clinical and Experimental Research*, 30(12), pp. 2037–2045. doi: 10.1111/j.1530-0277.2006.00250.x.

Keller, S. S. and Roberts, N. (2009) 'Measurement of brain volume using MRI: software, techniques, choices and prerequisites.', *Journal of anthropological sciences = Rivista di antropologia : JASS*, 87, pp. 127–51. Available at: http://www.ncbi.nlm.nih.gov/pubmed/19663172.

Klein, A. and Tourville, J. (2012) '101 Labeled Brain Images and a Consistent Human Cortical Labeling Protocol', *Frontiers in Neuroscience*, 6. doi: 10.3389/fnins.2012.00171.

Koo, T. K. and Li, M. Y. (2016) 'A Guideline of Selecting and Reporting Intraclass Correlation Coefficients for Reliability Research', *Journal of Chiropractic Medicine*, 15(2), pp. 155–163. doi: 10.1016/j.jcm.2016.02.012.

Kopera-Frye, K, Dehaene, S. and Streissguth, a P. (1996) 'Impairments of number processing induced by prenatal alcohol exposure.', *Neuropsychologia*, pp. 1187–96. Available at: http://www.ncbi.nlm.nih.gov/pubmed/8951830.

Koyama, M., Hasegawa, I., Osada, T., Adachi, Y., *et al.* (2004) 'Functional magnetic resonance imaging of macaque monkeys performing visually guided saccade tasks: Comparison of cortical eye fields with humans', *Neuron*, 41(5), pp. 795–807. doi: 10.1016/S0896-6273(04)00047-9.

Kruggel, F. (2018) 'The macro-structural variability of the human neocortex', *NeuroImage*, 172, pp. 620–630. doi: 10.1016/j.neuroimage.2018.01.074.

Lanphear, B. P. (2000) 'Cognitive Deficits Associated with Blood Lead Concentrations <10 microg/dL in US Children and Adolescents', *Public Health Reports*, 115(6), pp. 521–529. doi: 10.1093/phr/115.6.521.

Lebel, C., Mattson, S. N., Riley, E. P., Jones, K. L., *et al.* (2012) 'A Longitudinal Study of the Long-Term Consequences of Drinking during Pregnancy: Heavy In Utero Alcohol Exposure Disrupts the Normal Processes of Brain Development', *Journal of Neuroscience*, 32(44), pp. 15243–15251. doi: 10.1523/JNEUROSCI.1161-12.2012.

Lebel, C., Roussotte, F. and Sowell, E. R. (2011) 'Imaging the Impact of Prenatal Alcohol Exposure on the Structure of the Developing Human Brain', *Neuropsychology Review*, 21(2), pp. 102–118. doi: 10.1007/s11065-011-9163-0.

Lewis, J. W. and Van Essen, D. C. (2000a) 'Corticocortical connections of visual, sensorimotor, and multimodal processing areas in the parietal lobe of the macaque monkey', *Journal of Comparative Neurology*, 428(1), pp. 112–137. doi: 10.1002/1096-9861(20001204)428:1<112::AID-CNE8>3.0.CO;2-9.

Lewis, J. W. and Van Essen, D. C. (2000b) 'Mapping of architectonic subdivisions in the macaque monkey, with emphasis on parieto-occipital cortex', *Journal of Comparative Neurology*, 428(1), pp. 79–111. doi: 10.1002/1096-9861(20001204)428:1<79::AID-CNE7>3.0.CO;2-Q.

Lindquist, M. A. (2008) 'The Statistical Analysis of fMRI Data', *Statistical Science*, 23(4), pp. 439–464. doi: 10.1214/09-STS282.

Logothetis, N. K. (2008) 'What we can do and what we cannot do with fMRI', *Nature*, 453(7197), pp. 869–878. doi: 10.1038/nature06976.

Longo, C. A., Fried, P. A., Cameron, I. and Smith, A. M. (2014) 'The long-term effects of prenatal nicotine exposure on verbal working memory: An fMRI study of young adults', *Drug and Alcohol Dependence*. Elsevier Ireland Ltd, 144, pp. 61–69. doi: 10.1016/j.drugalcdep.2014.08.006.

Mancall, E. L. and Brock, D. G. (2011) *Gray's Clinical Neuroanatomy: The Anatomic Basis for Clinical Neuroscience*. 1st edn. Elsevier.

Martinez, A. M., Moro, A., Munhoz, R. P. and Teive, H. A. G. (2013) 'MacDonald Critchley', *Arquivos de Neuro-Psiquiatria*, 71(1), pp. 61–62. doi: 10.1590/S0004-282X2013000100013.

Matejko, A. A., Hutchison, J. E. and Ansari, D. (2019) 'Developmental specialization of the left intraparietal sulcus for symbolic ordinal processing', *Cortex*, 114, pp. 41–53. doi: 10.1016/j.cortex.2018.11.027.

Matthews, P. M. and Jezzard, P. (2004) 'Functional magnetic resonance imaging.', *Journal of neurology, neurosurgery, and psychiatry*, 75(1), pp. 6–12. Available at: http://www.ncbi.nlm.nih.gov/pubmed/14707297.

Mattson, S. N. and Riley, E. P. (1998) 'A review of the neurobehavioral deficits in children with fetal alcohol syndrome or prenatal exposure to alcohol.', *Alcoholism, clinical and experimental research*, 22(2), pp. 279–94. Available at: http://www.ncbi.nlm.nih.gov/pubmed/9581631 (Accessed: 7 August 2014).

Mattson, S. N., Riley, E. P., Sowell, E. R., Jernigan, T. L., *et al.* (1996) 'A decrease in the size of the basal ganglia in children with fetal alcohol syndrome.', *Alcoholism, clinical and experimental research*, 20(6), pp. 1088–93. Available at: http://www.ncbi.nlm.nih.gov/pubmed/8892532.

May, P. a, Brooke, L., Gossage, J. P., Croxford, J., *et al.* (2000) 'Epidemiology of fetal alcohol syndrome in a South African community in the Western Cape Province.', *American journal of public health*, 90(12), pp. 1905–12. Available at: http://www.pubmedcentral.nih.gov/articlerender.fcgi?artid=1446431&tool=pmcentrez&rendertype=abstract.

May, P. a., Gossage, J. P., Marais, A. S., Adnams, C. M., *et al.* (2007) 'The epidemiology of fetal alcohol syndrome and partial FAS in a South African community', *Drug and Alcohol Dependence*, 88, pp. 259–271. doi: 10.1016/j.drugalcdep.2006.11.007.

McRobbie, D. W., Moore, E. A., Graves, M. J. and Prince, M. R. (2006) *MRI from Picture to Proton*. 2nd edn. Cambridge University Press.

Meintjes, E. M., Jacobson, J. L., Molteno, C. D., Gatenby, J. C., *et al.* (2010) 'An FMRI study of number processing in children with fetal alcohol syndrome.', *Alcoholism, clinical and experimental research*, 34(8), pp. 1450–64. doi: 10.1111/j.1530-0277.2010.01230.x. **(b)**

Meintjes, E. M., Narr, K. L., der Kouwe, A. J. W. van, Molteno, C. D., *et al.* (2014) 'A tensor-based morphometry analysis of regional differences in brain volume in relation to prenatal alcohol exposure', *NeuroImage: Clinical*. Elsevier B.V., 5, pp. 152–160. doi: 10.1016/j.nicl.2014.04.001.

Meintjes, Ernesta M, Jacobson, J. L., Molteno, C. D., Gatenby, J. C., *et al.* (2010) 'An FMRI study of number processing in children with fetal alcohol syndrome.', *Alcoholism, clinical and experimental research*, 34(8), pp. 1450–64. doi: 10.1111/j.1530-0277.2010.01230.x. **(a)**

Menon, V., Rivera, S. M., White, C. D., Glover, G. H., *et al.* (2000) 'Dissociating prefrontal and parietal cortex activation during arithmetic processing', *NeuroImage*, 12(4), pp. 357–365. doi: 10.1006/nimg.2000.0613.

Migliorini, R., Moore, E. M., Glass, L., Infante, M. A., *et al.* (2015) 'Anterior cingulate cortex surface area relates to behavioral inhibition in adolescents with and without heavy prenatal alcohol exposure', *Behavioural Brain Research*. Elsevier B.V., 292, pp. 26–35. doi: 10.1016/j.bbr.2015.05.037.

Mikhael, S. S., Mair, G., Valdes-Hernandez, M., Hoogendoorn, C., *et al.* (2019) 'Manually-parcellated gyral data accounting for all known anatomical variability', *Scientific Data*, 6, p. 190001. doi: 10.1038/sdata.2019.1.

Molko, N., Cachia, A., Rivière, D., Mangin, J. F., *et al.* (2003) 'Functional and structural alterations of the intraparietal sulcus in a developmental dyscalculia of genetic origin', *Neuron*, 40(4), pp. 847–858. doi: 10.1016/S0896-6273(03)00670-6.

Moore, K. L., Persaud, T. V. N. and Torchia, M. G. (2016) *The Developing Human: Clinically Oriented Embryology*. 10th edn. Elsevier.

Mosby's Dictionary of Medicine, Nursing & Health Professions. 8th edn (2009). Elsevier.

Morey, R. A., Petty, C. M., Xu, Y., Pannu Hayes, J., *et al.* (2009) 'A comparison of automated segmentation and manual tracing for quantifying hippocampal and amygdala volumes', *NeuroImage*, 45(3), pp. 855–866. doi: 10.1016/j.neuroimage.2008.12.033.

Mtui, E., Gruener, G. and Dockery, P. (2016) *Fitzgerald's Clinical Neuroanatomy and Neuroscience*. Elsevier.

Naccache, L. and Dehaene, S. (2001) 'The Priming Method : Imaging Unconscious Repetition Priming Reveals an Abstract Representation of Number in the Parietal Lobes', *Cerebral Cortex Oct*, 11, pp. 966–974. doi: 10.1093/cercor/11.10.966.

Nunez, C. C., Roussotte, F. and Sowell, E. R. (2011) 'Focus on: structural and functional brain abnormalities in fetal alcohol spectrum disorders.', *Alcohol research & health : the journal of the National Institute on Alcohol Abuse and Alcoholism*, 34(1), pp. 121–31. Available at: http://pubs.niaaa.nih.gov/publications/arh341/121-131.htm.

Ogawa, S. (2012) 'Finding the BOLD effect in brain images', *NeuroImage*, 62(2), pp. 608–609. doi: 10.1016/j.neuroimage.2012.01.091.

Ogawa, S., Lee, T. M., Kay, A. R. and Tank, D. W. (1990) 'Brain magnetic resonance imaging with contrast dependent on blood oxygenation.', *Proceedings of the National Academy of Sciences*, 87(24), pp. 9868–9872. doi: 10.1073/pnas.87.24.9868.

Ogawa, S., Tank, D. W., Menon, R., Ellermann, J. M., *et al.* (1992) 'Intrinsic signal changes accompanying sensory stimulation: functional brain mapping with magnetic resonance imaging.', *Proceedings of the National Academy of Sciences*, 89(13), pp. 5951–5955. doi: 10.1073/pnas.89.13.5951.

Ogawa, Seiji, Lee, T.-M., Nayak, A. S. and Glynn, P. (1990) 'Oxygenation-sensitive contrast in magnetic resonance image of rodent brain at high magnetic fields', *Magnetic Resonance in Medicine*, 14(1), pp. 68–78. doi: 10.1002/mrm.1910140108.

Pa, J. and Hickok, G. (2008) 'A parietal-temporal sensory-motor integration area for the human vocal tract: evidence from an fMRI study of skilled musicians.', *Neuropsychologia*, 46(1), pp. 362–8. doi: 10.1016/j.neuropsychologia.2007.06.024.

Peters, L. and De Smedt, B. (2018) 'Arithmetic in the developing brain: A review of brain imaging studies', *Developmental Cognitive Neuroscience*, 30, pp. 265–279. doi: 10.1016/j.dcn.2017.05.002.

Pfefferbaum, A., Desmond, J. E., Galloway, C., Menon, V., *et al.* (2001) 'Reorganization of Frontal Systems Used by Alcoholics for Spatial Working Memory: An fMRI Study', *NeuroImage*, 14(1), pp. 7–20. doi: 10.1006/nimg.2001.0785.

Piazza, M., Giacomini, E., Le Bihan, D. and Dehaene, S. (2003) 'Single-trial classification of parallel pre-attentive and serial attentive processes using functional magnetic resonance imaging', *Proceedings of the Royal Society B: Biological Sciences*, 270(1521), pp. 1237–1245. doi: 10.1098/rspb.2003.2356.

Piazza, M., Izard, V., Pinel, P., Le Bihan, D., *et al.* (2004) 'Tuning curves for approximate numerosity in the human intraparietal sulcus.', *Neuron*, 44(3), pp. 547–55. doi: 10.1016/j.neuron.2004.10.014.

Pinel, P., Dehaene, S., Rivière, D. and LeBihan, D. (2001) 'Modulation of Parietal Activation by Semantic Distance in a Number Comparison Task', *NeuroImage*, 14(5), pp. 1013–1026. doi: 10.1006/nimg.2001.0913.

Poldrack, R. A., Nichols, T. and Mumford, J. (2011) *Handbook of Functional MRI Data Analysis*, *Handbook of Functional MRI Data Analysis*. doi: 10.1017/cbo9780511895029.

Rajaprakash, M., Chakravarty, M. M., Lerch, J. P. and Rovet, J. (2013) 'Cortical morphology in children with alcohol-related neurodevelopmental disorder', pp. 41–50. doi: 10.1002/brb3.191.

Randall, S. R., Warton, C. M. R., Holmes, M. J., Cotton, M. F., *et al.* (2017) 'Larger Subcortical Gray Matter Structures and Smaller Corpora Callosa at Age 5 Years in HIV Infected Children on Early ART', *Frontiers in Neuroanatomy*, 11. doi: 10.3389/fnana.2017.00095.

Rasmussen, C. and Bisanz, J. (2009) 'Exploring Mathematics Difficulties in Children With Fetal Alcohol Spectrum Disorders', *Child Development Perspectives*, 3(2), pp. 125–130. doi: 10.1111/j.1750-8606.2009.00091.x.

Riley, E. P., Clarren, S., Weinberg, J. and Jonsson, E. (2010) *Fetal Alcohol Spectrum Disorder: Management and Policy Perspectives of FASD*. Wiley-Blackwell.

Riley, E. P., Infante, M. A. and Warren, K. R. (2011) 'Fetal Alcohol Spectrum Disorders: An Overview', *Neuropsychology Review*, 21(2), pp. 73–80. doi: 10.1007/s11065-011-9166-x.
Rubin, M. and Safdieh, Joseph, E. (2016) *Netter's Concise Neuroanatomy*. 1st edn. Elsevier. Available at: https://www.elsevier.com/books/netters-concise-neuroanatomy-updated-edition/rubin/978-0-323-48091-8.

Rizzolatti, G. (1997) 'Adrian Lecture: Organization of cortical motor system: New concepts', *Electroencephalography and Clinical Neurophysiology*, 103(1), p. 3. doi: 10.1016/S0013-4694(97)87916-7.

Rosset, A., Spadola, L. and Ratib, O. (2004) 'OsiriX: An Open-Source Software for Navigating in Multidimensional DICOM Images', *Journal of Digital Imaging*, 17(3), pp. 205–216. doi: 10.1007/s10278-004-1014-6.

Sacks, O. (1985) *The Man Who Mistook His Wife For A Hat and Other Clinical Tales*. Gerald Duckworth.

Santhanam, P., Li, Z., Hu, X., Lynch, M. E., *et al.* (2009) 'Effects of prenatal alcohol exposure on brain activation during an arithmetic task: An fMRI study', *Alcoholism: Clinical and Experimental Research*, 33(11), pp. 1901–1908. doi: 10.1111/j.1530-0277.2009.01028.x.

Sattler, J. M. (1992) *Assessment of children*. 3rd edn.

Schild, H. H. (1990) *MRI Made Easy: (... Well Almost)*. Schering AG.

Schlack, A., Hoffmann, K. and Bremmer, F. (2002) 'Interaction of linear vestibular and visual stimulation in the macaque ventral intraparietal area (VIP)', *European Journal of Neuroscience*, 16(10), pp. 1877–1886. doi: 10.1046/j.1460-9568.2002.02251.x.

Schlack, A., Hoffmann, K. P. and Bremmer, F. (2003) 'Selectivity of macaque ventral intraparietal area (area VIP) for smooth pursuit eye movements', *Journal of Physiology*, 551(2), pp. 551–561. doi: 10.1113/jphysiol.2003.042994.

Schultz, J. and Lennert, T. (2009) 'BOLD signal in intraparietal sulcus covaries with magnitude of implicitly driven attention shifts', *NeuroImage*, 45(4), pp. 1314–1328. doi: 10.1016/j.neuroimage.2009.01.012.

Shikata, E., McNamara, A., Sprenger, A., Hamzei, F., *et al.* (2008) 'Localization of human intraparietal areas AIP, CIP, and LIP using surface orientation and saccadic eye movement tasks', *Human Brain Mapping*, 29(4), pp. 411–421. doi: 10.1002/hbm.20396.

Simmons, R. W., Nguyen, T. T., Levy, S. S., Thomas, J. D., *et al.* (2012) 'Children with Heavy Prenatal Alcohol Exposure Exhibit Deficits when Regulating Isometric Force', *Alcoholism: Clinical and Experimental Research*, 36(2), pp. 302–309. doi: 10.1111/j.1530-0277.2011.01625.x.

Simon, O., Mangin, J. F., Cohen, L., Le Bihan, D., *et al.* (2002) 'Topographical layout of hand, eye, calculation, and language-related areas in the human parietal lobe.', *Neuron*, 33(3), pp. 475–87. Available at: http://www.ncbi.nlm.nih.gov/pubmed/11832233 (Accessed: 14 June 2013).

Soares, J. M., Magalhães, R., Moreira, P. S., Sousa, A., *et al.* (2016) 'A Hitchhiker's Guide to Functional Magnetic Resonance Imaging', *Frontiers in Neuroscience*, 10. doi: 10.3389/fnins.2016.00515.

Sokol, R., Debanne, S., Ager, J., Martier, S., *et al.* (1985) 'Maximizing the Efficiency of a Study on Alcohol-Related Birth Defects by Means of Data Collection and Analytic Strategy Dissociation', *American Journal of Perinatology*, 2(03), pp. 245–249. doi: 10.1055/s-2007-999961.

Sowell, E. R., Mattson, S. N., Kan, E., Thompson, P. M., *et al.* (2008) 'Abnormal cortical thickness and brain-behavior correlation patterns in individuals with heavy prenatal alcohol exposure.', *Cerebral cortex (New York, N.Y. : 1991)*, 18(1), pp. 136–44. doi: 10.1093/cercor/bhm039.

Sowell, E. R., Thompson, P. M., Mattson, S. N., Tessner, K. D., *et al.* (2001) 'Voxel-based morphometric analyses of the brain in children and adolescents prenatally exposed to alcohol.', *Neuroreport*, 12(3), pp. 515–23. Available at: http://www.ncbi.nlm.nih.gov/pubmed/11234756.

Sowell, E. R., Thompson, P. M., Mattson, S. N., Tessner, K. D., *et al.* (2002) 'Regional brain shape abnormalities persist into adolescence after heavy prenatal alcohol exposure.', *Cerebral cortex (New York, N.Y. : 1991)*, 12(8), pp. 856–65. Available at: http://www.ncbi.nlm.nih.gov/pubmed/12122034.

Sowell, E. R., Thompson, P. M., Mattson, S. N., Tessner, K. D., *et al.* (2001) 'Voxel-based morphometric analyses of the brain in children and adolescents prenatally exposed to alcohol.', *Neuroreport*, 12(3), pp. 515–23. Available at: http://www.ncbi.nlm.nih.gov/pubmed/11234756.

Sowell, E. R., Thompson, P. M., Peterson, B. S., Mattson, S. N., *et al.* (2002) 'Mapping cortical gray matter asymmetry patterns in adolescents with heavy prenatal alcohol exposure', *NeuroImage*, 17(4), pp. 1807–1819. doi: 10.1006/nimg.2002.1328.

Streissguth, A. P., Barr, H. M., Olson, H. C., Sampson, P. D., *et al.* (1994) 'Drinking during pregnancy decreases word attack and arithmetic scores on standardized tests: adolescent data from a population-based prospective study.', *Alcoholism, clinical and experimental research*, 18(2), pp. 248–254. doi: 10.1111/j.1530-0277.1994.tb00009.x.

Streissguth, A. P., Bookstein, F. L., Sampson, P. D. and Barr, H. M. (1989) 'Neurobehavioral effects of prenatal alcohol: Part III. PLS analyses of neuropsychologic tests.', *Neurotoxicology and teratology*, 11(5), pp. 493–507. Available at: http://www.ncbi.nlm.nih.gov/pubmed/2593988.

Swayze, V. W., Johnson, V. P., Hanson, J. W., Piven, J., *et al.* (1997) 'Magnetic resonance imaging of brain anomalies in fetal alcohol syndrome.', *Pediatrics*, 99(2), pp. 232–40. Available at: http://www.ncbi.nlm.nih.gov/pubmed/9024452.

Tapert, S. F., Schweinsburg, A. D., Barlett, V. C., Brown, S. A., *et al.* (2004) 'Blood Oxygen Level Dependent Response and Spatial Working Memory in Adolescents With Alcohol Use Disorders', *Alcoholism: Clinical & Experimental Research*, 28(10), pp. 1577–1586. doi: 10.1097/01.ALC.0000141812.81234.A6.

Tisdall, M. D., Hess, A. T., Reuter, M., Meintjes, E. M., *et al.* (2012) 'Volumetric navigators for prospective motion correction and selective reacquisition in neuroanatomical MRI', *Magnetic Resonance in Medicine*, 68(2), pp. 389–399. doi: 10.1002/mrm.23228.

Tsutsui, K. I., Sakata, H., Naganuma, T. and Taira, M. (2002) 'Neural correlates for perception of 3D surface orientation from texture gradient', *Science*, 298(5592), pp. 409–412. doi: 10.1126/science.1074128.

Tunik, E., Frey, S. H. and Grafton, S. T. (2005) 'Virtual lesions of the anterior intraparietal area disrupt goal-dependent on-line adjustments of grasp.', *Nature neuroscience*, 8(4), pp. 505–11. doi: 10.1038/nn1430.

Turner, W. (1866) 'The Convolutions of the Human Cerebrum Topographically Considered.', *Edinburgh medical journal*, 11(12), pp. 1105–1122. Available at: http://www.ncbi.nlm.nih.gov/pubmed/29645562.

Turner, W. (1866) '5. Notes more especially on the Bridging Convolutions in the Brain of the Chimpanzee.', *Proceedings of the Royal Society of Edinburgh*, 5(1866), pp. 578–587. doi: 10.1017/S0370164600041432.

van der Kouwe, A. J. W., Benner, T., Salat, D. H. and Fischl, B. (2008) 'Brain morphometry with multiecho MPRAGE', *NeuroImage*, 40(2), pp. 559–569. doi: 10.1016/j.neuroimage.2007.12.025.

Venkatraman, V., Ansari, D. and Chee, M. W. L. (2005) 'Neural correlates of symbolic and non-symbolic arithmetic', *Neuropsychologia*, 43(5), pp. 744–753. doi: 10.1016/j.neuropsychologia.2004.08.005.

Vogel, S. E., Goffin, C., Bohnenberger, J., Koschutnig, K., *et al.* (2017) 'The left intraparietal sulcus adapts to symbolic number in both the visual and auditory modalities: Evidence from fMRI', *NeuroImage*, 153, pp. 16–27. doi: 10.1016/j.neuroimage.2017.03.048.

Warton, F. L., Meintjes, E. M., Warton, C. M. R., Molteno, C. D., *et al.* (2018) 'Prenatal methamphetamine exposure is associated with reduced subcortical volumes in neonates', *Neurotoxicology and Teratology*, 65, pp. 51–59. doi: 10.1016/j.ntt.2017.10.005.

Watkins, K. E. (2001) 'Structural Asymmetries in the Human Brain: a Voxel-based Statistical Analysis of 142 MRI Scans', *Cerebral Cortex*, 11(9), pp. 868–877. doi: 10.1093/cercor/11.9.868.

Weishaupt, D., Köchli, V. D. and Marincek, B. (2008) *How Does MRI Work? An Introduction to the Physics and Function of Magnetic Resonance Imaging*. 2nd edn, *Radiology*. 2nd edn. Springer- Verlag

Wessels, Q., Correia, J. C. and Taylor, A. M. (2016) 'Sir William Turner (1832–1916) – Lancastrian, anatomist and champion of the Victorian era', *Journal of Medical Biography*, 24(4), pp. 500–506. doi: 10.1177/0967772015575891.

Winer, B. (1971) *Statistical Principles in Experimental Design*. 2nd edn. McGraw-Hill.

Wisniewski, K., Dambska, M., Sher, J. H. and Qazi, Q. (1983) 'A clinical neuropathological study of the fetal alcohol syndrome.', *Neuropediatrics*, 14(4), pp. 197–201. doi: 10.1055/s-2008-1059578.

Woods, K. J., Jacobson, S. W., Molteno, C. D., Jacobson, J. L., *et al.* (2018) 'Altered Parietal Activation during Non-symbolic Number Comparison in Children with Prenatal Alcohol Exposure', *Frontiers in Human Neuroscience*, 11. doi: 10.3389/fnhum.2017.00627.

Woods, K. J., Meintjes, E. M., Molteno, C. D., Jacobson, S. W., *et al.* (2015) 'Parietal dysfunction during number processing in children with fetal alcohol spectrum disorders', *NeuroImage: Clinical*. Elsevier B.V., 8, pp. 594–605. doi: 10.1016/j.nicl.2015.03.023.

Woods, R. P. (2003) 'MultiTracer: A Java-based tool for anatomic delineation of grayscale volumetric images', *NeuroImage*, 19(4), pp. 1829–1834. doi: 10.1016/S1053-8119(03)00243-X.

Yushkevich, P. A., Piven, J., Hazlett, H. C., Smith, R. G., *et al.* (2006) 'User-guided 3D active contour segmentation of anatomical structures: Significantly improved efficiency and reliability', *NeuroImage*, 31(3), pp. 1116–1128. doi: 10.1016/j.neuroimage.2006.01.015.

Zamarian, L., Ischebeck, A. and Delazer, M. (2009) 'Neuroscience of learning arithmetic—Evidence from brain imaging studies', *Neuroscience & Biobehavioral Reviews*, 33(6), pp. 909–925. doi: 10.1016/j.neubiorev.2009.03.005.

Zlatkina, V. and Petrides, M. (2014) 'Morphological patterns of the intraparietal sulcus and the anterior intermediate parietal sulcus of Jensen in the human brain', *Proceedings of the Royal Society B: Biological Sciences*, 281(1797), pp. 20141493–20141493. doi: 10.1098/rspb.2014.1493.